

***In vitro and in vivo***  
**Drug Targeting using**  
**Biotinylated Immunoliposomes**

**INAUGURALDISSERTATION**

zur Erlangung der Würde eines Doktors der Philosophie  
vorgelegt der  
Philosophisch-Naturwissenschaftlichen Fakultät  
der Universität Basel

von

Anita Schnyder  
aus Halten (SO)

Basel, 2005

Genehmigt von der Philosophisch-Naturwissenschaftlichen Fakultät  
auf Antrag von:

PD Dr. Jörg Huwyler (Dissertationsleiter)

Prof. Dr. Stephan Krähenbühl (Fakultätsverantwortlicher)

Prof. Dr. Jürgen Drewe (Referent)

Prof. Dr. Hans Leuenberger (Vorsitzender)

Basel, den 5.4.2005

Dekan Prof. Dr. Hans-Jakob Wirz

*This work is dedicated to my parents  
Therese and Erwin*



## **ACKNOWLEDGEMENTS**

It gives me great pleasure to acknowledge the help and support I have received during the preparation of this thesis work.

First, I would like to thank my supervisors PD Dr. Jörg Huwyler, Prof. Dr. Stephan Krähenbühl and Prof. Dr. Jürgen Drewe for giving me the opportunity to accomplish the work presented here in their groups. I am grateful to PD Dr. Jörg Huwyler for the excellent working environment and the essential resources to learn and do research during the period of my study. His enthusiasm about pharmaceutical research and science was always constructive, motivating and indispensable. Thank you very much for everything!

I am particularly indebted to Dr. Philippe Coassolo for his continuous support during the last 3 years.

Thanks go also to all other members of the DMPK group in PRBD-E, F. Hoffmann-La Roche Ltd. in Basel who have contributed to the pleasant atmosphere I experienced in the laboratories. Special thanks to Marie-Elise Brun and Brigitte Notter for their technical support and for sharing many funny moments with me. The excellent technical help of Marie Stella Gruyer and Veronique Dall'Asen with animal surgery is acknowledged. I would like to express my thanks to Vittorio Bona, Elena Fontana, Roberto Bravo, Martine Buhler and Gerhard Zürcher for their contribution to this very agreeable environment and for all the interesting discussions!

I am also grateful to Dr. Michael Török and Dr. Lothar Lindemann for their patient and qualified help and for giving me some very interesting insights into molecular biology. I also thank Ursula Behrens for her technical assistance with cell-cultures.

The help of Dr. Bernd Bohrmann, Krisztina Orszolan-Szovik and Beat Erne with confocal microscopy is acknowledged.

I would like to express my thanks to Prof. Dr. Karsten Mäder for his valuable and competent help concerning ESR technique. Thanks to Dr. Hansruedi Lötscher and Hanspeter Kurt for their technical support and providing the antibody.

Special thanks go to all my friends who supported and helped me in many ways to get this work done. In particular the invaluable daily motivations and encouragements of Caroline, Michael and Thomas are sincerely thanked.

Finally, and most deeply, I would like to thank my family, especially my parents, for loving and supporting me always in my life. They have made a major contribution to all I have been able to achieve so far!

The Swiss National Science Foundation and F. Hoffmann-La Roche Ltd. Basel are thanked for the financial support.

## **ABBREVIATIONS**

- AT: 4-Amino-2,2,5,5,-tetramethyl-3-imidazoline-1-yloxy
- AUC: Area under the curve\$
- BBB: Blood-brain barrier
- bio-PEG-DSPE: biotinylated PEG-DSPE
- BSA: bovine serum albumine
- CL: Clearance
- DAPI: 4',6-Diamidino-2-phenylindole
- DMEM: Dulbecco's Modified Eagle Medium
- DSPC: distearoylphosphatidylcholine
- EGFR: human epidermal growth factor receptor
- FCS: fetal calf serum
- HIRmAb: monoclonal antibody to human insulin receptor
- HP: 2-Heptadecyl-2,3,4,5,5,-pentamethylimidazolidine-1-yloxy
- i.v. : intravenous
- IgG<sub>2a</sub> mAb: unspecific IgG monoclonal antibody
- MBS: m-maleimidobenzoyl-N-hydroxysuccinimide ester
- OX26 mAb: OX26 monoclonal antibody to the rat transferrin receptor
- OX26-streptavidin: OX26 mAb coupled covalently to streptavidin
- pI: isoelectric point
- PBS: phosphate buffered saline
- PEG: poly(ethylene glycol)
- PEG-DSPE: PEG derivatized distearoylphosphatidylethanolamine

PI: propidium iodide

PS: permeability surface area product

SA: streptavidin

SEC: size exclusion chromatography

SEM: standard error of the mean

SRB: sulforhodamine B

Tf: transferrin

TfR: transferrin receptor

$T_{1/2}$ : half-life

$V_0$ : organ volume of distribution of a plasma volume marker

$V_D$ : tissue volume of distribution

$2a_N$ : distance between the first and the third peak in the ESR spectrum



## TABLE OF CONTENTS

<b>ACKNOWLEDGEMENTS</b> .....	<b>5</b>
<b>ABBREVIATIONS</b> .....	<b>7</b>
<b>TABLE OF CONTENTS</b> .....	<b>9</b>
<b>SUMMARY</b> .....	<b>11</b>
<b>1 INTRODUCTION</b> .....	<b>13</b>
1.1 Liposomes.....	13
1.1.1 Structure .....	13
1.1.2 Pegylation of liposomes .....	15
1.2 Immunoliposomes .....	16
1.2.1 Targeting using immunoliposomes: a new technology.....	16
1.2.2 Targeting of small molecules – state of the art.....	19
1.2.3 OX26 and the transferrin receptor .....	20
1.2.4 Antibody conjugation .....	23
1.3 Non-covalent streptavidin-biotin binding method.....	27
1.4 Loading of liposomes .....	28
1.5 Clinical use of immunoliposomes .....	32
1.6 Gene targeting .....	33
<b>2 AIMS OF THE THESIS</b> .....	<b>38</b>
<b>3 MATERIALS AND METHODS</b> .....	<b>39</b>
3.1 Materials.....	39
3.2 Methods: Preparation and characterization of a novel liposomal carrier system.....	41
3.2.1 Synthesis of streptavidin-conjugated OX26 mAb .....	41
3.2.2 Gel electrophoresis.....	41
3.2.3 Biotin binding assay.....	42
3.2.4 Preparation of liposomes .....	43
3.2.5 Loading of immunoliposomes by pH gradient .....	43
3.2.6 Passive loading of immunoliposomes.....	44
3.2.7 Preparation of pH-sensitive liposomes .....	44
3.2.8 Preparation of fluorescent biotinylated OX26-immunoliposomes.....	45
3.3 Methods: In vitro assays and results .....	46
3.3.1 Cell-cultures .....	46
3.3.2 Immunohistochemistry .....	47
3.3.3 Immunocytochemistry and uptake experiments .....	48
3.3.4 Endosomal release of propidium iodide .....	49
3.3.5 Microscopy.....	49
3.3.6 DNA incorporation into immunoliposomes .....	50
3.3.7 Confirmation of DNA incorporation into liposomes.....	51
3.3.8 Liposomal administration of pGL3 expression vector.....	52

Table of contents

3.3.9	Expression of $\beta$ -galactosidase in RG2 cells .....	53
3.3.10	Uptake of liposomal, labeled oligonucleotides by RG2 cells .....	54
3.3.11	In vitro IC <sub>50</sub> determination of daunomycin.....	55
3.3.12	Cellular uptake of liposomal [ <sup>3</sup> H]daunomycin .....	56
3.3.13	Pharmacological effects of daunomycin loaded Immunoliposomes on RBE4 cells.....	56
3.3.14	Sulforhodamine B assays for determination of daunomycin cytotoxicity.....	57
3.4	Methods: In vivo assays and results.....	57
3.4.1	Pharmacokinetics and tissue delivery of (immuno) liposomes in the rat.....	57
3.4.2	Statistics.....	59
<b>4</b>	<b>RESULTS.....</b>	<b>60</b>
4.1	Characterization and optimization of a novel liposomal carrier system .....	60
4.1.1	Synthesis of streptavidin-conjugated OX26 mAb .....	60
4.1.2	Gel electrophoresis .....	62
4.1.3	Biotin binding assay .....	63
4.1.4	Loading of immunoliposomes by pH gradient.....	64
4.1.5	Passive loading of immunoliposomes.....	66
4.2	In vitro assays and results .....	67
4.2.1	Immunohistochemistry .....	67
4.2.2	Immunocytochemistry and uptake experiments .....	68
4.2.3	Endosomal release of propidium iodide.....	71
4.2.4	Gene uptake and expression using immunoliposomes .....	73
4.2.5	Liposomal administration of pGL3 expression vector.....	75
4.2.6	Expression of $\beta$ -galactosidase in RG2 cells .....	76
4.2.7	Uptake of liposomal, labeled oligonucleotides by RG2 cells .....	77
4.2.8	Cytotoxicity of liposomal daunomycin.....	79
4.2.9	Cellular uptake of liposomal [ <sup>3</sup> H]daunomycin .....	81
4.2.10	Pharmacological effects of daunomycin loaded immunoliposomes on RBE4 cells.....	82
4.3	In vivo assays and results .....	87
4.3.1	Plasma concentrations of free and liposomal daunomycin in rat .....	87
4.3.2	Tissue distribution of free daunomycin and daunomycin loaded liposomes or immunoliposomes.....	90
<b>5</b>	<b>DISCUSSION AND FUTURE PERSPECTIVES.....</b>	<b>95</b>
5.1	Characterization and optimization of a novel liposomal carrier system .....	95
5.2	In vitro assays.....	103
5.3	In vivo assays .....	113
5.4	Future perspectives .....	117
<b>6</b>	<b>CONCLUSIONS .....</b>	<b>127</b>
<b>7</b>	<b>REFERENCES.....</b>	<b>128</b>
<b>8</b>	<b>CURRICULUM VITAE .....</b>	<b>140</b>

## SUMMARY

The aim of my thesis was the optimization, characterization and application of a new, innovative drug carrier system which can be used to target pharmaceuticals to diseased tissues and organs. In the present study, a non-covalent biotin-streptavidin coupling procedure for the preparation of pegylated immunoliposomes is presented which simplifies the attachment of targeting vectors to sterically stabilized liposomes. The OX26 monoclonal antibody against the rat transferrin receptor was used as a targeting vector.

Immunostaining experiments with the OX26 monoclonal antibody followed by fluorescent confocal microscopy revealed immunofluorescence labeling of the transferrin receptor on muscle and on glioma cells. Uptake experiments with these cells demonstrated cellular uptake and accumulation of small molecules (daunomycin, fluorescent probes) or macromolecules such as fluorescent oligonucleotides, within an intracellular compartment.

Cellular uptake of liposomal daunomycin by multidrug-resistant cells was dose- and time-dependent and was associated with a clear pharmacological (i.e. cytotoxic) effect. Cytotoxic effects of liposomal formulations of daunomycin, in contrast to the free drug, were apparent only after prolonged incubation periods being indicative of a slow intracellular unpacking and release of liposomal daunomycin. With respect to expression plasmids (i.e. gene targeting), only marginal levels of gene expression were observed *in vitro*.

Pharmacokinetics and tissue distribution studies in the rat revealed a substantially increased plasma half-life of liposomal drug compared to free drug. Brain accumulation of daunomycin in OX26-immunoliposomes occurred in higher levels as compared to brain uptake of free daunomycin or daunomycin incorporated within pegylated liposomes or unspecific IgG<sub>2a</sub> isotype control immunoliposomes. Such OX26-mediated effects were not observed in other tissues such as spleen, liver, muscle or kidney.

Our experiments indicate that immunoliposomes can be used to target small drug molecules as well as macromolecules, such as oligonucleotides and expression plasmids, to cells and tissues.

These findings demonstrate that immunoliposomes are a versatile and promising tool for future drug development in regard to both, galenic and therapeutical research. For clinical administrations, a better understanding of cellular uptake and release mechanisms are needed.

# 1 INTRODUCTION

Drug targeting is an innovative and challenging topic in contemporary drug development and galenic research. The use of immunoliposomes offers a promising approach to improve controlled drug delivery. The molecule of interest is thereby incorporated into immunoliposomes that are directed by a coupled antibody against a defined target that is present in diseased tissues or organs. The ideal vector antibody exhibits specificity for one sole antigen. Therewith, liposomal drug is delivered only to the targeted, diseased tissue or organs and not to unintentional, not diseased sites. Adverse side effects are a major drawback in drug development and pharmaceutical research. By using immunoliposomes as a specific drug delivery system, adverse reactions can be circumvented or reduced. It presents an enhancement of efficacy as the drug is delivered completely to the sites of disease, yielding in lower required doses. Thus, immunoliposomes, the topic of present work, describe a promising tool for the targeted delivery of small drugs to organs or tissues.

## 1.1 LIPOSOMES

### 1.1.1 *Structure*

Liposomes are vesicles in which an aqueous volume is entirely enclosed by a membrane composed of lipid molecules, usually phospholipids (Figure 1). Spontaneously formed upon dispersion in aqueous media, the size of such vesicles can range from tens of nanometres to tens of microns in diameter (New, 1990). In pharmaceutical sciences, liposomes have been used traditionally as formulation ingredients to assist in formulation of poorly soluble therapeutic agents for oral or parenteral administration. The antibiotic amphotericin B is an example of a marketed

drug that makes use of this formulation principle for intravenous infusion (Gulati et al., 1998).

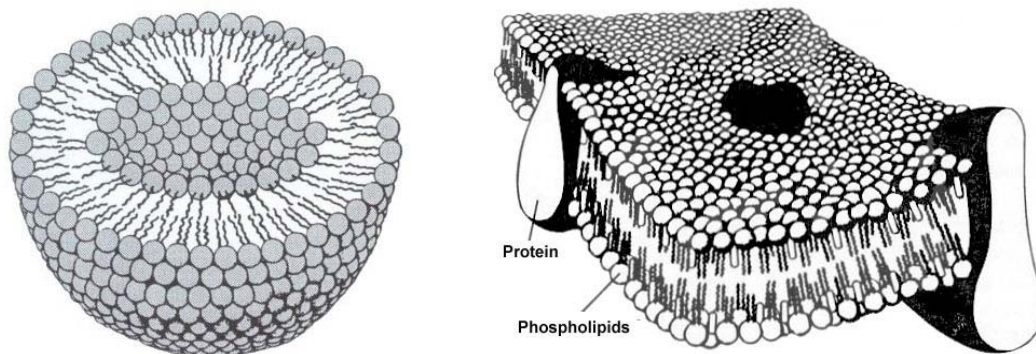


**Figure 1:** Schematic representation of membranes: Liposome structure (left panel) and human cell membrane (right panel). Both of them are formed by phospholipid molecules that have arranged themselves to form a membrane. Under certain physical conditions they will spontaneously form liposomes (left panel) whose walls are very similar in construction to the actual cell membrane shown on the right side.

Liposomes can contain large amounts of small molecules either within their aqueous interior or dissolved in the lipophilic region of their membrane bilayers (Cerletti et al., 2000). Enzymes have no longer access to the encapsulated substance which is hence protected from degradation and metabolism. This is one of the reasons why such liposomal delivery systems acquired much attention during the last years (Storm and Crommelin, 1998).

Liposomes can be made of natural constituents. Their membrane is very similar to natural cell membranes (Figure 1) and provides great convenience as models for membrane systems (New, 1990). Such naturally occurring constituents are cholesterol, phospholipids or fatty acids that make them a biocompatible and safe vehicle for medical *in vivo* applications. Those favourable properties can be adjusted by chemical

modifications of the phospholipid-bilayer membrane of the liposome. Chemical modifications, such as saturation or pegylation of phospholipids are well established and numerous possibilities are described, which results in a vast versatility and flexibility of such phospholipid-bilayer membrane liposomes.

### *1.1.2 Pegylation of liposomes*

Pharmacokinetics of conventional liposomes, i.e. liposomes that consist of naturally occurring phospholipids and cholesterol, are characterized by a very high systemic plasma clearance. After intravenous administration, such vesicles are rapidly removed from the circulation by macrophages of the reticuloendothelial system, namely the liver, the spleen, and the bone marrow (Frank, 1993). The liposome half-life in the circulation can considerably be prolonged by incorporation of gangliosides (such as monosialoganglioside GM1 derived from bovine brain (Allen and Chonn, 1987)) or polyethylene glycol (PEG) derivatized lipids within the phospholipid bilayer of conventional liposomes (Papahadjopoulos et al., 1991; Woodle et al., 1992; Uster et al., 1996). Conventional liposomes coated with the inert and biocompatible polymer PEG are often referred to as 'sterically stabilized' liposomes. The PEG coating is believed to prevent binding of opsonins from physiological fluids such as plasma, which in turn avoids the recognition by phagocytotic cells (Moghimi and Patel, 1992). PEG phospholipids are safe and can be prepared synthetically at high purity and in large quantities, which has led to their acceptance for clinical applications. Animal and human studies (Gabizon et al., 2003) have demonstrated pronounced differences with respect to pharmacokinetic parameters between conventional and sterically stabilized PEG-liposomes: in humans, pegylation of liposomes resulted in a 50-fold decrease in plasma volume of distribution to a value similar to the plasma volume (from 200 to 4.5 liters), a

200-fold decrease in systemic plasma clearance (from 22 to 0.1 l/hour) and a nearly 100-fold increase in area under the time-concentration curve (Allen, 1994a). The apparent terminal half-life of PEG-liposomes reached up to 90 h in humans (Gabizon et al., 2003). The extended circulation half-life of sterically stabilized liposomes in combination with an increased permeability of tumor vasculature results in passive accumulation of PEG-liposomes in solid end-stage tumors (Gabizon and Papahadjopoulos, 1988). This principle of passive targeting to tumor tissue has been applied to commercial formulations of doxorubicin used for the chemotherapy of malignant Kaposi's sarcoma or breast cancer (Gabizon, 2001).

Aside from the effects described above, pegylation of liposomes offers an additional advantage. As it has been shown several times, incorporation of PEG derivatized lipids within the phospholipid bilayer provides liposomes with an enhanced stability (Allen, 1994b; Kirpotin et al., 1996; Mori et al., 1991). The underlying mechanism is in particular inhibition of membrane fusion, whereat PEG acts on three independent levels: First, inhibition of phospholipase C-induced liposome fusion, second, prevention of membrane apposition and third, stabilization of the lamellar phase (Basanez et al., 1997). These effects may act together and lead, along with formerly discussed items, to a remarkably enhanced lifetime of liposomal carrier systems *in vivo*.

## **1.2 IMMUNOLIPOSOMES**

### *1.2.1 Targeting using immunoliposomes: a new technology*

Long-circulating, sterically stabilized PEG-liposomes show minimal interactions with cells *in vitro* and not diseased tissues and organs *in vivo* and can be considered to be neutral and inert carriers for encapsulated molecules. They therefore provide a biologically inert and safe platform for the design of drug delivery systems. The organ



and tissue distribution of sterically stabilized liposomes can be modulated by conjugation of an appropriate targeting vector. Examples of such vectors include proteins, peptides, and small molecules such as the vitamin folate, which was used to target folate-receptor overexpressing tumor cells (Goren et al., 2000; Lee and Low, 1994). Pharmacokinetics therefore largely depend on the nature of the coupled targeting vector. Only the attachment of certain specific ligands makes liposomes targeted. Protein-conjugated liposomes have attracted a great deal of interest, principally because of their potential use as targeted drug delivery systems (Heath et al., 1983; Leserman et al., 1981) and in diagnostic applications (Kung et al., 1986; O'Connell et al., 1985). Examples of vectors include proteins such as Staphylococcus aureus protein A (Leserman et al., 1981), plant lectins and enzymes (Shek and Heath, 1983). However, the most commonly conjugated proteins are antibodies that lead to the denomination of “immunoliposomes”, represented schematically in Figure 2.

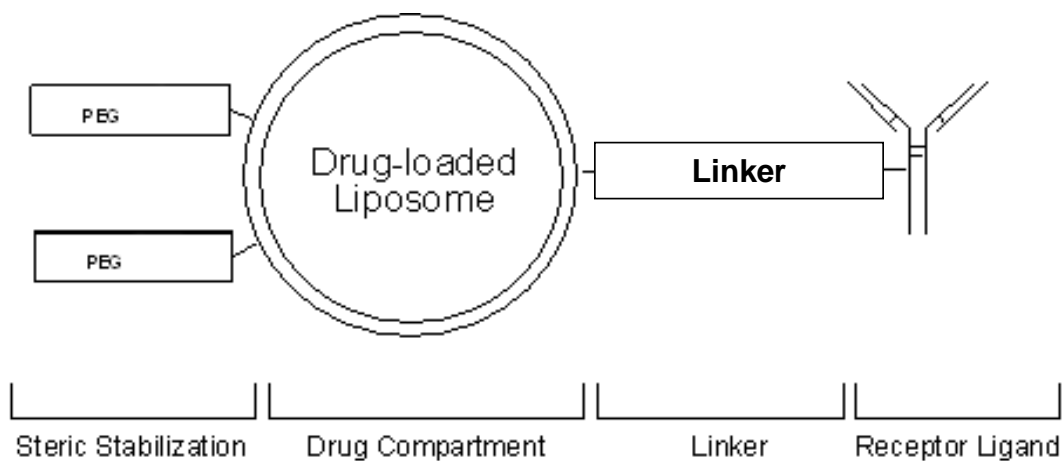


**Figure 2:** Schematic representation of an immunoliposome-based delivery system for *in vitro* and *in vivo* drug targeting. The design of immunoliposomes combines four different functional units responsible for steric stabilization *in vivo*, encapsulation of drug, targeting and linkage of a receptor-specific monoclonal antibody. Immunoliposomes are prepared by attachment of monoclonal antibodies via linker molecules to pegylated liposomes. PEG, polyethylene glycol.

Immunoliposomes consist of four different functional units:

- a) The inert and biocompatible PEG derivatized lipids incorporated in the phospholipid bilayer membrane of the liposome which provide steric stabilization or coating of the liposome surface.
- b) The liposome itself, acting as a container for several thousand molecules that can be incorporated.
- c) The linker molecule in order to combine steric stabilization of liposomes with efficient immuno-targeting by attaching a cell-specific ligand to the distal end of a few lipid-conjugated and in liposome bilayer anchored PEG molecules.
- d) The vector itself, responsible for the specific delivery.

With respect to brain drug delivery vectors, modified proteins or antibodies are used that undergo absorptive-mediated or receptor-mediated transcytosis through the blood-brain barrier. Examples of brain targeting vectors include cationized albumin, the OX26 monoclonal antibody to the rat transferrin receptor, or monoclonal antibodies to the insulin receptor (Pardridge, 1993; Wu et al., 1997).

Site-specific delivery of drugs to diseased cells can lead to increased therapeutic effects and to significant reductions of toxicity. Drug targeting by antibody-conjugated liposomes or immunoliposomes (Heath et al., 1980) represents a technology which has been applied for the targeting of specific sites of drug action such as the brain (Huwlyer et al., 1996), lungs (Maruyama et al., 1990a), cancer cells (Allen et al., 1995; Emanuel et al., 1996; Kirpotin et al., 1997; Moradpour et al., 1995; Nassander et al., 1992; Suzuki et al., 1995a), HIV-infected cells (Gagne et al., 2002; Zelphati et al., 1993) or cells of the immune system (Dufresne et al., 1999). Site-specific targeting is in particular mediated by the high affinity binding of monoclonal antibodies, i.e. the targeting vectors, to their specific antigens. The efficacy of the method depends first, on the target specificity of the vector and, second, on the cellular uptake and intracellular delivery of

the liposomal load. In addition, a sufficient stability in the circulation is in equal measure an essential requirement of those methods.

### *1.2.2 Targeting of small molecules – state of the art*

Immunoliposome-based drug delivery systems are of special interest for targeting of molecules that can not be coupled directly to a transport vector. This can be small drugs that have to achieve micromolar concentrations in a target tissue to reach a pharmacological effect (Carlsson et al., 2003; Wang and Low, 1998). Possible indications are the chemotherapy of neoplastic diseases as liposomal formulations of anthracycline antibiotics are often characterized by quantitative encapsulation and retention in liposomes (Lasic, 1996). The first clinical application of antibody-conjugated liposomes was a recent phase I trial in oncology (Matsumura et al., 2004). Doxorubicin encapsulated in long-circulating PEG-immunoliposomes was administered by 1-h infusions every 3 weeks in raising dose levels to 23 patients with metastatic or recurrent stomach cancer. The duration of the treatment period was between 48 and 135 days. The used targeting vector was a F(ab')<sub>2</sub> fragment of a cancer-reactive human monoclonal antibody (GAH), which showed high binding (with a positive ratio of > 90 %) to cells obtained from cancerous stomach tissues (Hosokawa et al., 2003). The antibody was grafted by a post-insertion method to the surface of PEG-liposomes. Stable disease (but no antitumor response) was observed in 10 out of 18 evaluable patients with a tolerance similar to Doxil, a doxorubicin formulation based on pegylated liposomes (Gabizon et al., 1994). This study is an impressive demonstration of the technical feasibility of the clinical application of antibody-conjugated liposomes. However, the pharmacological efficacy of this particular design of immunoliposomes

(where the antibody was conjugated to the surface of the liposome and not to the tip of the PEG chains) remains to be shown.

In addition to therapeutic applications, a possible future application of immunoliposomes might include their use as diagnostic tools to localize, for example, tumor tissue (Gabizon et al., 1994) or amyloid plaques in Alzheimer's Disease (Kurihara and Pardridge, 2000; Lee et al., 2002). Such applications rely on brain delivery of quantitative amounts of contrast agents such as magnetoferritin (Bulte et al., 1994) or gadolinium (Arnold and Matthews, 2002). Recent *in vivo* studies using a C6 glioma rat brain tumor model indicate that liposomal gadolinium might indeed be used for the visualization of tumor tissue by *in vivo* magnetic resonance imaging (MRI) (Saito et al., 2004). In these studies, gadolinium loaded liposomes were delivered to tumor tissue by convection-enhanced delivery, an invasive technique where drugs are infused under pressure into brain white matter (Bobo et al., 1994).

### 1.2.3 OX26 and the transferrin receptor

The murine monoclonal antibody to the rat transferrin receptor, the OX26 mAb, conjugated to pegylated liposomes, was used in first attempts to use liposomes for brain targeting (Huwyler et al., 1996). OX26 is shown to trigger receptor-mediated transcytosis through the blood-brain barrier upon binding to its target, the transferrin receptor, which mediates endocytosis of iron bound to the plasma glycoprotein transferrin. The transferrin receptor is a cell membrane-associated glycoprotein that serves as a gatekeeper in regulating cellular uptake of iron from transferrin, a plasma protein which transports iron in the circulation (Richardson and Ponka, 1997). Cellular iron uptake from transferrin is reasonably well understood, and involves the binding of transferrin to the transferrin receptor, internalization of transferrin within an endocytotic

vesicle by receptor-mediated endocytosis, and the release of iron from the protein by a decrease in endosomal pH (Ponka and Lok, 1999). It is a frequent statement in literature that only proliferating cells express the transferrin receptor excessively. However, there are many examples of non-proliferating cells that show high transferrin receptor expression, such as endothelial cells of the blood-brain barrier, Sertoli cells of the blood-testis barrier, hepatocytes, and trophoblast cells of the hemochorial type of placenta (Ponka and Lok, 1999).

The model of how transferrin receptors function in mediating cellular uptake of iron from transferrin is reproduced from Ponka and Lok (Ponka and Lok, 1999) and shown in Figure 3.

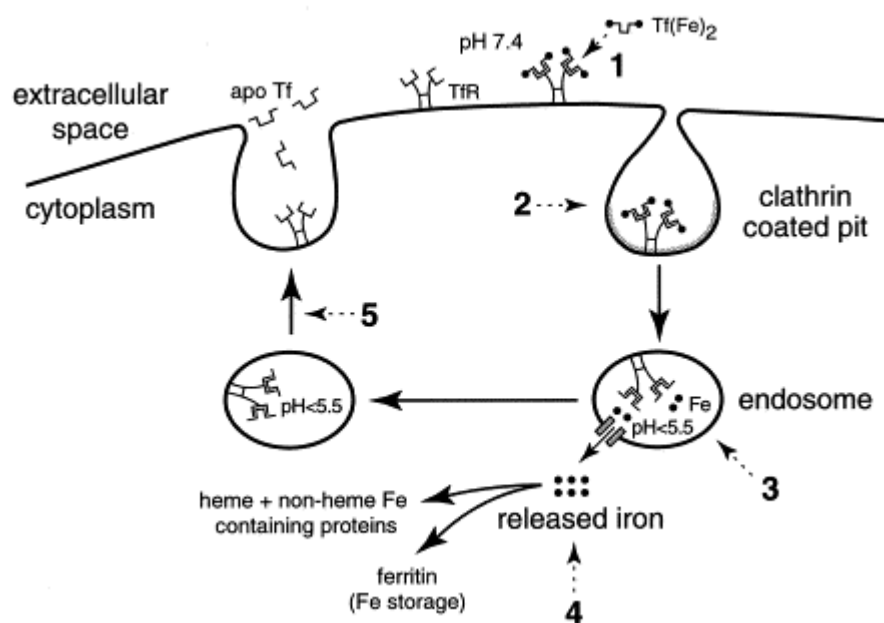


**Figure 3:** Schematic representation of iron uptake from transferrin via receptor-mediated endocytosis in mammalian cells. Tf, transferrin; TfR, transferrin receptor.

(1) In the first step, transferrin (Tf) attaches to the receptors on the cell surface by a physicochemical interaction. Bound transferrin receptor (TfR) complexes then cluster into clathrin-coated pits; (2) the transferrin receptor complexes, enclosed within

endocytic vesicles, are internalized by the cells. Transferrin receptor containing endosomes are diverted from lysosomes and this deflection prevents receptor degradation; (3) iron is released from transferrin within the endocytic vesicles. The low pH in endosomes (approximately 5.3) is conducive to iron release; (4) iron released from transferrin is then transported through the endosomal membrane; (5) the iron free apotransferrin, which remains attached to the receptor at pH ~5.5, returns to the cell surface, where the apotransferrin is released from the cells. Iron that is taken up by the cell can be used for metabolic functioning or it can be stored in ferritin.

Transferrin receptors are expressed in all cells, but their expression levels vary greatly (Ponka and Lok, 1999). On cells such as RBE4 cells, a receptor density of approximately 70000 receptors per cell has been described (Huwlyer et al., 1999). Receptor mapping studies using different antibodies to the human transferrin receptor have demonstrated binding to different organs and tissues in cynomolgus monkeys (Friden et al., 1996). The highest percentage of the injected dose of antibody was found in the brain where it bound almost exclusively to the parenchyma, indicating transcytosis over the blood-brain barrier. Quite interestingly, skeletal muscle as well showed a very high accumulation of antibody, compared to other tissues (Friden et al., 1996).

The OX26 monoclonal antibody was shown before to achieve a high degree of brain delivery. Following a single intravenous injection, 0.26 % of the injected dose per gram can be found in brain tissue at 60 min (Bickel et al., 1993) as a result of both a high blood-brain barrier PS product (i.e. blood-brain barrier permeability) as well as high plasma AUC (area under the curve) of the antibody. Using the internal carotid artery brain perfusion and capillary depletion technique (Triguero et al., 1990), it could be shown that the OX26 monoclonal antibody is transported across the blood-brain barrier by receptor-mediated transcytosis (Friden et al., 1996; Pardridge et al., 1991). *In vivo*,

brain uptake of the OX26 monoclonal antibody is not inhibited by endogenous transferrin despite the saturation of the BBB transferrin receptor (which has a KD of 6 nM) by the micromolar transferrin concentrations in plasma (Pardridge et al., 1987). This is due to the fact that the antibody recognizes a binding site on the transferrin receptor which is distant to the one of the natural ligand transferrin (Pardridge, 1995b).

Based on these findings, we decided to explore if the OX26 mAb to the rat transferrin receptor would bind to rat skeletal muscle, and if this antibody subsequently could serve as a targeting vector in a novel design of biotinylated immunoliposomes.

#### 1.2.4 *Antibody conjugation*

Different types of coupling strategies have been developed to attach proteins to phospholipids or pegylated phospholipids while preserving their biological activity. Covalent coupling to phospholipids can be achieved using amino-reactive homobifunctional cross-linkers (Hermanson, 1996; Torchilin et al., 1978) for example. Water-soluble carbodiimides can be used to catalyze the formation of an amide linkage between amines of the phospholipid headgroups and carboxyl moieties of proteins (Dunnick et al., 1975). Thiolated F(ab')<sub>2</sub> fragments and maleimidated phosphatidylethanolamine (Martin and Papahadjopoulos, 1982; Suzuki et al., 1995b) can be linked by disulfide bonds. A major drawback of the direct coupling of proteins to the liposome surface is the observation that the PEG chains may have a strong shielding effect that prevents the interaction between the bound receptor ligand and its receptor (Kaasgaard et al., 2001). In a liposome agglutination assay, as little as 0.72 mol % of PEG<sup>5000</sup>-phosphatidylethanolamine (PEG molecular mass 5000 Da) completely abolished the interaction between phospholipid-bound biotin and

streptavidin (Klibanov et al., 1991). The shielding effect also reduced target binding *in vivo* of immunoliposomes by up to 50 % and was highly dependent on PEG chain length (Mori et al., 1991). The effect of pegylation was less pronounced or not present for PEG molecular masses of 2000 or 750 Da.

As opposed to direct coupling to the phospholipid headgroup region on the liposome surface, ligands can be attached at the terminus of the PEG chains (Figure 4 A and 3 C). Thus, PEG is used as a spacer that results in a better accessibility and flexibility of the vector (Allen et al., 1995; Maruyama et al., 1995; Shahinian and Silvius, 1995). By this strategy, the immunoliposome target binding efficiency increases by a factor of two to three as well *in vitro* (Bendas et al., 1999) as *in vivo* (Maruyama et al., 1995). The PEG interactions associated with different coupling strategies and the dimensions of an immunoliposome are visualized in Figure 4.

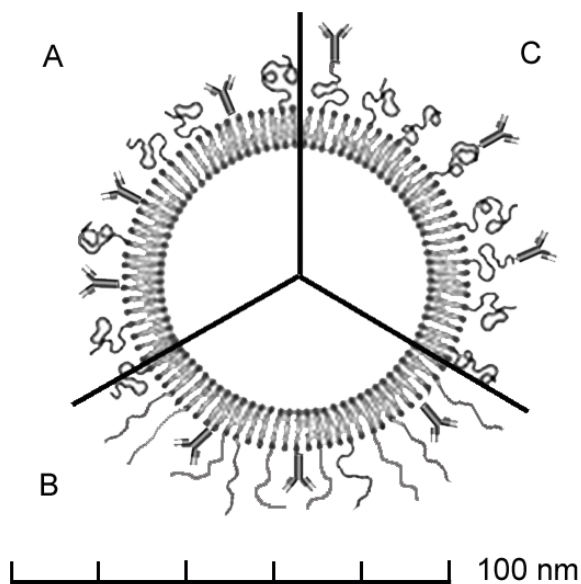


**Figure 4:** Schematic representation of a pegylated immunoliposome where the antibody is bound directly to the liposome surface (**A**) or to the distal tip of the PEG chains (**C**). The relative sizes are representative for a 80 nm liposome decorated with PEG<sup>2000</sup> (PEG of molecular weight 2000 Da). When attached to the liposome surface, steric hindrance between the PEG chains in their coiled (**A**) as well as extended (**B**) conformation and the antigen-recognition site of the antibody can be expected.



The minimal size of a unilamellar liposome is determined by the maximal tolerated proximity of the phospholipid headgroups imposed by the curvature of the inner leaflet. This minimal size is approximately 80 nm for liposomes that have as main constituents lecithin-analogs and cholesterol (New, 1990). Approximately 30 % of the inner volume of a 80 nm liposome are occupied by the phospholipid bilayer which thickness represents 4 - 5 nm. The hydrophilic PEG<sup>2000</sup> corona has a thickness of 5 nm as shown by electron microscopy (Bendas et al., 1999). By the same technique, the apparent dimensions of an antibody are determined to be in the range of 10 - 15 nm. Direct measurement of PEG tethered ligand-receptor interaction potentials confirms a thickness of 5 nm for PEG<sup>2000</sup> in its coiled state (Figure 4 A) and an overall length of an extended PEG<sup>2000</sup> chain of 15 nm (Wong et al., 1997) (Figure 4 B). These considerations emphasize that a corona of PEG<sup>2000</sup> substantially blocks the access of a surface-bound antibody to its epitope. This steric hindrance will further increase using PEG molecules of higher molecular weights.

Different techniques have been developed for the covalent binding of proteins to pegylated phospholipids by cleavable (i.e. disulfide) or metabolically stable (i.e. thioether, amide, or imide) linker strategies (Hansen et al., 1995; Huwyler et al., 1996; Maruyama et al., 1995; Shahinian and Silvius, 1995). In general, the choice of a specific coupling procedure is guided by practical considerations such as coupling efficiency and the need to retain the antigenicity of the coupled antibody despite the introduced chemical modifications. The target recognition by the coupled antibody may also depend on the orientation (i.e. random or defined) of the antibody or a Fab' on the liposome surface and the resulting accessibility of the antibody binding sites to their respective epitopes (Allen et al., 2002).

Covalent binding protocols rely generally on chemical reactive PEG phospholipid derivatives which are part of the phospholipid/cholesterol mix used for the synthesis of the PEG-liposomes. The liposomes are loaded with the drug, reduced in size and purified before the actual coupling procedure is performed by addition of the vector. The latter may undergo a chemical modification (i.e. chemical introduction of functional groups) before use. The disadvantage of such protocols is the observation that the efficiency of the coupling procedure is very difficult to control due to competing (hydrolytic) reactions.

In attempts to develop more reproducible and flexible coupling procedures that may be used for the large-scale production of immunoliposomes, alternative methods have been recently introduced (Iden and Allen, 2001; Tan et al., 2003).

Iden et al. (Iden and Allen, 2001) developed a postinsertion technique that involves the coupling of ligands to the terminus of PEG lipid derivatives in a micellar phase. At a later time point, the ligand-coupled PEG lipids are transferred into the bilayers of preformed liposomes during a simple incubation step (1 hour at 60°C). The final product is purified by size exclusion chromatography (SEC). Therapeutic effect, cytotoxicity and binding of immunoliposomes prepared by the postinsertion technique were comparable to the ones of immunoliposomes made by a conventional coupling technique (Allen et al., 2002).

In the present work the OX26 murine monoclonal antibody (mAb) to the rat transferrin receptor (Jefferies et al., 1985) has been used as vector. As mentioned, this antibody has been shown to bind to an extracellular epitope on the receptor, at a site removed from the transferrin binding site (Pardridge, 1995b). In cultured cells, such as the RG2 rat glioma cell line, the immortalised rat brain capillary endothelial RBE4 cell line, and the L6 cell line derived from rat skeletal muscle, receptor mediated endocytosis and

thus intracellular accumulation of the OX26 mAb as well as OX26 conjugated liposomes is observed (Huwyler et al., 1997).

We presented in this work a new coupling procedure for the preparation of pegylated immunoliposomes. A biotinylated PEG phospholipid (bio-PEG-DSPE) is used for a non-covalent (biotin-streptavidin) method of attachment of the OX26 mAb to sterically stabilized liposomes (Schnyder et al., 2004).

### **1.3 NON-COVALENT STREPTAVIDIN-BIOTIN BINDING METHOD**

We have designed a linker lipid, DSPE-PEG-biotin (distearoylphosphatidylethanolamin-PEG-biotin), based on a common phospholipid with two (saturated) fatty acids (stearoyl). The phosphatidyl moiety was linked to a PEG molecule and a biotin molecule, being attached on its tip (Figure 5 B). This biotinylated linker lipid was introduced into the liposome lipid-bilayer during fabrication. Preformed and purified biotin-PEG-liposomes are subsequently simply mixed with the streptavidin-conjugated antibody to result immediately in a quantitative coupling. The biotin-streptavidin interaction is among the strongest non-covalent affinities known and is characterized by a dissociation constant of about  $1.3 \times 10^{-15}$  M. One streptavidin molecule has four biotin binding sites. Consequently, excess binding sites on the streptavidin molecule need to be blocked by free biotin to avoid cross-linking and thus aggregation of the biotinylated immunoliposomes. The biotin is coupled at the PEG terminus that allows optimal target recognition of the bound mAb (Figure 5 A). Coupling of a streptavidin-conjugated antibody is simple, rapid and highly reproducible. Streptavidin conjugated OX26 mAb was used since streptavidin has a much lower isoelectric point (pI 5 - 6) as compared to the highly basic pI of 10 of avidin.

In addition, streptavidin is not a glycoprotein and that reduces its potential for binding to carbohydrate receptors (Hermanson, 1996). Both factors reduce the amount of nonspecific binding and thereby the systemic clearance *in vivo* (Kang and Pardridge, 1994).

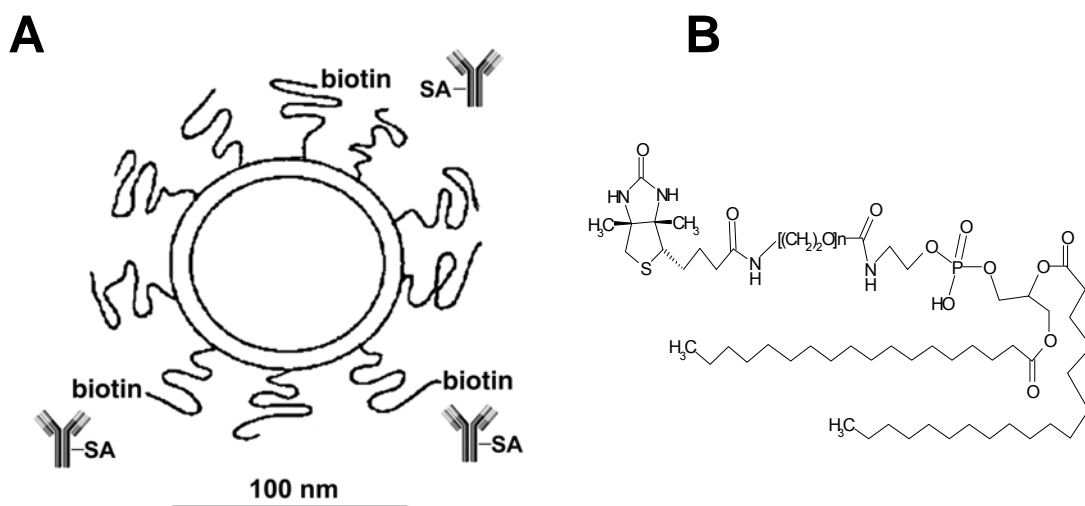


**Figure 5:** Preparation of OX26-immunoliposomes by coupling of streptavidin-conjugated OX26 mAbs to biotinylated PEG-liposomes (A), and chemical structure of bio-PEG-DSPE, the biotinylated linker phospholipid (B). There are approximately 5500 strands of PEG of molecular mass 2000 Da attached to the liposome surface, of which approximately 30 carry a biotin group at their distal end. SA, streptavidin.

#### 1.4 LOADING OF LIPOSOMES

The use of immunoliposomes as drug delivery systems requires adequate techniques for the generation of unilamellar vesicles and for the encapsulation of drugs and macromolecules. With respect to drug loading, several methods have been described. Whereas first attempts relied on passive entrapment methods with low loading efficiencies. Recent methods make use of more efficient strategies such as loading by transmembrane ion gradients (i.e. a pH or specific salt gradient).

Passive entrapment can be done by hydration of dried phospholipids. Liposomes are prepared in presence of the molecule of interest followed by purification of the liposomes and their separation from nonincorporated material by gel-filtration chromatography (Torchilin and Weissig, 2003). Lipophilic or amphiphilic drugs will thereby partition into the lipid bilayer which leads to a quantitative and efficient loading of the liposomes.

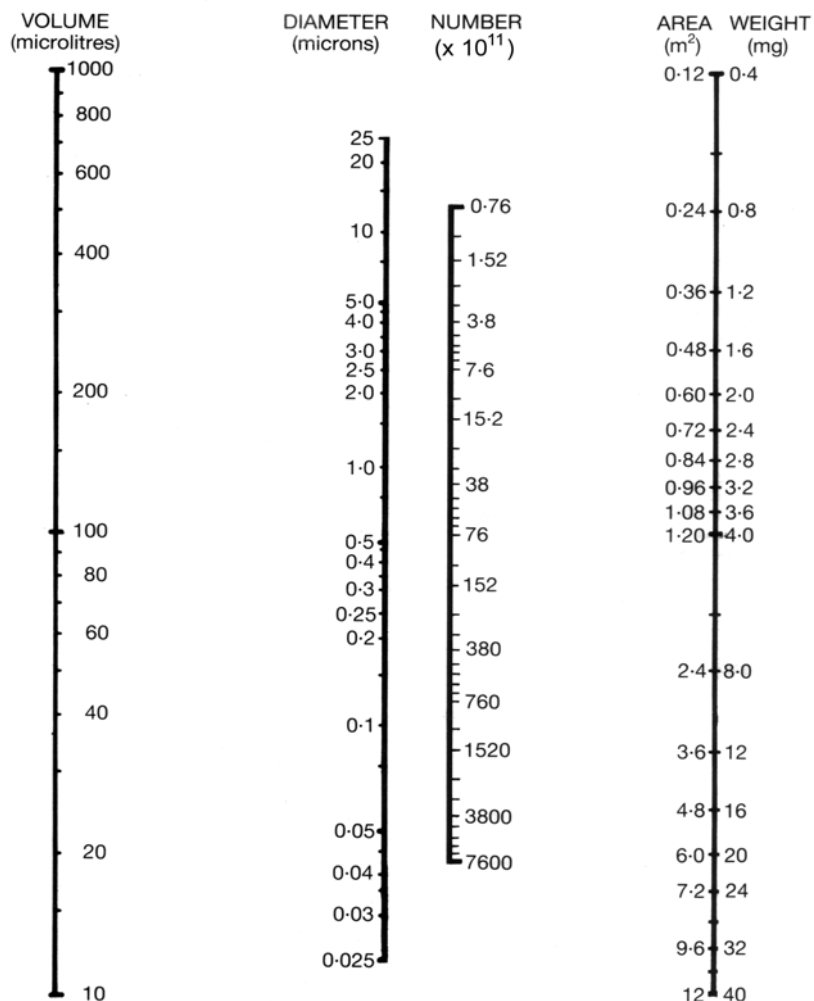


**Figure 6:** Nomogram relating theoretical captured volume, diameter, number, area, and lipid weight of unilamellar liposomes. To read the nomogram, two known parameters are connected by a straight line and the unknown parameter where this line intersects the third scale is read off. The calculation is based on the assumption that the phosphatidyl choline headgroup occupies an area of the membrane bilayer of  $42 \text{ \AA}^2$ . Note: the smallest possible diameter for an unilamellar liposome is on theoretical grounds 25 nm.

For water-soluble compounds, which partition into the aqueous phase of the lumen of the liposome, the amount of entrapped drug is directly proportional to the initial drug concentration used in the incubation mix and the total inner volume of the resulting liposomes. The latter depends on liposome diameter, and lipid concentration and can be related to these parameters using a nomogram (Figure 6) (New, 1990). Because the inner volume of liposomes represents only a small percentage of the whole liposome suspension, the efficiency of this method is low and a considerable amount of (expensive) material is not incorporated and therefore lost. This can be illustrated based on theoretical considerations with the help of the nomogram in Figure 6: liposomes with a diameter of 100 nm that are prepared using 4 mg of lecithin will have an outer surface of 1.2 m<sup>2</sup>. These  $6 \times 10^{13}$  liposomes will capture a theoretical volume of as little as 15  $\mu$ l. One single 100-nm liposome will be made up of approximately 150000 phospholipid molecules assuming that the phosphatidyl choline headgroup occupies an area of the membrane bilayer of 42 Å<sup>2</sup>.

The loss of hydrophilic biological macromolecules such as proteins, plasmids and enzymes during the passive loading process can be reduced using highly concentrated liposomal solutions. Solutions of preformed liposomes are thereby concentrated by ultrafiltration or partial lyophilization. The molecule of interest is added and incorporated into the liposomes by several freeze-thaw cycles. The freezing and thawing is used to rupture and re-fuse the liposomes, during which time the solute equilibrates between the inside and outside. This method has been used recently. For example, to incorporate DNA into neutral liposome formulations (Shi and Pardridge, 2000). Disadvantages of this method are the poor entrapment stability (i.e. leakage of the encapsulated molecules after dilution and purification of the liposomes) and influences on size and heterogeneity of the preformed liposomes (Lasic et al., 1995).

The remote (active) loading of drug molecules into preformed liposomes is generally a very efficient loading technique and can result in a sustained incorporation of small molecules. The underlying principle is the use of pH or ion gradients to create an electrochemical potential across the phospholipid-bilayer of the liposome that in turn leads to active uptake and entrapment of a given drug within the liposome. The gradient is generated by a two-step process: after preparation of liposomes in a buffer of a certain pH and ion strength, the external medium is exchanged by size exclusion chromatography (Goren et al., 2000; Hwang et al., 1999; Lasic et al., 1995). This method has been applied with success to small, weakly basic molecules such as doxorubicin and vincristine. Under appropriate conditions, they precipitate as a gel within the liposome (Lasic et al., 1995). This leads to quantitative uptake with incorporation efficiencies approaching 100 % as well as a stable retention within the liposome. It is important to note that the use of such liposomal formulations greatly enhances the carrying capacity of the coupled vector. For example, approximately 28000 small molecules of daunomycin can be packed within a single 100-nm liposome and can be directed to a target tissue using just a few conjugated antibodies (Huwylar et al., 1996). Thus, antibody to drug ratios of 1000 are possible using 100-nm immunoliposomes. This value is in sharp contrast to the 1:1 ratios obtained by individual attachment of drugs to a targeting vector (Pardridge, 1995b).

In general, the choice, the optimization, and the validation of a specific loading technique may be a complex problem depending on the physico-chemical properties of a given drug. To assess suitability of a liposome-based drug delivery system for *in vivo* use, careful *in vitro* tests should be performed to evaluate loading efficiency, loading capacity and stability of entrapment upon large dilutions in physiological fluids.

## 1.5 CLINICAL USE OF IMMUNOLIPOSOMES

Recent phase I clinical trials with immunoliposomes (Matsumura et al., 2004) demonstrate that liposome-based targeting technologies have the potential to find their way from the bench to the bedside. Formulations of pegylated liposomes have been on the market for many years. We now have the technologies at hand (using efficient coupling strategies for vectors such as post-insertion techniques (Allen et al., 2002) and biotin-streptavidin coupling strategies (Schnyder et al., 2004)) to expand the use of such liposomal formulations to the targeted delivery of drugs to organs and tissues. Once produced, liposomal formulations should be applied immediately or within short periods of time to minimize leakage of the liposomal content. As discussed earlier, remote loading techniques are available for selected drugs which are characterized by high loading efficiencies and a stable retention of the transported drug within the liposomal carrier. However, loading of peptides, plasmids and DNA is in general still problematic and expensive due to the low efficiency of entrapment.

Lyophilization may be an alternative to stabilize liposomal formulations and to minimize storage in a dissolved and diluted state. A formulation kit for doxorubicin composed of lyophilized liposomes was developed recently by Stevens et al. (Stevens and Lee, 2003), providing a strategy to expand the shelf-life of liposomal formulations.

With respect to any targeting of liposomes, the success of this as well as any other physiological and non-invasive targeting strategy will depend on the availability of efficient and specific targeting vectors. For instance in the field of brain targeting, there does not exist an 'ideal' brain vector to date. Such a molecule would have to recognize a target which is expressed exclusively at the brain capillary endothelium, would not compete with endogenous ligands, and would be transported with high efficiency across the blood-brain barrier by receptor-mediated transcytosis. The transferrin receptor, to



name a well characterized example, is expressed in several other organs than the brain. As a consequence, targeting of immunoliposomes coupled to anti-transferrin receptor antibodies is not confined solely to the brain. Other organs such as the liver (Huwlyer et al., 1997) or skeletal muscle (Schnyder et al., 2004) are recognized as well. It is therefore tempting to speculate that in the future the design of immunoliposomes using alternative brain delivery vectors (such as antibodies directed at the insulin receptor) (Slepushkin et al., 1997; Stevens and Lee, 2003) might allow for higher targeting efficiencies bringing this technology to its full potential.

## **1.6 GENE TARGETING**

Gene therapy is a promising technique for correcting defective genes responsible for certain diseases. This technique has attracted more and more attention in the last few years. One of the most challenging difficulties dealing with this advanced therapeutic strategy is how to bring a certain gene to the desired site of action and, within the target tissue to the nucleus of a diseased cell. However, due to limits of current technology, this is a very ambitious goal. Above all, it is very difficult to deliver a gene exclusively to the site of disease in order to reduce side effects and exposure to healthy tissue. This is of special importance when it comes to the treatment of CNS diseases.

Past strategies have often used direct intracerebral implantation of a therapeutic gene by means of a viral vector, such as adenovirus or herpes simplex virus. However, this provokes an inflammatory response and demyelination in many animals and virtually all humans (Herrlinger et al., 1998; Kajiwara et al., 2000). The incorporation of DNA in the interior of stealth immunoliposomes would therefore inhibit such immune reactions due

to viral antigens and, additionally, prevent supercoiled plasmid DNA from degradation by ubiquitous nucleases *in vivo*.

Complexes between cationic lipids and DNA are often used to transfect cultured cells or tissues. An application of this technology for *in vivo* gene delivery is problematic because DNA-cationic liposome form micrometer-scale aggregates, particularly at lipid to DNA ratios where the overall charge of the complex is neutral (Radler et al., 1997). As a consequence, their pharmacokinetics and tissue distribution is characterized by a very short plasma half-life (i.e. a few minutes in a mouse) and an unspecific accumulation in different organs (Osaka et al., 1996). Microautoradiography of tissue samples at 24 h after injection of cationic lipid-DNA complexes revealed uptake of expression-plasmid DNA in cells of the reticuloendothelial system, i.e. alveolar macrophages, hepatic Kupffer cells, and macrophages of the spleen. DNA uptake per tissue occurred in this, as well as in other studies, significantly higher in the lung (up to 1000 fold) than in the liver or spleen (Liu et al., 1997). It is tempting to speculate that the efficient transfection of lung tissue might be a direct consequence of quantitative first-pass filtration of particulate DNA-lipid aggregates in the lung.

An alternative to DNA/cationic liposome complexes is the use of neutral liposome formulations. The DNA is thereby encapsulated within the liposome. The neutral liposome can be pegylated and subsequently coupled to a targeting vector. Such a targeted gene delivery system is characterized by a high stability of the encapsulated DNA under physiological conditions and a prolonged circulation half-life *in vivo* (Shi and Pardridge, 2000; Zhang et al., 2002a). Several studies have demonstrated that exogenous gene expression in the brain can be achieved using such a gene-delivery system: Shi et al. (Shi et al., 2001a; Shi and Pardridge, 2000) incorporated an expression plasmid coding for either  $\beta$ -galactosidase or luciferase in the interior of pegylated OX26-immunoliposomes. *In vivo* gene expression was shown at 2 - 6 days

after a single intravenous administration. Similar expression plasmids were incorporated into PEG-immunoliposomes which were targeted to the rhesus monkey brain *in vivo* with a monoclonal antibody to the human insulin receptor (HIR) by Zhang et al. (Zhang et al., 2003b). Widespread neuronal expression of the  $\beta$ -galactosidase gene in primate brain was demonstrated after 48 hours (Figure 7).

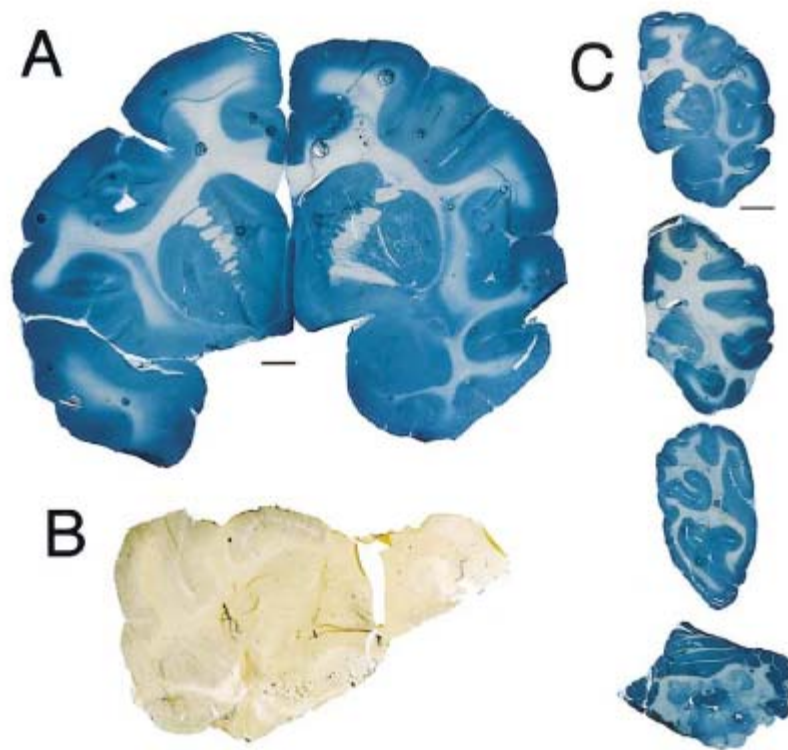


**Figure 7:**  $\beta$ -galactosidase histochemistry of brain removed from either the HIRmAb-immunoliposomes injected rhesus monkey (**A** and **C**) or the control, uninjected rhesus monkey (**B**). The plasmid DNA encapsulated in the immunoliposomes is the pSV- $\beta$ -galactosidase expression plasmid driven by the SV40 promoter. (**A**) Reconstruction of the 2 halves of a coronal section of the forebrain. (**C**) Half-coronal sections through the primate cerebrum and a full coronal section through the cerebellum; the sections from top to bottom are taken from the rostral to caudal parts of brain. All specimens are  $\beta$ -galactosidase histochemistry without counter-staining. The magnification in panels **A** and **B** is the same and the magnification bar in panel **A** is 3 mm; the magnification bar in panel **C** is 8 mm. HIRmAb, monoclonal antibody to human insulin receptor.

The tissue specificity of gene expression in a given target tissue can be further enhanced by the combined use of such a gene targeting technology and tissue-specific gene promoters. In a recent study (Shi et al., 2001b),  $\beta$ -galactosidase exogenous expression plasmids under the control of either the unspecific simian virus 40 (SV40) promoter or by a brain-specific promoter (taken from the 5' flanking region of the GFAP gene), were incorporated in pegylated immunoliposomes and injected intravenously into mice. The used targeting vector was a monoclonal antibody against the mouse transferrin receptor (8D3 mAb). The expression in mice of the  $\beta$ -galactosidase gene was restricted to brain tissue in experiments where the  $\beta$ -galactosidase gene was under the control of the brain-specific GFAP promoter.

In contrast, immunoliposomes loaded with expression plasmids controlled by the unspecific SV40 promoter caused  $\beta$ -galactosidase expression in all transferrin receptor rich organs, i.e. brain, liver, spleen and lung. Several studies indicate that gene expression in the brain following immunoliposome-based gene therapy may translate to pharmacological effects *in vivo*. OX26-immunoliposomes were used to normalize tyrosine hydroxylase activity in an animal model of Parkinson's disease (Zhang et al., 2003a), which did result in reversal of apomorphine-induced rotation behavior in 6-hydroxydopamine-lesioned rats.

In another study, the immunoliposome-mediated gene targeting technology was used for brain delivery of a therapeutic gene in a human brain tumor model consisting of scid mice implanted with intracranial U87 human glial brain tumors (Zhang et al., 2004). The expression plasmid did encode a short hairpin RNA directed at a nucleotide sequence within the human epidermal growth factor receptor (EGFR). The used targeting vectors were the murine 83-14 mAb to the human insulin receptor and the rat 8D3 mAb to the mouse transferrin receptor. This intravenous RNA interference gene therapy resulted in silencing of EGFR expression in tumor cells both *in vitro* as well as *in vivo* leading to a

significant increase in survival time of mice with implanted brain tumors. The pharmacological effect on brain cancer cells *in vivo* provides evidence that macromolecules such as plasmid DNA can be delivered across consecutive series of biological barriers that included in the discussed gene therapy studies the blood-brain barrier, the plasma membrane of the target cells within the brain tissue and the nuclear membrane (Zhang et al., 2003b).

## 2 AIMS OF THE THESIS

Specific drug delivery using immunoliposomes is an innovative promising approach to target pharmaceuticals to diseased tissues and organs. It was the aim of the work presented here:

1. To optimize and characterize an immunoliposome based drug delivery system using a novel antibody linker technology.
2. To test *in vitro* uptake of drugs incorporated within immunoliposomes by specific target cells, such as rat muscle cells or rat glioma cells. The transported drugs can be small molecules or macromolecules such a DNA plasmids for gene therapy.
3. To investigate uptake, intracellular fate and endosomal release of the liposomal carrier system, using technologies such as confocal microscopy, ESR spectroscopy, molecular biological and biochemical methods.
4. To determine if such a delivery translates to a pharmacological effect *in vitro* by incorporating a cytotoxic substance (daunomycin) or an expression plasmid into the immunoliposomal carrier system.
5. To characterize *in vivo* the pharmacokinetics and tissue distribution of this immunoliposome based drug delivery system after i.v. injection into the rat.

### 3 MATERIALS AND METHODS

#### 3.1 MATERIALS

Dioleoylphosphatidylethanolamin (DOPE), Cholesteryl hemisuccinate (CHEMS), 1-palmitoyl-2-oleoyl-sn-glycerol-3-phosphocholine (POPC), Cholesterol, and Distearoylphosphatidylcholine (DSPC) were from Sigma (St. Louis, MI). Pegylated distearoylphosphatidylethanolamine (PEG-DSPE) was purchased from Avanti Polar Lipids (Alabaster, AL). Didodecyldimethylammoniumbromide (DDAB), was from Fluka Chemie (Buchs, CH). For conjugation of the OX26 mAb to the liposome, a biotin-derivatized linker lipid was used which consists of a bifunctional 2000-Da polyethylene-glycol (PEG) that contains a lipid on one end (distearoylphosphatidylethanolamine (DSPE)) and a biotin molecule at the other end. Biotinylated PEG-DSPE (bio-PEG-DSPE) was custom synthesized by Shearwater Polymers (Huntsville, AL). 5(6)-Carboxyfluorescein was purchased from Acros Organics (Geel, Belgium), Sephadex G-75 and Sephacryl S-200 High Resolution were from Amersham Pharmacia Biotech (Uppsala, Sweden). Cy2-conjugated secondary antibody was from Jackson Laboratories (West Grove, PA). Biotin-labeled with fluorescein was from Pierce (Rockford, IL). The IgG<sub>2a</sub> anti-rat transferrin receptor OX26 monoclonal antibody (MRC OX-26) (Jefferies et al., 1985) was harvested from cell-culture supernatants of the OX26 hybridoma cell line and was purified by protein G Sepharose affinity chromatography as described (Kang and Pardridge, 1994). The OX26 mAb was thiolated using 2-iminothiolane (Traut's reagent) (Sigma) as described previously (Huwyler et al., 1996) by conversion of one primary amine per mAb and then linked to streptavidin (Sigma) by activation of the latter with m-maleimidobenzoyl-N-hydroxysuccinimide ester (MBS) (Pierce, Rockford, IL). Unspecific mouse IgG<sub>2a</sub> isotype monoclonal antibody was from Sigma. (Yoshikawa and Pardridge,

1992). The protein concentration was quantified by the Pierce BCA Protein Assay (Pierce, Rockford, IL) using bovine serum albumin (Sigma, St. Louis, MO) as reference. Equipment for electrophoresis, such as Novex® 4 - 20 % Tris-Glycine polyacrylamide gels, pre-stained protein standard SeeBlue Plus2, running buffer, reducing and non-reducing buffer and the XCell II Mini Cell electrophoresis apparatus were from Invitrogen (Carlsbad, CA). The GelCode® Blue Stain Reagent was from Pierce (Rockford, IL). Centrifree® MPS micropartition devices for separation of biotin bound to OX26 mAb from free biotin, were from Millipore (Bedford, MA) and [<sup>3</sup>H]Biotin was from Amersham Pharmacia Biotech. [<sup>3</sup>H]Daunomycin (16 Ci/mmol) was from PerkinElmer Life Sciences (Wellesley, MA). Daunomycin was from Merck (Darmstadt, FRG). The Bright-Glo™ Luciferase Assay System and luciferase expression vectors were from Promega (Madison, WI). β-galactosidase plasmid DNA, pcDNA™3.1/myc-His/lacZ, was purchased from Invitrogen (Carlsbad, CA), phosphorothioate oligonucleotides-labeled at the 5'-end with Cy3 was synthesized by Microsynth AG (Balgach, CH). DNase I for digestion of not incorporated DNA was from Roche Diagnostics (Rotkreuz, CH). Lipofectamine for gene transfection was from Gibco-BRL (Paisley, Scotland), Plus™ reagent was purchased from Invitrogen (Carlsbad, CA). Sulforhodamine for sulforhodamine B assay was from Fluka (Buchs, CH). For tissue solubilization, Soluene-350 was purchased from Packard (Meriden, CT). The spin labels 4-Amino-2,2,5,5,-tetramethyl-3-imidazoline-1-yloxy (AT) and 2-Heptadecyl-2,3,4,5,5,-pentamethylimidazolidine-1-yloxy (HP) and were purchased from Magnostech GmbH (Berlin, FRG).

All other chemicals were of analytical grade and were obtained from commercial sources.



## **3.2 METHODS: PREPARATION AND CHARACTERIZATION OF A NOVEL LIPOSOMAL CARRIER SYSTEM**

### *3.2.1 Synthesis of streptavidin-conjugated OX26 mAb*

The OX26 mAb (1.65 mg, 11.2 nmol) was thiolated by using a 20:1 molar excess of 2-iminothiolane (Traut's Reagent) as described previously (Huwyler et al., 1996). By this procedure a single thiol reactive group is introduced into the OX26 mAb. In parallel with the antibody thiolation, streptavidin (2 mg, 33 nmol) was dissolved in 200  $\mu$ l 0.1 M phosphate buffered saline (PBS) (100 mM phosphate, 150 mM sodium chloride, pH 7.4) and activated by using a 20:1 molar excess of m-maleimidobenzoyl-N-hydroxysuccinimide ester (MBS, Pierce, Rockford, IL) (Hermanson, 1996). After incubation for 1 h at room temperature with gentle shaking, the reaction mix was purified by Sephadex G-75 gel filtration chromatography and UV detection at 280 nm. The thiolated antibody was conjugated to the activated streptavidin at a molar ratio of 1:3 (OX26:streptavidin) by incubation over night at room temperature and gentle shaking. The reaction products were purified by Sephacryl S-200 gel filtration chromatography and OX26-containing samples were detected by absorbance measurements at 280 nm. The protein concentration was quantified by the Pierce BCA Protein Assay (Pierce, Rockford, IL) using bovine serum albumin (BSA) as reference. OX26-streptavidin was stored in 0.01 M PBS (10 mM phosphate, 150 mM sodium chloride, pH 7.4) at -20°C.

### *3.2.2 Gel electrophoresis*

Purified peak samples of OX26 mAb conjugated to streptavidin were prepared for electrophoresis under reducing and non-reducing conditions. 5  $\mu$ l of samples were

mixed with 10  $\mu$ l of reducing or non-reducing buffer, respectively, and denatured at 90°C for 5 min. A Novex® 4 - 20 % Tris-Glycine polyacrylamide gel (Invitrogen, Carlsbad, CA) was loaded with two concentrations (2  $\mu$ l and 10  $\mu$ l) of each sample and with a pre-stained protein standard (SeeBlue Plus2, Invitrogen, Carlsbad, CA) to determine molecular mass and consequently identify the reaction products. One-dimensional vertical gel electrophoresis was performed according to the method of Laemmli (Laemmli, 1970) by using the XCell II Mini Cell apparatus (Invitrogen, Carlsbad, CA). Novex® Tris-Glycine Running Buffer from Invitrogen (Invitrogen, Carlsbad, CA) was used for electrophoresis (2 h, 34 mA, 200 V), to identify fractions that contain streptavidin-coupled, uncoupled, and aggregated antibody fractions. The gel was stained for 1 hour in (Coomassie) GelCode® Blue Stain Reagent (Pierce, Rockford, IL) and washed.

### 3.2.3 *Biotin binding assay*

Binding of [<sup>3</sup>H]biotin to the neutral streptavidin-OX26 conjugate was determined by an ultrafiltration method using Centrifree® MPS micropartition devices (Millipore, Bedford, MA) containing a low-adsorptive hydrophilic membrane with a 30 kDa exclusion. The binding measurements were performed in a final volume of 1 ml of 10 mM PBS containing 0.1  $\mu$ Ci of [<sup>3</sup>H]biotin and unlabeled biotin at concentrations ranging from 16 to 500 nM. The assay was initiated by the addition of neutral streptavidin-OX26 to a final concentration of 32 nM. Samples were incubated for 15 min at 37°C and unbound biotin was separated from the bound fraction by centrifugation (10 min at 1250 x g, 3 times). The percentage of unbound biotin in the filtrates was determined by liquid scintillation counting (Packard beta counter, Downers Grove, IL).

### 3.2.4 *Preparation of liposomes*

DSPC (4.2  $\mu\text{mol}$ ), cholesterol (1.8  $\mu\text{mol}$ ), PEG-DSPE (0.24  $\mu\text{mol}$ ) and linker lipid (bio-PEG-DSPE, 0.66 nmol) were dissolved in chloroform. A lipid film was prepared by vacuum evaporation using a Rotavapor (Büchi, CH). Dried lipid films were hydrated at 40°C in PBS or, in case of drug loading by pH gradient, in 0.1 M citrate buffer respectively, such that a final lipid concentration of 4.4 mM was achieved. Lipids were dispersed by addition of glass beads and gentle agitation. Lipids were subjected to 5 freeze-thaw cycles followed by extrusion (6 times) at room temperature through a 200 nm pore-size polycarbonate membrane employing an extruder (Avestin, Ottawa, Canada). Extrusion was repeated 9 times using a 100 nm polycarbonate membrane. Mean vesicle diameters were 150 nm as determined by dynamic light scattering using a Zetasizer 4 Particle Analyzer (Malvern Instruments, Worcestershire, UK).

### 3.2.5 *Loading of immunoliposomes by pH gradient*

Loading of liposomes with [ $^3\text{H}$ ]daunomycin was done via a pH gradient (Mayer et al., 1986) as described elsewhere (Huwlyer et al., 1996). Dried lipids were rehydrated in 0.1 M citrate buffer pH 4.0 (4.4  $\mu\text{mol}$  of lipid). By addition of NaOH, the pH of the external buffer was raised to at least pH 7.1. [ $^3\text{H}$ ]daunomycin (5  $\mu\text{l}$ , 1  $\mu\text{Ci}/\mu\text{l}$ ) and Daunomycin (880 nmol) was added and the incubation mix was incubated for 10 min at 53°C. External buffer was exchanged by passing the liposomes over a Sephadex G-75 column and eluting with 0.001 M PBS (0.001 M Na-phosphate, 0.15 M NaCl, pH 7.4). Aliquots of column eluates were analyzed by scintillation counting. Efficiency of entrapment of daunomycin was determined by analysis of the column elution profiles. Fractions containing daunomycin loaded biotinylated liposomes were used immediately for conjugation with streptavidin-linked OX26 mAb by addition of antibody (using a

molar ratio of bio-PEG-DSPE:OX26-streptavidin of 1:1). Excess biotin-binding sites on the OX26-streptavidin vector were blocked before coupling to the biotinylated liposomes, using free biotin (in a molar ratio of OX26-streptavidin:biotin of 1:1) in order to minimize cross-linking and thus precipitation of immunoliposomes as described earlier (Schnyder et al., 2004). In cases of IgG<sub>2a</sub>-coupled immunoliposomes, the same procedure was performed with a streptavidin-linked IgG<sub>2a</sub> mAb.

The average number of bio-PEG-DSPE molecules and thus mAb bound per liposome, was calculated to be 30, assuming that one 100 nm liposome contains 100000 phospholipid molecules (Hansen et al., 1995).

#### 3.2.6 *Passive loading of immunoliposomes*

The passive entrapment method was performed for DNA, fluorescent markers and all other drugs. Dried lipids were hydrated in 0.01 M or 0.001 M PBS pH 7.4 containing the corresponding material to be incorporated. Lipids were subjected to five freeze-thaw cycles, followed by extrusion through a 200 nm and 100 nm pore-size membrane, as described before (3.2.4).

#### 3.2.7 *Preparation of pH-sensitive liposomes*

pH-sensitive liposomes were prepared following the protocol as for conventional liposomes. DOPE (7  $\mu$ mol), CHEMS (3  $\mu$ mol) and linker lipid (bio-PEG-DSPE, 3.15 nmol) were dissolved in chloroform. A lipid film was prepared by vacuum evaporation using a Rotavapor (Büchi, CH). Dried lipid films were hydrated at 40°C in PBS such that a final lipid concentration of 10 mM was achieved. Lipids were dispersed by addition of glass beads and gentle agitation. Lipids were subjected to 5 freeze-thaw cycles followed by extrusion (6 times) at room temperature through a 200 nm pore-size polycarbonate

membrane employing an extruder (Avestin, Ottawa, Canada). Extrusion was repeated 9 times using a 100 nm polycarbonate membrane.

### 3.2.8 *Preparation of fluorescent biotinylated OX26-immunoliposomes*

DSPC (5.2  $\mu\text{mol}$ ), cholesterol (4.5  $\mu\text{mol}$ ), PEG-DSPE (0.3  $\mu\text{mol}$ ) and linker lipid (bio-PEG-DSPE, 0.015  $\mu\text{mol}$ ) were dissolved in chloroform. A lipid film was prepared by vacuum evaporation using a Rotavapor (Büchi, CH). Dried lipid films were hydrated at 40°C in 0.01 M PBS, such that a final lipid concentration of 10 mM was achieved. For the preparation of carboxyfluorescein filled immunoliposomes, the dried lipids were hydrated in 0.01 M PBS containing 0.1 mM 5(6)-carboxyfluorescein. Lipids were subjected to 5 freeze-thaw cycles followed by extrusion (5 times) at room temperature through a 100 nm pore-size polycarbonate membrane employing an extruder (Avestin, Ottawa, Canada). Extrusion was repeated 9 times using a 50 nm polycarbonate membrane. Mean vesicle diameters were 150 nm as determined by dynamic light scattering using a Zetasizer 4 Particle Analyzer (Malvern Instruments, Worcestershire, UK).

Buffer was exchanged for 10 mM PBS by applying the liposome suspension to a 1.6 x 20 cm Sephadex G-75 column. Aliquots of column eluates were analyzed by on-line absorbance measurements at 280 nm. Fractions containing fluorescent biotin-liposomes were used immediately for conjugation with streptavidin linked OX26 mAb by addition of antibody (bio-PEG-DSPE:OX26-streptavidin = 1:1, molar ratio). Excess biotin binding sites on the OX26-streptavidin vector were blocked prior to coupling to the biotinylated liposomes using free biotin (OX26-streptavidin:biotin = 1:1, molar ratio) in order to minimize cross-linking and thus precipitation of immunoliposomes. The average number of biotin-PEG-DSPE and thus bound mAb per liposome was

calculated to be 30 assuming that one 100 nm liposome contains 100000 phospholipid molecules (Hansen et al., 1995).

### **3.3 METHODS: IN VITRO ASSAYS AND RESULTS**

#### *3.3.1 Cell-cultures*

Early passages of L6 cells (ATCC catalog No. CRL-1458) (Mandel and Pearson, 1974) were obtained from ATCC (Manassas, VA) and were grown using Dulbecco's Modified Eagle Medium (DMEM, Gibco-BRL) supplemented with 4 mM L-glutamine, 1.0 mM sodium pyruvate, 4.5 g/L glucose, 1.5 g/L sodium bicarbonate, 10 % heat-inactivated fetal calf serum (FCS), 100 µg/ml streptomycin and 100 units/ml penicillin G (all Gibco-BRL, Paisley, Scotland). They were characterized with respect to transferrin receptor expression by Hyde et al. (Hyde et al., 2002) and others.

Passages between 30 and 40 of the immortalised rat brain capillary endothelial RBE4 cell line were used for toxicology experiments. The immortalized rat brain microvessel endothelial cell line was kindly provided by Neurotech SA (Orsay, France). RBE4 cells were cultured as described (Huwyler et al., 1999). They were characterized with respect to transferrin receptor (Huwyler et al., 1999) and P-glycoprotein (Begley et al., 1996) expression. The cells were grown in a culture medium consisting of  $\alpha$ -minimal essential medium ( $\alpha$ MEM) and Ham's F-10 (1:1 vol/vol), supplemented with 2 mM glutamine, 10 % heat-inactivated FCS, 1 ng/ml bFGF (basic fibroblast growth factor), 100 µg/ml streptomycin and 100 units/ml penicillin G (all Gibco-BRL, Paisley, Scotland). The experiments were conducted 2 - 4 days after seeding when the cells reached 70 - 100 % confluence.

RG2 cells (ATCC catalog No. CRL-2433) expressing the transferrin receptor (Nakano et al., 1996) were grown using Ham's F-12 medium supplemented with 10 % heat-inactivated fetal calf serum FCS, 100 µl/ml streptomycin and 100 units/ml penicillin G (Gibco-BRL, Paisely, Scotland). This cell line does not reach a confluence of 100 %, cells start to detach at approximately 60 % confluence.

### 3.3.2 *Immunohistochemistry*

For immunohistochemistry of skeletal rat muscle tissue, fresh rat muscle tissue fragments were transferred to plastic moulds (Tissue-Tek Cryomould, Miles, Torrance, CA), embedded in Tissue-Tek OCT reagent and were frozen immediately in a mixture of isopropanol and dry ice. Samples were kept at -70°C until use. Sections (6 µm) of the frozen OCT-embedded tissue samples were made using a HM560 cryostat (Microm, Volketswil, CH), mounted on uncoated coverslips, dried for 24 hours at room temperature, fixed with ice-cold 4 % paraformaldehyde for 20 min and washed with PBS. All subsequent incubations were done using PBS containing 3 % FCS to reduce unspecific binding. Sections were incubated with mAb OX26 (125 µg/ml) for 30 min at room temperature, washed with PBS containing 3 % FCS and incubated with rabbit Cy2 secondary anti-mouse antibody (Jackson Laboratories, West Grove, PA) for 1 hour (1:200 dilutions of antibody). Fluorophor protector (FluorSafe Reagent, Calbiochem, San Diego, CA) was added to the sections, slides were sealed and analyzed by confocal microscopy using a Zeiss LSM 510 confocal microscope. Control experiments done in parallel did include incubations with secondary antibody only. Alternatively, the primary OX26 mAb was substituted by an unspecific mouse monoclonal IgG<sub>2a</sub> isotype control antibody.

### 3.3.3 *Immunocytochemistry and uptake experiments*

Cell surface expression of the transferrin receptor as well as intracellular accumulation of the OX26 mAb by L6 and RG2 cells was visualized by immunostaining experiments: L6 and RG2 cells were grown on chamber slides (Nalge Nunc, Naperville, IL). In order to visualize surface expression of the transferrin receptor, cells were incubated on ice for 30 min with the OX26 mAb (50 µg/ml). Cellular uptake and intracellular accumulation of the OX26 mAb was visualized by incubations for 30 min at 37°C under cell-culture conditions with OX26 mAb (30 µg/ml). Cells were washed and fixed for 20 min with ice-cold 4 % paraformaldehyde, permeabilized by incubation for 5 min at room temperature with 0.5 % Triton X-100 in PBS, transferred for 15 min at room temperature to PBS containing 3 % FCS and incubated with rabbit Cy2 secondary anti-mouse antibody (Jackson Laboratories) for 1 hour (Cerletti et al., 2000). All incubations with antibody were done using PBS containing 3 % FCS to reduce unspecific binding. Cells were mounted in FluorSafe Reagent (Calbiochem, San Diego, CA) and analyzed by confocal microscopy (Leica TCS NT confocal microscope). Control experiments performed in parallel did include incubations with secondary antibody only, or the use of an unspecific mouse monoclonal IgG<sub>2a</sub> isotype control antibody.

Uptake experiments with OX26-conjugates (i.e. OX26 conjugated to streptavidin or not pH-sensitive OX26 immunoliposomes) were performed with L6 and RG2 cells grown on chamber slides (Nalge Nunc). Fluorescent OX26-immunoliposomes (carrying 70 µg/ml of bound OX26 mAb) or biotin-fluorescein bound to OX26-streptavidin (70 µg/ml) in 10 mM PBS were diluted with one volume of cell-culture medium. Incubations with cells were done for 1 hour at 37°C. Competition experiments were done in presence of 200 µg/ml of OX26 after 15 min pre-incubation of the cells with the free OX26. Cells of



control experiments were incubated with normal growth medium, representing background fluorescence of the cells. Cells were washed four times with ice-cold 10 mM PBS and fixed (20 min at 4°C) using 200 µl of 4 % paraformaldehyde. Cells were washed and mounted using FluorSafe Reagent (Calbiochem). Slides were sealed and analyzed by confocal fluorescence microscopy (Leica TCS NT confocal microscope).

#### 3.3.4 *Endosomal release of propidium iodide*

Confocal microscopy studies using RG2 cells were performed to investigate endosomal release and accumulation of propidium iodide to the cytosol. Cells were grown onto chamber slides (Nalge Nunc) until they reached a confluence of 50 %. Cells were incubated with not pH-sensitive immunoliposomes consisting of DSPC and linker lipid only, or pH-sensitive immunoliposomes (33.3 µg/ml OX26-streptavidin). Liposomes were filled preliminary with propidium iodide by the freeze-thaw technique and mixed 1:1 with cell-culture medium. Cells were incubated for 1, 3 or 24 hours at 37°C, liposomes were either removed after 3 hours or left on cells till the end of the experiment. Cells were washed, fixed for 20 min at 4°C using 4 % paraformaldehyde as described before and were mounted in FluorSafe Reagent (Calbiochem). Confocal microscopy was performed with a Leica TCS NT inverted fluorescent microscope (Leica). (Excitation = 544 nm; emission = 603 nm).

#### 3.3.5 *Microscopy*

Tissue sections and L6 cells of Figure 13 were analysed with a Zeiss LSM 510 inverted scanning confocal microscope using 20 x and 40 x Zeiss Plan-Neofluor lenses with a numerical aperture of 0.5 and 1.3, respectively. A 488 nm argon laser was used in combination with fluorescein bandpass filters. Optical sections of 5.3 µm (muscle

tissue) or 1.4  $\mu\text{m}$  (L6 cells) were acquired and processed on a silicon graphics workstation (Silicon Graphics, Mountain View, CA, USA) using Zeiss software.

All other confocal microscopy images were recorded with a Leica TCS NT confocal microscope (Leica) using 25 x and 40 x Plan Fluotar or 63 x Plan Apochromat oil immersion objectives with numerical apertures of 0.75, 1.0 and 1.32, respectively. Optical sections of 0.7 - 1  $\mu\text{m}$  were analyzed using the Imaris software (Bitplane AG, Zurich, CH) and processed using Photoshop software (Adobe Systems, Mountain View, CA).

### 3.3.6 *DNA incorporation into immunoliposomes*

Immunoliposomes were synthesized by using a total of 40  $\mu\text{mol}$  of lipids, including 37.6  $\mu\text{mol}$  of 1-palmitoyl-2-oleoyl-snglycerol-3-phosphocholine (POPC), 0.8  $\mu\text{mol}$  of didodecyldimethylammoniumbromide (DDAB), 1.2  $\mu\text{mol}$  of distearoylphosphatidylethanolamine (DSPE-PEG), and 12 nmol of DSPE-PEG-maleimide, as described by Shi et al. (Shi et al., 2001b) with minor modifications: 400  $\mu\text{g}$  DNA (pGL3-Basic Luciferase Vector (Promega),  $\beta$ -galactosidase plasmid DNA (pcDNA<sup>TM</sup>3.1/myc-His/lacZ, Invitrogen, Carlsbad, CA) or Cy3-labeled phosphorothioate oligonucleotides (Microsynth AG, Balgach, CH) were encapsulated in the pegylated liposomes by the passive freeze-thaw method. Dried lipid film was resuspended in PBS containing the DNA to be incorporated, following the same protocol as for fabrication of carboxyfluorescein-filled immunoliposomes (3.2.8). There are two methods to remove not incorporated DNA from liposomes. That is the enzymatic method where exteriorized DNA is degraded by nuclease digestion, and the mechanic, more gentle method of purification by size exclusion chromatography (SEC). If not mentioned otherwise,

exteriorized DNA was removed by the mechanic SEC method, using a 1.6 cm x 20 cm Sephadex G-75 column. Fractions containing biotinylated liposomes were used immediately for conjugation with streptavidin-linked OX26 mAb by addition of antibody (using a molar ratio of bio-PEG-DSPE:OX26-streptavidin of 1:1). Excess biotin-binding sites on the OX26-streptavidin vector were blocked, before coupling to the biotinylated liposomes, using free biotin (in a molar ratio of OX26-streptavidin:biotin of 1:1) in order to minimize cross-linking and thus precipitation of immunoliposomes. The average number of OX26 mAbs conjugated to one liposome was 30 as described before.

### 3.3.7 *Confirmation of DNA incorporation into liposomes*

To confirm the presence of DNA in the liposome fraction, original DNA liposome samples were analyzed by agarose gel electrophoresis prior and after to size exclusion chromatography. Experiments were done with a pGL3-Basic Luciferase Vector (Promega). Biotinylated PEG-immunoliposomes were formulated in a total volume of 1 ml Tris/HCl pH 8.5 prior to gel purification, using 20  $\mu$ mol of lipids and 200  $\mu$ g of plasmid DNA. 650  $\mu$ l were subjected to DNase I (Roche Diagnostics, CH) treatment to digest not incorporated DNA. DNase I treatment was done in the presence of 68  $\mu$ l 50 mM MgCl<sub>2</sub> and 10 U RNase free DNase I (10 U/ $\mu$ l), during 1 hour at 37°C and stopped by addition of EDTA at a final concentration of 7 mM. As control for the DNase I digest, 10  $\mu$ g of not liposomal plasmid DNA (pCDNA3.1-lacZ plasmid, 8.5 kb) in an equal volume of Tris/HCl pH 8.5 were treated under identical conditions. Liposome samples were analyzed directly or purified by SEC with or without DNase I digest. For DNA extraction, pCDNA3.1-lacZ plasmid and pGL3 containing immunoliposomes were subjected to phenol/chloroform extraction and precipitated with ethanol/acetate using glycogen as a carrier in order to achieve maximal DNA recovery. In the case of SEC

purified samples, as well peak fractions, as post-peak fractions were analyzed. The DNA pellets were resuspended in 17  $\mu$ l of 10 mM Tris/HCl pH 7.5 and linearized by restriction digest with Xho I. The restriction digest was supplemented with 25 % gel loading buffer, and aliquots of the DNA were analyzed by electrophoresis on a 0.8 % agarose gel with subsequent ethidium bromide staining.

### 3.3.8 *Liposomal administration of pGL3 expression vector*

pGL3 expression experiments were carried out according to Shi et al. (Shi et al., 2001b) with minor modifications: Liposomes were composed of POPC, DDAB, DSPE-PEG and DSPE-PEG-biotin and prepared according to the standard protocol (3.3.6). The DNA content of the liposomes was calculated as approximately 10 % of the initial amount of DNA added to the suspension (assumption of internal unpublished data), that is about 40  $\mu$ g per 40  $\mu$ mol lipid, according to published data (Shi et al., 2001b; Zhang et al., 2002a). 40  $\mu$ g plasmid DNA in a liposome volume of 1 ml before column purification results in approximately 0.01  $\mu$ g/ml after column purification (estimated dilution factor). RG2 and L6 cells were cultured in a 24-well plate (2.0 cm<sup>2</sup>/well) and incubated with approximately 0.4  $\mu$ g of liposomal DNA per well for 24 and 48 hours prior to analysis with the bright glow reagent (Promega, Madison, WI) according to manufacturer's protocol (Bright-Glo™ Luciferase Assay System, Promega). Lipofectamine transfected cells were used as positive controls which were transfected with 5  $\mu$ g of the plasmid and 2  $\mu$ l of lipofectamine (Gibco-BRL, Paisley, Scotland). In brief, 5  $\mu$ g of plasmid were diluted to a total volume of 25  $\mu$ l DMEM. 8  $\mu$ l of Plus™ reagent (Invitrogen) for pre-complexing DNA was added and incubated 15 min at room temperature before mixing with 2  $\mu$ l lipofectamine in 50  $\mu$ l DMEM that was incubated likewise 15 min at room temperature. After another 15 min incubation at room temperature, 300  $\mu$ l of

transfection mix and 500  $\mu$ l of opti-Mem (Gibco-BRL) per well were placed on cells for 6 hours at 37°. Transfection mixture was replaced with 1.5 ml complete growth medium supplemented with 150  $\mu$ l PBS per well. Transfected cells were harvested 24 and 48 h after transfection for analysis of cellular luciferase activity by the Bright-Glo™ Luciferase Assay System (Promega), according to manufacturer's protocol. Cells were lysed for 2 hours with Glo Lysis Buffer and 20  $\mu$ l of the lysate were transferred on a 96-well plate and mixed with 100  $\mu$ l Bright-Glo™ Assay Regent (n = 2 for each well). Plates were immediately placed in a TECAN fluorescence and luminescence plate reader (Spectrafluor plus, TECAN, Männedorf, CH), and peak light emission was measured at 20°C for 2 s and recorded as relative light units.

### 3.3.9 *Expression of $\beta$ -galactosidase in RG2 cells*

Gene expression experiments were performed with a  $\beta$ -galactosidase exogenous expression plasmid under the control of the unspecific SV40 promoter (pcDNA™3.1/myc-His/lacZ, invitrogen, Carlsbad, CA). RG2 cells were grown on purified coverslips placed in 12-well cell-culture plates in the normal cell growth medium. The surface area was 3.8 cm<sup>2</sup>/well. The experiments were conducted 2 - 3 days after seeding when cells reached a confluence higher than 50 %. RG2 cells were incubated for 24 or 48 hours with  $\beta$ -galactosidase expression plasmid filled immunoliposomes, medium or, the negative control, with unconjugated liposomes loaded with plasmid. The amount of liposomes per well was 13.3 pmol, and accordingly 399 pmol OX26-streptavidin (30 antibodies per liposome). In order to confirm experimental proceeding, RG2 cells were transfected with  $\beta$ -galactosidase expression plasmid DNA using lipofectamine (Gibco-BRL, Paisley, Scotland) according to the manufacturer's protocol. In brief, 5  $\mu$ g of the plasmid was diluted to a total volume of 25

$\mu$ l DMEM. 8  $\mu$ l of Plus<sup>TM</sup> reagent (Invitrogen) for pre-complexing DNA and enhancing cationic lipid-mediated transfection of DNA into cultured adherent eukaryotic cells, was added and incubated 15 min at room temperature before mixing with 2  $\mu$ l lipofectamine in 50  $\mu$ l DMEM that was incubated likewise 15 min at room temperature. After another 15 min incubation at room temperature, 300  $\mu$ l of transfection mix and 500  $\mu$ l of Opti-Mem (Gibco-BRL) per well were placed on cells for 6 hours at 37°. Transfection mixture was replaced with 1.5 ml complete growth medium supplemented with 150  $\mu$ l PBS per well. The transfected cells were harvested 24 and 48 h after transfection for analysis of mRNA expression and newly synthesized protein.

Cells were washed 3 times with PBS, fixed and incubated overnight at 37°C in X-Gal solution (1 mg/ml X-gal, 2 mM MgCl<sub>2</sub>, 5 mM K<sub>4</sub>Fe(CN)<sub>6</sub> and 5 mM (K<sub>3</sub>Fe(CN)<sub>6</sub> in PBS pH 7.3). When lipofectamine transfected control cells reached sufficient staining intensity (after 2 - 24 h), cells were washed again 2 x with PBS.

#### *3.3.10 Uptake of liposomal, labeled oligonucleotides by RG2 cells*

In order to confirm gene uptake and intracellular distribution of administered liposomal cargo in RG2 cells, fluorescent Cy3-labeled phosphorothioate oligonucleotides ((Cy3)5'-CAGATCCTCTTCTGAGATGAGTTTTTGTTC-3', Microsynth AG, Balgach, CH) were incorporated into OX26-conjugated immunoliposomes and incubated with RG2 cells. RG2 cells were grown in 12-well cell-culture plates in normal growth medium. The surface area was 3.8 cm<sup>2</sup>/well. The experiments were conducted 2 - 3 day after seeding, when cells reached a confluence higher than 50 %. RG2 cells were incubated for 1, 24 or 48 h either with liposomes that were filled with labeled oligonucleotide or with medium only, as negative control. Liposomes were coupled to OX26 mAb (immunoliposomes) or, as additional negative control, kept in unbound, unspecific

original state alternatively. The amount of liposomes per well was 13.3 pmol, and accordingly 399 pmol OX26-streptavidin (30 antibodies per liposome). The transfected cells were washed 1, 24 and 40 h after transfection, fixed for 30 min at 4°C using 4 % paraformaldehyde and stored in 0.1 % sodium azide until fluorescent microscopy analysis. In order to visualize every cell, 4',6-Diamidino-2-phenylindole (DAPI) was used. DAPI staining is one of the most frequently used nucleic acid stains; it binds to the minor groove of DNA at AT-rich sequences.

Microscopy was performed with a Zeiss Axioplan fluorescent microscope with common epifluorescence equipment. Excitation at 565 nm and emission at 552 nm was provided by optics intended for Cy3.

#### 3.3.11 *In vitro* IC<sub>50</sub> determination of daunomycin

LD<sub>50</sub> were defined as the concentration of daunomycin deleting 50 % of the cells. LD<sub>50</sub> were determined for RG2 and for RBE4 cells. Serial dilutions of daunomycin in normal cell growth medium were used at 0.001, 0.01, 0.1, 1, 10 and 100 µM daunomycin. All cell lines were seeded in 96-well microplates and experiments were performed when cells reached 50 – 70 % confluency and divided into control and treatment groups (n = 6). Controls were treated with same volume of solvents without any treatment. RG2 cells between passage 35 and 40 and RBE4 cells between passages 25 and 35 respectively, were incubated for 3, 6 and 24 hours with according serial daunomycin dilutions. After indicated incubation times, cells were washed with PBS and kept in normal growth medium until analysis. When all incubation times were performed (24 h), cell viability (% of control) was determined by the sulforhodamine B (SRB) assay.

### 3.3.12 Cellular uptake of liposomal [<sup>3</sup>H]daunomycin

The immortalized rat brain microvessel endothelial cell line RBE4 was kindly provided by Neurotech SA (Orsay, France). For uptake experiments, cells between passages 25 and 35 were seeded at a density of  $10^4$  -  $10^5$  cells/cm<sup>2</sup> into 24-well cell-culture plates. The surface area was 2 cm<sup>2</sup> per well. The cells were grown in culture medium described above for 3 - 4 days until they reached confluence. For uptake assays, cells were incubated for one or three hours respectively with [<sup>3</sup>H]daunomycin (free drug, 0.375 μCi/well) or [<sup>3</sup>H]daunomycin loaded immunoliposomes (5.5 pmol liposomes, 165 pmol OX26-streptavidin, 0.2 μCi/well). Where pre-incubation is indicated, cells were incubated preliminary with 200 μg free OX26 per well for 15 min. Cells were washed after the incubation using ice-cold PBS, detached from the cell-culture plate by incubation with 250 μl trypsin-EDTA (0.05 % and 0.02 % (w/v)) and subsequently transferred to scintillation vials. 2 ml of scintillation fluid (Ultima Gold by Packard BioSciences, Meriden, CT) were added, cells were solubilized overnight and the amount of radiolabeled substrate taken up by the cells was quantified by scintillation counting.

### 3.3.13 Pharmacological effects of daunomycin loaded immunoliposomes on RBE4 cells

Toxicology experiments were performed using the immortalised rat brain capillary endothelial RBE4 cell line. RBE4 cells were cultured as described (Huwyler et al., 1999). For pharmacological effect studies, cells between passages 30 and 40 were seeded into 96-well plates. The cells were grown in a culture medium as described above. The experiments were conducted 2 - 4 days after seeding when the cells reached 70 - 100 % confluence. For pharmacological effect experiments, cells were incubated 45 min at 37°C with free OX26 where pre-incubation is indicated. Pre-



incubated and other cells were incubated for 1 or 3 hours respectively with 1 or 5  $\mu\text{M}$  of free or liposomal daunomycin (1  $\mu\text{M}$  and 5  $\mu\text{M}$ ). Cells were washed two times with PBS and incubated for another 48 h in fresh culture medium, before sulforhodamine B assay was conducted.

#### *3.3.14 Sulforhodamine B assays for determination of daunomycin cytotoxicity*

The protocol used for the SRB assay was similar to that previously described by Skehan et al. (Skehan et al., 1990). Cell layers were washed and fixed to the well bottoms by adding 20  $\mu\text{l}$  of cold 50 % trichloroacetic acid (TCA) to the 200  $\mu\text{l}$  of medium in each well (final concentration 5 %) and incubating the plate at 4°C for 1 h. The wells were then drained, rinsed five times with pure water, and air dried at 37°C. 0.4 % (w/v) sulforhodamine B (SRB) in 1 % glacial acetic acid was then added (100  $\mu\text{l}$ /well), and the plate incubated for 15 min. Unbound dye was drained and removed by washing four times with 1 % glacial acetic acid. After air drying the plate, the dye was solubilized by adding 100  $\mu\text{l}$ /well of 10mM Tris base, pH 10.5, and swirling for 5 min. Absorbance at 562 nm was measured on a microtiter plate reader (SOFTmax Pro, Molecular devices, California).

### **3.4 METHODS: IN VIVO ASSAYS AND RESULTS**

#### *3.4.1 Pharmacokinetics and tissue delivery of (immuno) liposomes in the rat*

Pharmacokinetic experiments were performed as described (Bittner et al., 2003) by cannulating the right jugular vein of male Wistar rats for blood sampling. Surgery was performed under 10 mg/kg xylazine and 90 mg/kg ketamine anaesthesia two days before the experiment. During the study, the freely moving animals were kept individually in

plastic metabolism cages. All rat experiments were performed in accordance with the current Swiss legislation on the welfare of experimental animals.

In brief, the right jugular vein of male rats was cannulated and injected with 0.001 M PBS containing 20  $\mu\text{Ci}/\text{kg}$  (specific activity: 16 Ci/mmol) of free [ $^3\text{H}$ ]daunomycin, [ $^3\text{H}$ ]daunomycin loaded pegylated liposomes (biotinylated or not) and [ $^3\text{H}$ ]daunomycin loaded OX26- or IgG<sub>2a</sub>-immunoliposomes. The injected dose of monoclonal antibodies and lipids was always  $\leq 100 \mu\text{g}$  per rat and  $\leq 2 \mu\text{mol}$  per rat, respectively. Blood samples were collected via the jugular vein catheter at 2, 5, 10, 15, 30 and 60 min after intravenous injection of the isotope. After 60 min, the animals were anesthetized with isofluorene, decapitated and brain, lung, spleen, heart, liver, kidney, testes and muscle tissue was collected. The plasma (50  $\mu\text{l}$  aliquots) and organ samples (approximately 0.2 g) were weighted, solubilized with Soluene-350 (Packard, Meriden, CT) and neutralized with glacial acetic acid before liquid beta-scintillation counting. Pharmacokinetic parameters such area under the plasma concentration curve ( $\text{AUC}_{0-t}$ ), clearance (CL) or half-live ( $T_{1/2}$ ) were calculated by non-compartmental data analysis of plasma concentrations (percent injected dose (%ID) per ml plasma) using WinNonlin 4.1 software (Pharsight, Mountain View, CA).

The tissue volume of distribution ( $V_D$ ) of the [ $^3\text{H}$ ]daunomycin sample at 60 min after i.v. injection is defined as the amount of drug in tissue (%ID per g tissue) divided by the concentration of drug (%ID/ml) in terminal phase. The tissue clearance (i.e. organ permeability surface area (PS) product) was determined as:

$$PS = \frac{[V_D - V_0]C_p(T)}{\int_0^t C_p(t) dt},$$

where  $C_p(T)$  = the terminal plasma concentration and  $V_0$  = the organ volume distribution of a plasma volume marker, i.e. sterically stabilized liposomes (biotinylated

PEG-liposomes) (Huwyler et al., 1996). Organ uptake was expressed as %ID/g tissue and was calculated from:  $\%ID/g(t) = PS \times AUC_{0-t}$  (Pardridge, 1995b). It is important to note that tissue levels of [<sup>3</sup>H]daunomycin were solely determined by radiolabel analysis. We can thus not distinguish between the parent drug and possible metabolites.

### 3.4.2 *Statistics*

Statistical tests were performed using excel software (Microsoft). Multiple groups at the same time point were compared using ANOVA. The difference between two groups was tested using Student's t test for single comparison. The level of significance was set at  $p < 0.05$ .

## 4 RESULTS

### 4.1 CHARACTERIZATION AND OPTIMIZATION OF A NOVEL LIPOSOMAL CARRIER SYSTEM

#### 4.1.1 Synthesis of streptavidin-conjugated OX26 mAb

A novel design of biotinylated immunoliposomes was tested, where a streptavidin-conjugated targeting vector, OX26 mAb, is attached to the surface of the liposome using a PEG spacer (Figure 5). PEG-liposomes containing in addition pegylated phospholipids with a biotin molecule coupled to the top (bio-PEG-DSPE), can be used for the non-covalent conjugation of a streptavidin-conjugated ligand. In the present study, streptavidin was chemically combined with the OX26 mAb by using MBS as a hetero-bifunctional cross-linker reactive for primary amines in streptavidin.

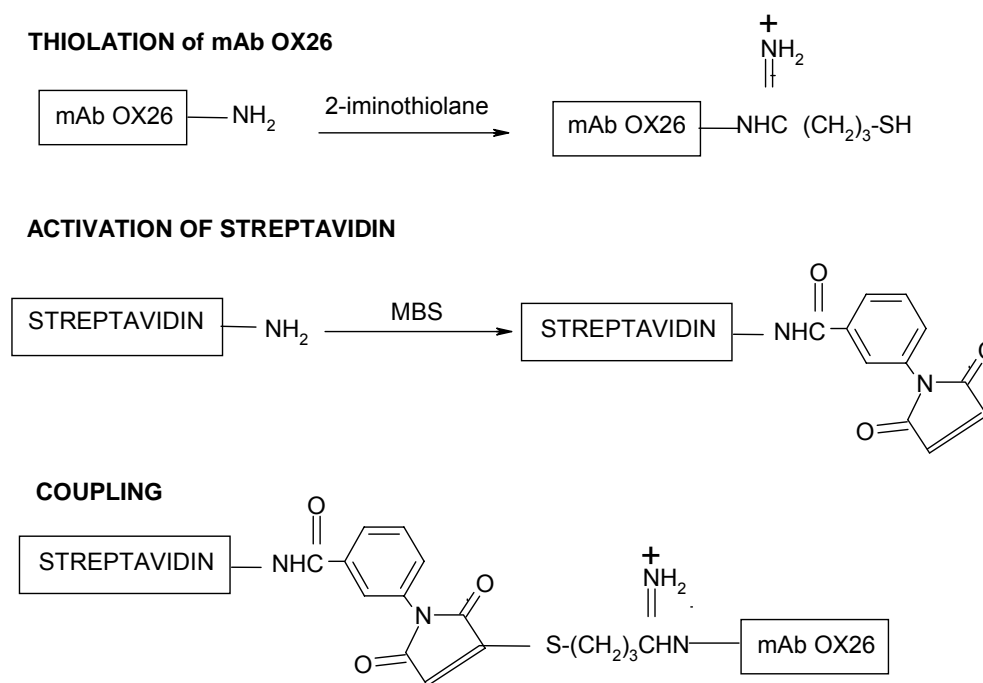


**Figure 8:** Coupling reaction by the use of MBS as cross-linker reactive and introduction of a single thiol group into the antibody via Traut's reagent (2-iminothiolane).

The amine-containing streptavidin is first modified via the N-hydroxysuccinimide ester end of MBS (its most reactive functional group) to create a stable amide bond. The derivative at this point contains reactive maleimide groups able to couple with the available sulfhydryl groups of a second molecule (New, 1990). A single thiol group was introduced into the OX26 mAb by thiolation with Traut's reagent (2-iminothiolane) to achieve this reaction and complete the coupling of OX26 to streptavidin. The three steps of the coupling reaction with MBS and Traut's reagent are shown in Figure 8.

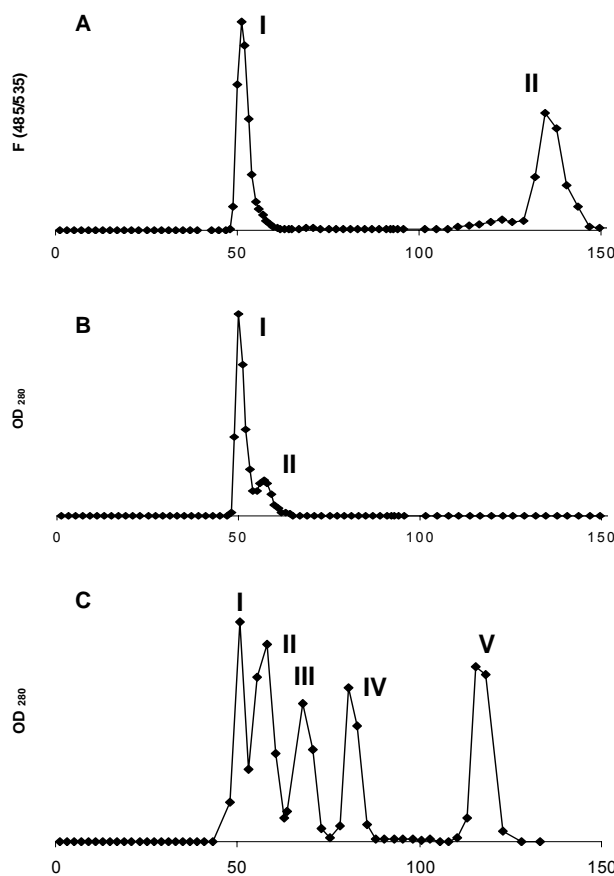


**Figure 9:** (A) Elution profile by fluorescence detection (excitation wavelength of 485 nm; emission wavelength of 535 nm) of OX26-streptavidin (I) labeled with an excess of fluorescein-labeled biotin (II). (B) Chromatographic separation after synthesis of OX26-streptavidin (210 kDa; I) and unconjugated OX26 (150 kDa; II). (C) Elution profile of molecular-mass markers: thyroglobulin (of 670 kDa; void volume; I),  $\gamma$ -globulin (of 158 kDa; II), ovalbumin (of 44 kDa; III), and myoglobin (of 17 kDa; IV), Vitamin-B12 (of 1.3 kDa, V). OD, absorbance.

The OX26-streptavidin conjugate was purified and analysed by gel-filtration chromatography (Figure 9). The conjugate was identified by a shift in molecular mass as compared to unconjugated OX26 mAb, and its ability to bind the fluorescent label biotin-fluorescein (Figure 9 A). A separation was achieved between the cross-linked precipitates OX26-streptavidin (Figure 9 B, peak I), and unbound OX26 mAb (Figure 9 B, peak II). This was confirmed as well by calibration of the used column with a set of molecular-mass markers (Figure 9 C) and comparison of the elution profiles, as by gel electrophoresis (4.1.2). The approximate yield of streptavidin-conjugated OX26 recovered after purification was 40 %.

#### 4.1.2 *Gel electrophoresis*

One-dimensional gel electrophoresis was performed on a Novex® 4 - 20 % Tris-Glycine polyacrylamide gel (Invitrogen, Carlsbad, CA), to resolve molecular weights of proteins in peak fractions. Figure 10 shows the coomassie stained protein pattern of peak samples before and after purification by SEC, shown in Figure 9 B. Under reducing conditions (lanes IV-VII), the interchain disulfide bonds of the antibody are cleaved, resulting in decomposition into heavy and light chains of the antibody. Lane IV is the positive control, OX26 which shows a staining pattern characteristic for this antibody which shows the heavy chain at approximately 55 kDa (high molecular weight band) which is homogeneous, and the light chains, resolved into two principal bands in the proximity of 25 kDa (Yoshikawa and Pardridge, 1992). All other lanes of reduced samples present these bands equally with additional signals which will be discussed in the section "results". Lane V (reduced peak I) and lane VII (unpurified reaction mix) exhibit additionally a slight band around 60 kDa and a blurred signal around 250 kDa. As expected, not denaturated samples (lanes I-III) all aggregate in the upper part of the

gel, indicating high molecular weight of the proteins or complexes of protein. Lane II (not reduced peak II) and low concentration of reaction mix before gel filtration in lane III show roughly bands at about 200 kDa.

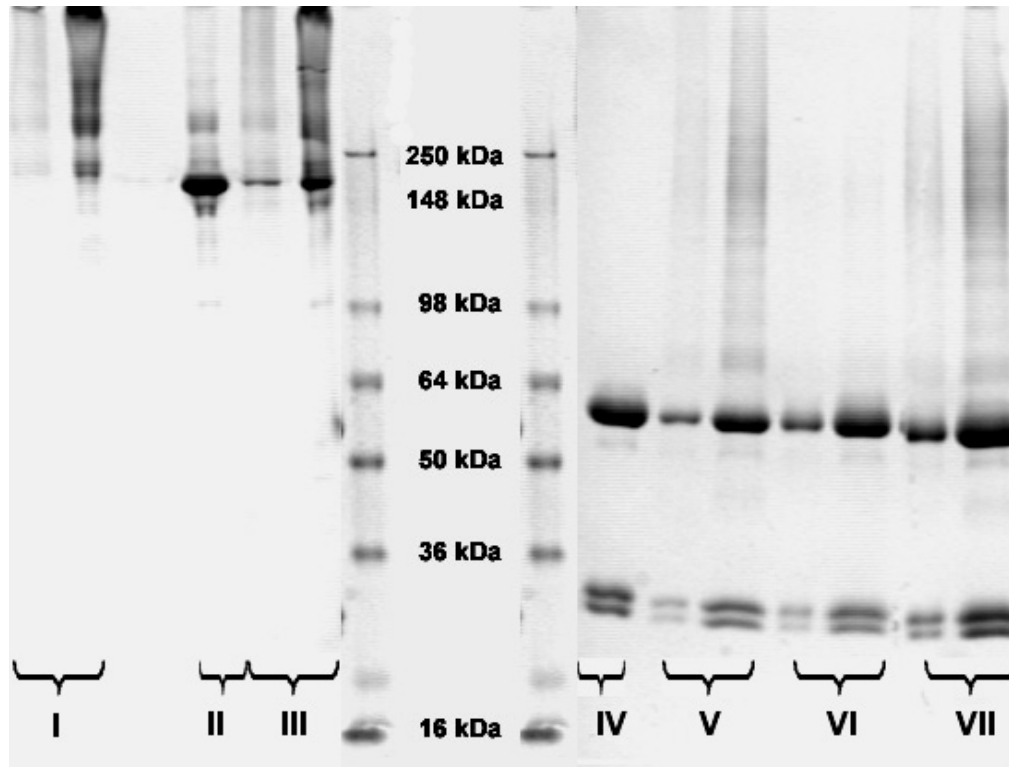


**Figure 10:** Tris-Glycine-Gel electrophoresis under non-reducing (left side, lanes I-III) and reducing (right side, lanes IV-VII) conditions, for identification of samples containing the conjugate OX26-streptavidin, before and after purification by the gel chromatography depicted in Figure 9 B (peak I and II). Lanes: I: two concentrations of peak I; II: high concentration of peak II; III: two concentrations of reaction mix before gel filtration; middle: molecular weight marker SeeBlue® Plus2, Invitrogen; IV: OX26 mAb; V: two concentrations of peak I; VI: two concentrations of peak II; VII two concentrations of reaction mix before gel filtration.

#### 4.1.3 Biotin binding assay

The binding capacity of the OX26-streptavidin conjugate for [<sup>3</sup>H]biotin was determined by an ultrafiltration method (Figure 11). Analysis of the biotin binding curve indicates that biotin binding is only partially impaired as a consequence of the coupling of streptavidin with the OX26 mAb. Using 32 nM OX26-streptavidin conjugate, saturation

of biotin binding is observed between 64 and 100 nM biotin, indicating the presence of two to three biotin-binding sites on each OX26-streptavidin conjugate. There are normally four biotin-binding sites on the tetrameric streptavidin (Hermanson, 1996).

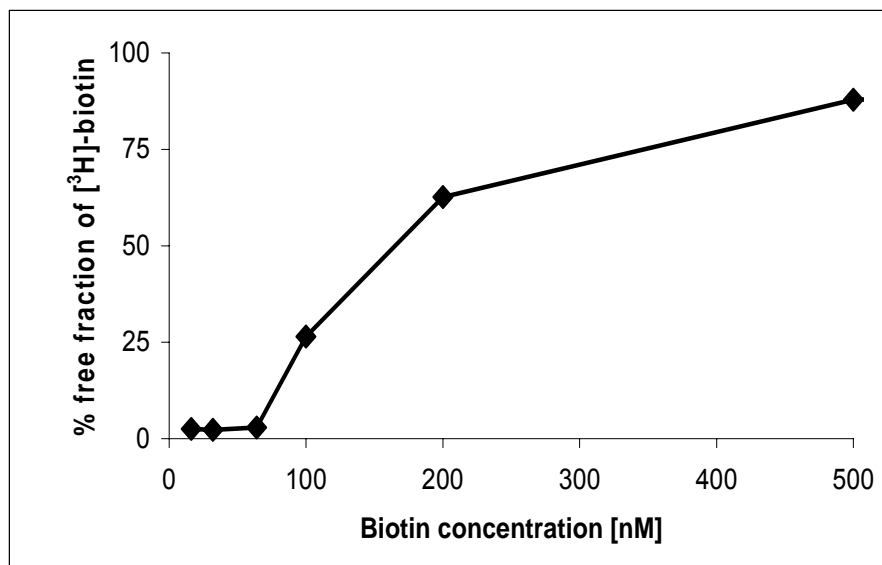


**Figure 11:** Concentration-dependent binding of [<sup>3</sup>H]biotin to a streptavidin-OX26 conjugate. Unbound [<sup>3</sup>H]biotin was separated from streptavidin-OX26 by ultrafiltration using a filter membrane with a molecular-mass cut-off of 30 kDa. Saturation of total [<sup>3</sup>H]biotin binding in the presence of 32 nM streptavidin-OX26 was observed at biotin concentrations of 64 - 100 nM.

#### 4.1.4 Loading of immunoliposomes by pH gradient

Encapsulation of daunomycin into liposomes was achieved using a pH gradient across the liposome bilayer. The pH gradient was established by preparing liposomes in presence of an acidic buffer with substantial buffering capacity, such as 0.1 M citrate pH 4.0, and adjustment of the external buffer by addition of NaOH to a pH between 7.1 and 7.7. Daunomycin was spiked with 5  $\mu$ Ci [<sup>3</sup>H]daunomycin as radioactive tracer. Labeled drug was added to external buffer and mixed with liposomes at a drug-to-lipid ratio of 0.2 (wt/wt). Not incorporated drug was separated from liposomal drug by SEC with 0.001 M



PBS pH 7.4. Using this method, external buffer is exchanged with a low phosphate PBS buffer (0.001 M) and liposomes are eluted in a physiological environment. The percentage of encapsulated daunomycin was determined by scintillation counting and is shown in Figure 12 to be approximately 90 %. This figure is representative for all experiments where daunomycin was encapsulated into liposomes using a pH gradient. Loading efficiencies were high throughout all experiments, i.e. in Figure 12 it was 95 %. In general, the range of pH gradient loading efficiencies was between 89 and 95 %.

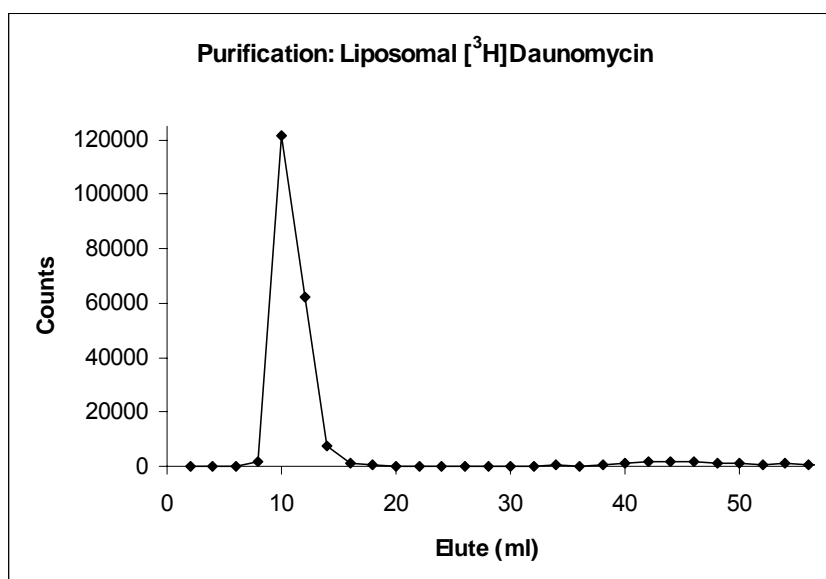


**Figure 12:** Loading of OX26-immunoliposomes with [ $^3\text{H}$ ]daunomycin by pH-gradient. Loading efficiencies were calculated by scintillation counting of eluates after purification by size exclusion chromatography. Loading efficiencies were 89 - 95 %.

Stability of entrapment of biotinylated PEG-liposomes was analyzed after storage at 4°C during four days. Liposomes were purified from leaked drug by gel chromatography. The leakage after this time was 2.6 % (data not shown).

#### 4.1.5 *Passive loading of immunoliposomes*

Substances to be incorporated by the pH gradient method have to fulfill two requirements. First, this technique necessitates a certain pK of the compound to be incorporated. Thereby, active uptake into the liposomes follows an existing electrochemical transmembrane gradient (i.e. daunomycin). Second, the substance has to be insensitive towards changes in pH and high temperatures (incorporation by pH gradient is done at 50 - 60°C). In the present work, ESR spin labels, fluorescent markers (i.e. carboxyfluorescein and propidium iodide), expression plasmids and oligonucleotides have been entrapped into liposomes by an alternative passive method. As passive loading presents a fast and simple approach, it is the method of choice for low priced substances (i.e. used ESR spin labels and fluorescent dyes), because entrapment efficiency is poor.

pH-sensitive liposomes do not tolerate low pH and can thereby not be loaded by the more efficient pH gradient method. Manufactured pH-sensitive liposomes contained dioleoylphosphatidylethanolamine (DOPE), a lipid that adopts the nonbilayer inverted hexagonal (H<sub>II</sub>) phase in isolation (Cullis and de Kruijff, 1978), and an ionizable acidic lipid such as cholesteryl hemisuccinate. Liposomes can only be formed with a mixture of both lipids, where CHEMS stabilizes DOPE and allows the adoption of a bilayer structure. Protonation of CHEMS at pH below its pK (5.8 (Hafez and Cullis, 2000)) diminishes the ability of this component to stabilize DOPE in the bilayer organization (Lai et al., 1985) leading to membrane inversion, membrane fusion and thus decomposition of liposomal structures. For this reason, we used a passive entrapment method in this case, with the disadvantage of a poor efficacy of 6 %. Stability of entrapment of pH-sensitive liposomes was analyzed after four days of storage at 4°C. These liposomes contained only 2 % of the initial substance (data not shown).

## 4.2 IN VITRO ASSAYS AND RESULTS

### 4.2.1 Immunohistochemistry

By immunostaining experiments using the OX26 mAb, the presence of the transferrin receptor in rat skeletal muscle tissue was examined (Figure 13). Tissue sections perpendicular to the muscle fibres (Figure 13 A) showed an intense immunostaining at the periphery of the myofibres, as well as at the periphery of the enclosed myofibrils. The staining of the myofibre surface can also be seen in longitudinal sections (Figure 13 B). Little or no fluorescent signal was observed in control experiments using secondary antibody only (Figure 13 B, inset) or an unspecific mouse IgG<sub>2a</sub> isotype control antibody (results not shown).

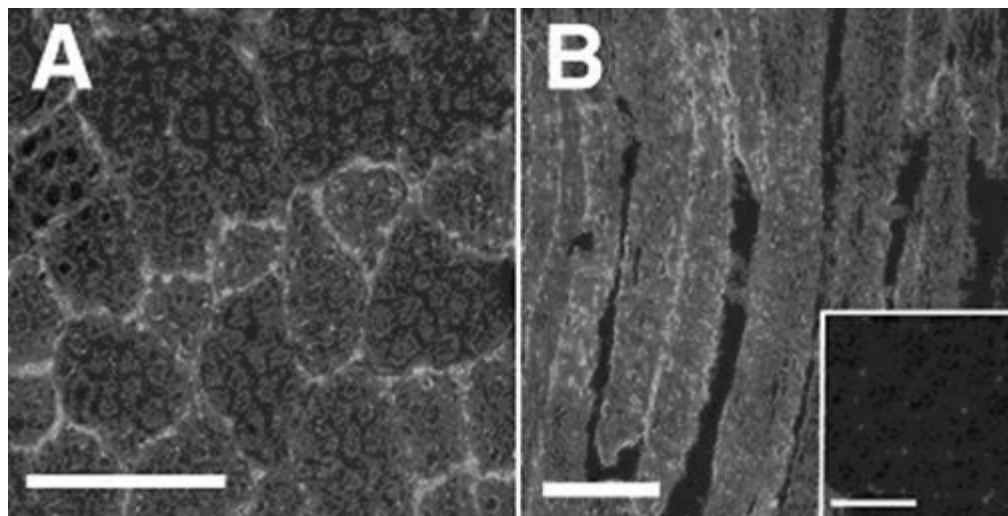


**Figure 13:** Analysis of muscle tissue sections by confocal microscopy using the OX26 mAb (125  $\mu\text{g}/\text{ml}$ ) and a secondary Cy2-labeled polyclonal antibody. Immunostaining of rat muscle tissue which is cryo-sectioned (**A**) orthogonal or (**B**) parallel to the muscle fibres. The inset to (**B**) shows the control experiment (incubation with secondary antibody only). Scale bars represent 100  $\mu\text{m}$ .

#### 4.2.2 Immunocytochemistry and uptake experiments

Immunocytochemistry was done in parallel with immunohistochemistry. The rat skeletal muscle derived L6 cell line was incubated with OX26 mAb at 37°C and analyzed with a fluorescent secondary antibody against mouse antibody (Cy2). Figure 14 A and 14 B shows a conspicuous fluorescent signal on the cell surface and a particulate staining pattern in the cells. Nearly all cells were positive when incubated at 37°C (Figure 14 A). The percentage of positive cells in these experiments was not investigated analytically; however, the overlay of fluorescence image with phase contrast image allows the assumption that more than 90 % of the cells showed a fluorescent signal. At 4°C, binding of OX26 accumulates on the cell surface and only the periphery of cells appears in fluorescence visualization. Figure 14 C shows one single cell incubated at 4°C.

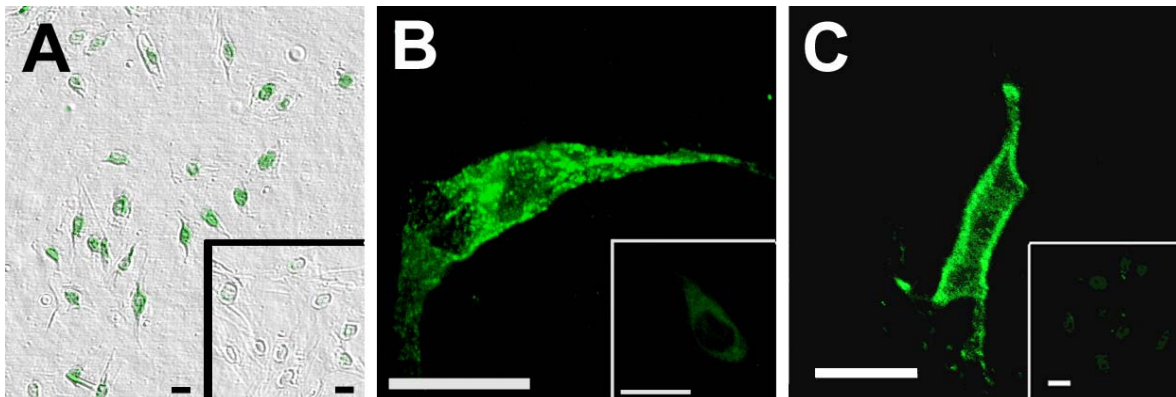


**Figure 14:** Immunocytochemistry and uptake experiments using the OX26 mAb and L6 cells. **(A)** Cellular uptake of the OX26 mAb (100 µg/ml) by L6 cells at 37°C and visualization of internalized antibody using a Cy2-labeled secondary antibody: overlay between a phase contrast image of L6 cells and the corresponding fluorescence image. The inset shows the negative control, using an unspecific IgG<sub>2a</sub> isotype antibody. **(B)** Magnification of a single L6 cell (incubation with 30 µg/ml OX26 at 37°C) reveals a particulate intracellular staining pattern. The inset shows the control (secondary antibody only). **(C)** Immunolabeling of surface receptors by incubation of L6 cells with OX26 mAb (100 µg/ml) at 4°C. The inset shows the control (unspecific IgG<sub>2a</sub> isotype antibody). Scale bars represent 20 µm.

Same immunostaining experiments were done with the RG2 rat glioma cell line, resulting in similar results (Figure 15). Figure 15 A and B display cellular uptake of the OX26 mAb (50  $\mu\text{g/ml}$ ) by the RG2 cells at 37°C. The phase contrast image overlaid with the corresponding fluorescence image confirms that every cell has taken up the OX26 mAb whereas in control experiments (inset, Figure 15 A), little or no fluorescence occurs. Similar as in L6 cells, at 4°C, OX26 mAb accumulates in RG2 cells at the periphery of the cell, indicating that receptor-mediated endocytosis and thus internalization of the labeled antibody is inhibited (Figure 15 C).

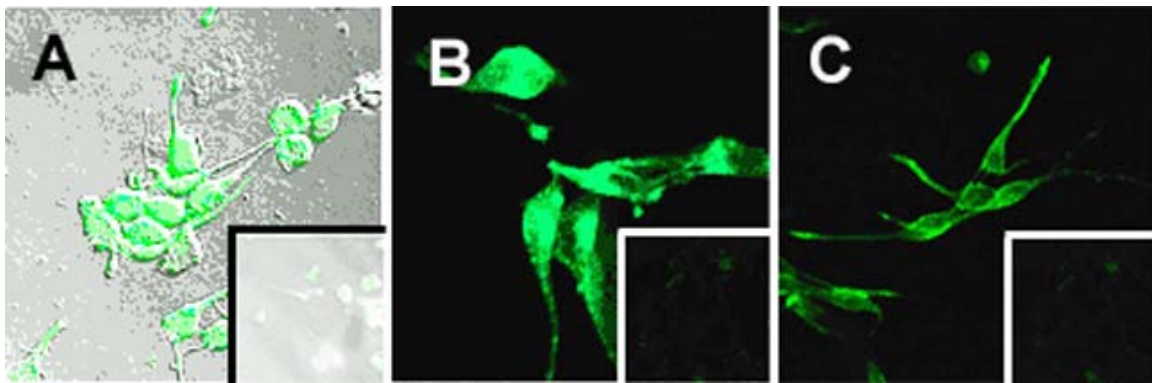


**Figure 15:** Immunocytochemistry and uptake experiments using the OX26 mAb and RG2 cells. **(A)** Cellular uptake of the OX26 mAb (50  $\mu\text{g/ml}$ ) by RG2 cells at 37°C and visualization of internalized antibody using a Cy2-labeled secondary antibody: overlay between a phase contrast image of RG2 cells and the corresponding fluorescence image. The inset shows the negative control (secondary antibody only). **(B)** Magnification of RG2 cells (incubation with 30  $\mu\text{g/ml}$  OX26 at 37°C) reveals a particulate intracellular staining pattern. The inset shows the control (secondary antibody only). **(C)** Immunolabeling of surface receptors by incubation of RG2 cells with OX26 mAb (30  $\mu\text{g/ml}$ ) at 4°C. The inset shows the control (secondary antibody only).

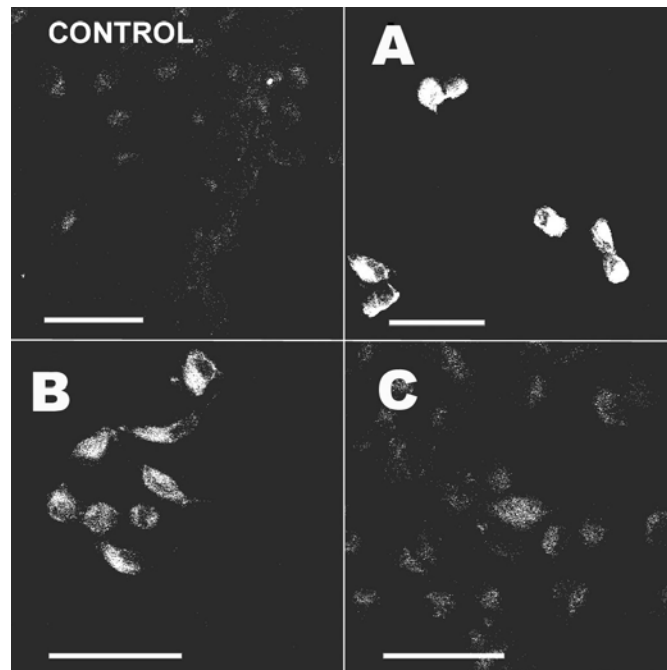


**Figure 16:** Cellular uptake of fluorescence-labeled OX26-streptavidin (OX26-streptavidin biotin-fluorescein) and fluorescent OX26 immunoliposomes by cultured L6 muscle cells. Cells were fixed after 1 h incubation and analyzed by confocal microscopy. The concentration of OX26 was always 70 µg/ml. **(A)** Incubation with OX26-streptavidin and biotin-fluorescein; **(B)** Incubation with OX26 immunoliposomes loaded with carboxyfluorescein; **(C)** Competition of cellular uptake of OX26 immunoliposomes in presence of 200 µg/ml free OX26; (Control) Background fluorescence of L6 cells. Scale bars represent 50 µm.

Results of uptake experiments for L6 cells are shown in Figure 16, and for RG2 cells in Figure 17. OX26-streptavidin was fluorescence-labeled by adding biotin-fluorescein. Intracellular fluorescent signal is presented in either of the cell lines, the muscular L6 line and the glioma RG2 line. In another set of experiments, liposomes were loaded with carboxyfluorescein and subsequently connected to OX26-streptavidin. Figure 16 B (L6) and 17 B (RG2) reveal a considerable intracellular staining of the cells, confirming previous experiments where OX26-streptavidin was labeled with biotin-fluorescein (A in Figure 16 and 17). Pre-incubation of cells with free OX26, in the purpose of occupying OX26-binding sites on the transferrin receptor, resulted in a lesser fluorescence intensity in both cell lines (C in Figures 16 and 17).

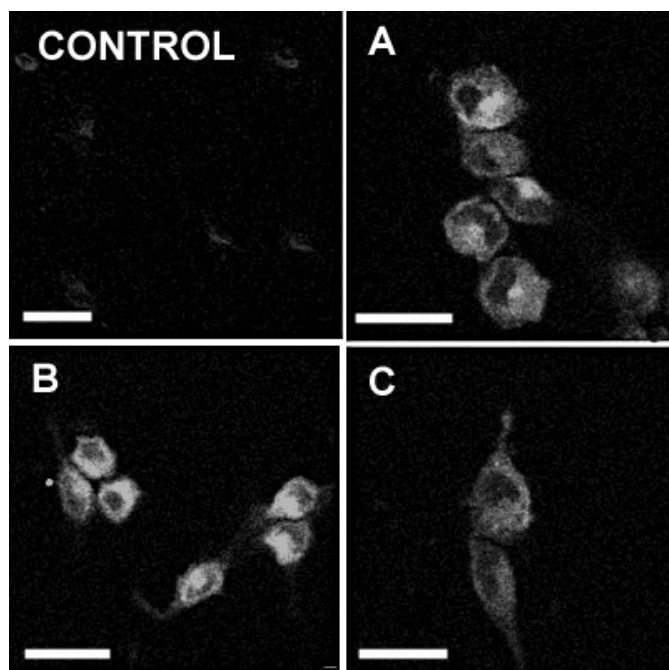


**Figure 17:** Cellular uptake of fluorescence-labeled OX26-streptavidin (OX26-streptavidin biotin-fluorescein) and fluorescent OX26 immunoliposomes by cultured RG2 rat glioma cells. Cells were fixed after 1 h incubation and analyzed by confocal microscopy. The concentration of OX26 was always 70  $\mu\text{g}/\text{ml}$ . **(A)** Incubation with OX26-streptavidin and biotin-fluorescein; **(B)** Incubation with OX26 immunoliposomes loaded with carboxyfluorescein; **(C)** Competition of cellular uptake of OX26 immunoliposomes in presence of 200  $\mu\text{g}/\text{ml}$  free OX26; (Control) Background fluorescence of RG2 cells. Scale bars represent 20  $\mu\text{m}$  apart from control (50  $\mu\text{m}$ ).

#### 4.2.3 Endosomal release of propidium iodide

Endosomal release of OX26-immunoliposomes was visualized by confocal fluorescence microscopy as described by Cerletti et al. (Cerletti et al., 2000). For this purpose, OX26-immunoliposomes were synthesized and loaded with propidium iodide (PI), a fluorescent dye that was shown to be impermeable to both, living cells and liposomal membranes. PI has spectral characteristics, changing dramatically upon binding to nucleic acids (Vogel et al., 1996). A shift in fluorescence of propidium iodide of a factor of 8 in presence of 0.5 mg/ml DNA was shown. This increase was accompanied by a shift of the excitation and emission wavelength maxima from 494 nm to 544 nm and from 627 nm to 603 nm, respectively, which makes the dye detectable

when it is released from liposomes and binds to DNA. RG2 cells were incubated with propidium iodide filled OX26-immunoliposomes for 1, 3 or 24 h prior to analysis by fluorescent confocal microscopy using settings of the microscope which were optimized for detection of propidium iodide associated with DNA (equipment settings Leica, installed in instrument). For pH-sensitive immunoliposomes, cells showed particulate fluorescence after one hour incubation which after 3 hours was at least of similar intensity after 3 hours and diminished after 24 hours incubation (Figure 18). Results were the same whether liposomes were removed after 3 hours or left on the cells for 24 hours (not shown). Different from published data where particularly the nucleus was stained (Cerletti et al., 2000), fluorescence in RG2 cells was increased in the cytosol and nucleolus. For not pH-sensitive immunoliposomes, fluorescence was most significant after 1 hour incubation and clearly less pronounced after 3 and 24 hours (Figure 19). However, it was less intensive throughout the experiment than the corresponding fluorescence of cells incubated with pH-sensitive immunoliposomes.

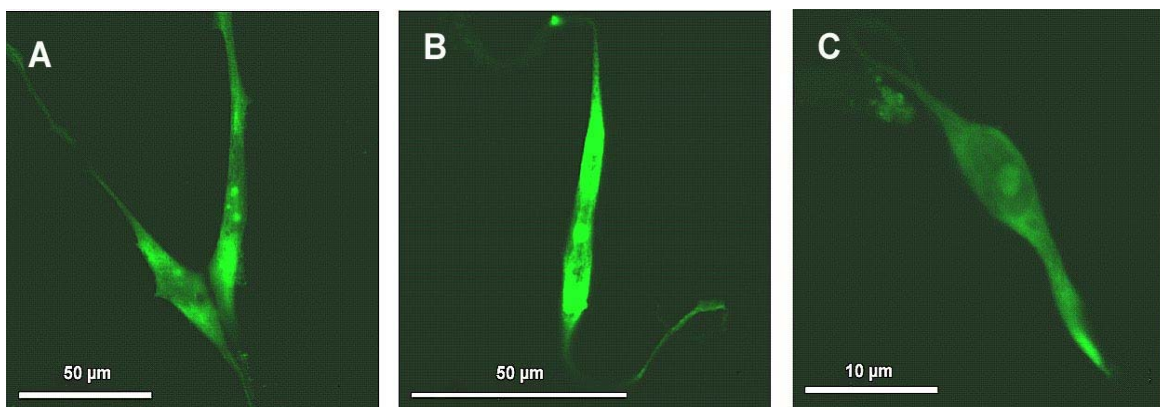


**Figure 18:** Uptake and endosomal release of pH-sensitive OX26-immunoliposomes by RG2 rat glioma cells. RG2 cells were incubated with propidium iodide loaded immunoliposomes and analyzed by confocal microscopy after (A) 1 h, (B) 3 h, or (C) 24 h. Immunoliposomes were removed after 3 h and cells were washed with normal growth medium.



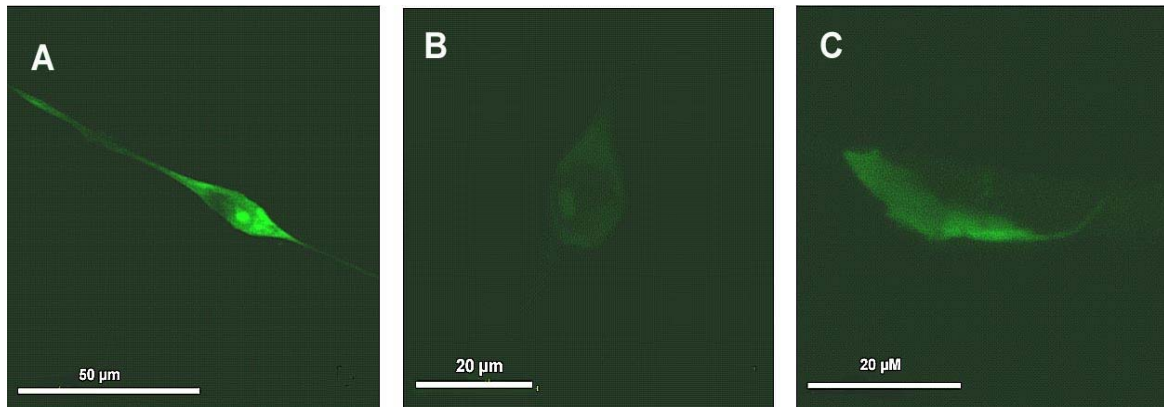


**Figure 19:** Uptake and endosomal release of not pH-sensitive OX26-immunoliposomes by RG2 rat glioma cells. RG2 cells were incubated with propidium iodide loaded immunoliposomes and analyzed by confocal microscopy after (A) 1 h, (B) 3 h, or (C) 24 h. Immunoliposomes were removed after 3 h and cells were washed with normal growth medium.

#### 4.2.4 Gene uptake and expression using immunoliposomes

After these promising results we decided to focus on uptake studies with the objective of gene uptake and expression. For this purpose, DNA was incorporated into liposomes by the freeze-thaw technique, which entails a low efficacy. For the purpose to remove external DNA, two different methods were carried out. By DNase digestion, not incorporated DNA is decomposed and can not be expressed by cells. SEC chromatography is a mechanic method that separates external DNA from liposomes as molecular weight is significantly lower and therefore is retained for a longer time in the column than liposomes. To confirm the presence of DNA in the immunoliposomes, analysis by agarose gel electrophoresis before and after size exclusion chromatography was performed (Figure 20). A plasmid of known molecular mass was examined to control experiment. Figure 20 shows the analysis of liposomal plasmid DNA by electrophoresis. 25  $\mu$ l-aliquots of the initial reaction mixture before SEC purification (Figure 20, lanes 3 and 4) and 500  $\mu$ l-aliquots of SEC purified (pooled) fractions (lanes 5 and 6) were applied on a 0.8 % agarose gel for electrophoresis. As control for the

DNase I digest, pCDNA1.3-lacZ (8.5 kb) was used. The DNA band in lane 1 (after digestion) in the proximity of the 8 kb band of the DNA ladder, together with its complete absence in lane 2 (with digest), confirms functionality of electrophoresis and DNase digestion. The DNA bands of the original liposome mixture (reaction mixture after incorporation process), are in the area of the 5 kb band of the DNA ladder, independent of DNase digestion (lane 4) or not (lane 3). This agrees with manufacturer's molecular mass indication of pGL3 (4.8 kb). Bands of the original liposome mixture differ considerably in intensity and dimension when treated with DNase (lanes 3 and 4), the signal becomes narrow-banded and well defined. Analysis of liposomal fractions after SEC (lane 6) and post-peak fractions (lane 5) exhibit similarly a 5 kb band that is well-defined and exact. Peak-fractions are more intensive than post-peak fractions which also contains certain amounts of DNA.

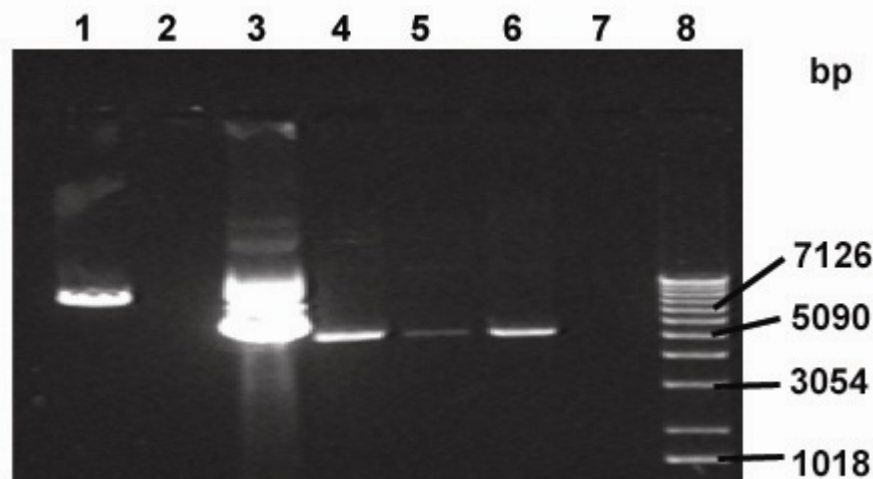


**Figure 20:** Agarose electrophoresis to confirm DNA incorporation into immuno-liposomes: (liposomal) plasmid DNA before and after purification by size exclusion chromatography and optional DNase I digestion. Lanes: **1:** pCDNA3.1-lacZ plasmid (8.5 kb) without DNase; **2:** pCDNA3.1-lacZ plasmid with DNase; **3:** Immunoliposomes containing pGL3 (4.8 kb) without DNase, not purified by chromatography; **4:** Immunoliposomes containing pGL3 with DNase, not purified by chromatography; **5:** DNase treated immunoliposomes after chromatography: post-peak fraction; **6:** DNase treated immunoliposomes after chromatography: peak fraction; **7:** buffer control; **8:** 1 kb DNA ladder (Invitrogen Cat. # 15615-024, Carlsbad, CA)

#### 4.2.5 *Liposomal administration of pGL3 expression vector*

The expression of liposome-incorporated luciferase gene in RG2 rat glioma and L6 rat muscle cells was determined by pGL3 Luciferase Reporter Vector under the control of the unspecific SV40 promoter (Promega, Madison, WI), using lipofectamine transfection as control. Lipofectamine transfections were conducted under standard conditions, as recommended by the manufacturer's protocol. Transcriptional activity was measured with a TECAN fluorescence and luminescence plate reader (Spectrafluor plus, TECAN, Männedorf, CH), and peak light emission was measured at 20°C and recorded as relative light units. Figure 21 shows L6 cells incubated with pGL3 Luciferase Reporter Vector for 24 hours. Plasmid DNA was either transfected with lipofectamine (not shown) or encapsulated in pegylated immunoliposomes that were conjugated to the OX26 mAb or the unspecific IgG<sub>2a</sub> mAb. OX26-immunoliposomes were examined in normal (1 x) or double concentration (2 x). Negative controls (Figure 21, control) were cells without plasmid administration, treated the same. Experiments were conducted with n = 6 wells per sample. Only double concentrated liposomal plasmids resulted in a luciferase expression higher than background (untreated cells). It was not tested whether further enhancement of concentration leads to an increase in luciferase expression of transfected cells. These results suggest that gene expression of cells transfected with liposomal plasmids can be enhanced by the OX26 mAb to a certain extend. However, it seems not to be the most adapted targeting vector and better results may be achieved with a more adapted antibody. The positive control, cells transfected with lipofectamine, exhibited strong luminescence (> 30000 relative light units in the same scale, data not shown). Rat glioma RG2 cells did not show differences between negative untreated control cells and cells incubated with liposome incorporated DNA (data not shown).

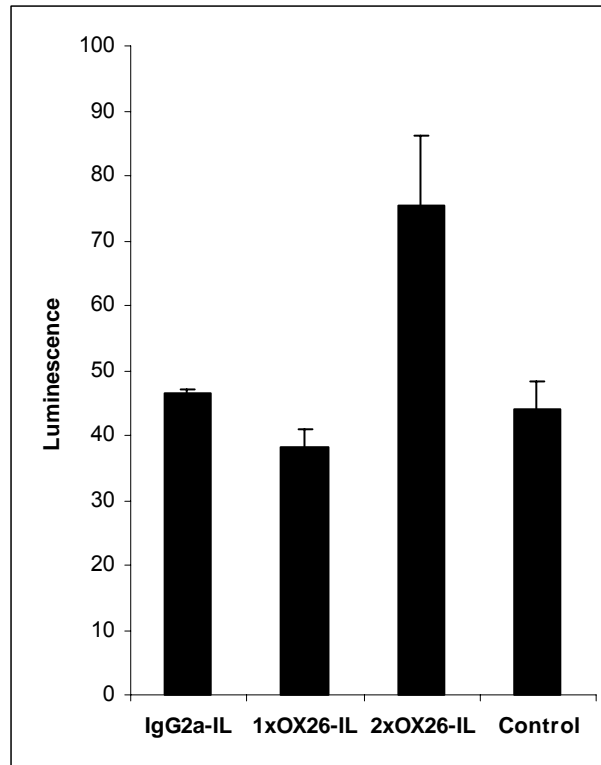


**Figure 21:** The luciferase activity in L6 cells, expressed as relative light units (luminescence), is shown for L6 cells after 24 h of administration of the pGL3 plasmid DNA encapsulated in pegylated immunoliposomes that were conjugated to the OX26 mAb or the unspecific IgG<sub>2a</sub> mAb. Controls are not treated at all. Data are mean ± SEM (n = 6). Positive control cells were transfected with lipofectamine (not shown).

#### 4.2.6 Expression of $\beta$ -galactosidase in RG2 cells

Additionally to liposomal plasmid delivery of the  $\beta$ -galactosidase vector, gene expression experiments were also performed with lipofectamine transfection as positive control for the expression plasmid. Lipofectamine transfections were conducted under standard conditions, as recommended by the manufacturer's protocol. In brief, 5  $\mu$ g of the plasmid per well was used for lipofectamine transfection. The initial amount of plasmid used for incorporation into liposomes was 400  $\mu$ g, 6.6 % from pooled liposome fractions after purification by SEC were placed per well. Loading efficiency was not determined; data from other experiments give efficiencies of about 5 % incorporation by

the passive freeze-thaw technique. In samples 24 and 48 hours after transfection, positive lipofectamine transfected controls showed intense blue staining ( $\beta$ -galactosidase expression) at 1 hour after staining with X-gal solution. Cells incubated with liposomal  $\beta$ -galactosidase expression vector did not reveal any signals, even after a staining treatment of 24 h (pictures not shown).

#### 4.2.7 *Uptake of liposomal, labeled oligonucleotides by RG2 cells*

After this limited success with  $\beta$ -galactosidase expression vector, uptake of fluorescent Cy3-labeled phosphorothioate oligonucleotides was examined. The intention was to investigate the location and endosomal release of liposomal cargo after cellular uptake. Targeted immunoliposomes under control of OX26 mAb were compared to unconjugated biotinylated PEG-liposomes and uptake was analyzed after 1, 24 and 40 hours (Figures 22 and 23). Fluorescent microscopy after one hour didn't reveal any difference, fluorescence was not detected in neither of the two formulations (Figure 22, inset A and C). Comparison after 24 h represented a more intensive fluorescence of cells incubated with OX26-immunoliposomes (Figure 22 A). However, unconjugated liposomes showed also fluorescence, but in a less extent (Figure 22 B). Analysis of DAPI staining brings out cell nucleus of stained cells and allows to discern the rate of cells that have taken up the labeled liposomal content.

Visualization of fluorescence after 40 h incubation demonstrates no appreciable difference between targeted and unconjugated liposomes (Figure 23). Comparison with DAPI staining indicates that approximately every cell exhibits fluorescence and has taken up the labeled oligonucleotides. The punctuated staining pattern of fluorescence is located rather in the cytosol than in nucleus and is distributed all-over the cell plasma.

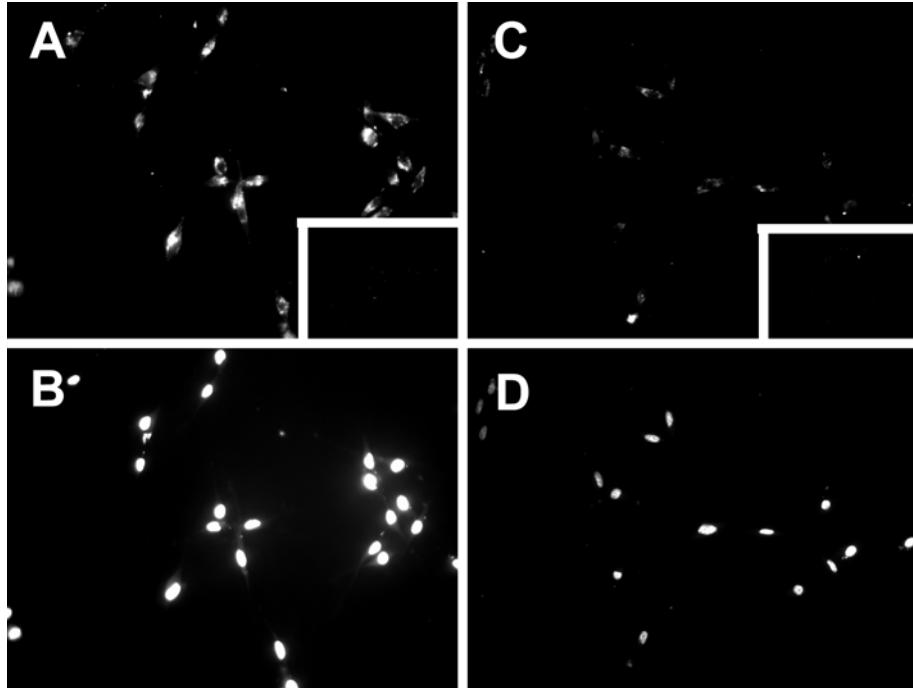


**Figure 22:** Uptake of liposomes by RG2 cells: fluorescent microscopy of Cy3-labeled oligonucleotides incorporated into OX26-immunoliposomes or into unconjugated liposomes after addition to cultured RG2 cells. (A) and (B) RG2 cells were incubated with OX26-immunoliposomes for 24 h prior to visualization by fluorescence microscopy of Cy3 (A) and DAPI staining (B); Inset (A) identical fluorescence microscopy of Cy3 after 1 h incubation; (C) and (D) RG2 cells were incubated with unconjugated liposomes for 24 hours prior to analysis by fluorescence microscopy of Cy3 (C) and DAPI staining (D); Inset (C) fluorescence microscopy of Cy3 after one hour incubation.

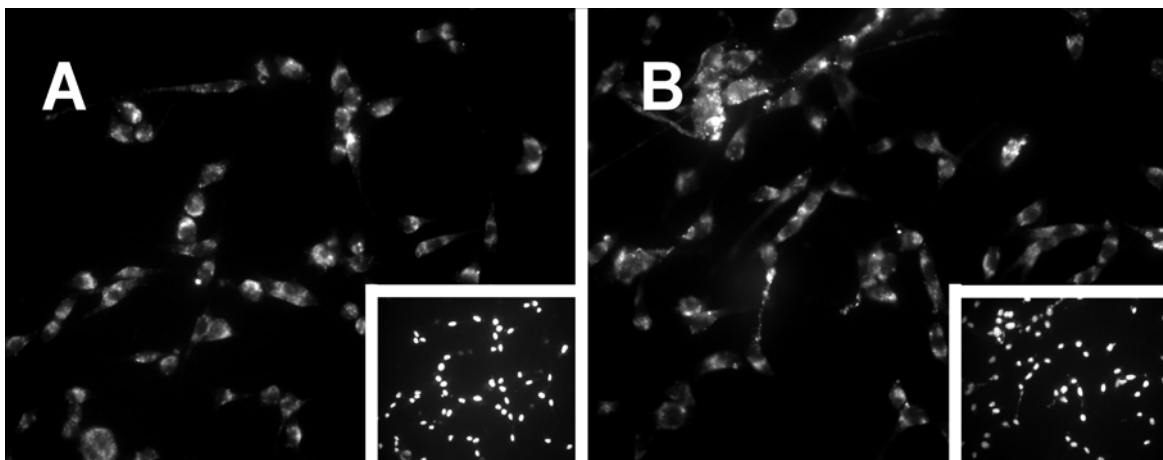


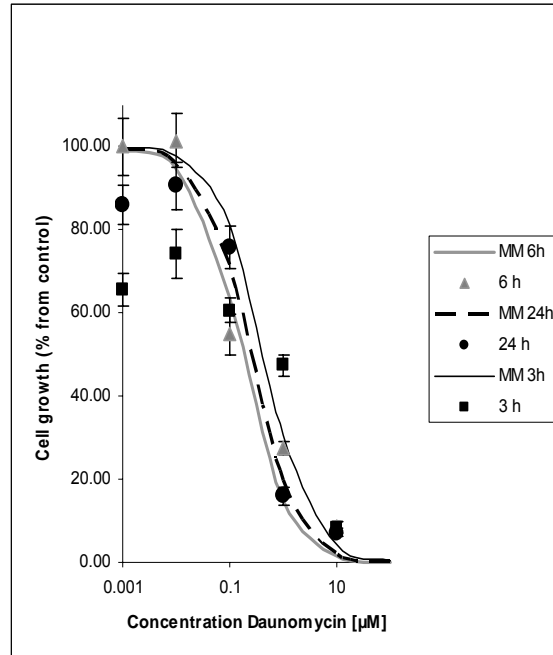
**Figure 23:** Uptake of liposomes by RG2 cells: fluorescent microscopy of Cy3-labeled oligonucleotides incorporated into OX26-immunoliposomes or into unconjugated liposomes after addition to cultured RG2 cells and incubation of 40 h prior to visualization by fluorescent microscopy. (A) RG2 cells were incubated with OX26-immunoliposomes prior to visualization of Cy3 and DAPI staining (inset); (B) RG2 cells were incubated with unconjugated liposomes prior to visualization of Cy3 and DAPI staining (inset).

#### 4.2.8 Cytotoxicity of liposomal daunomycin

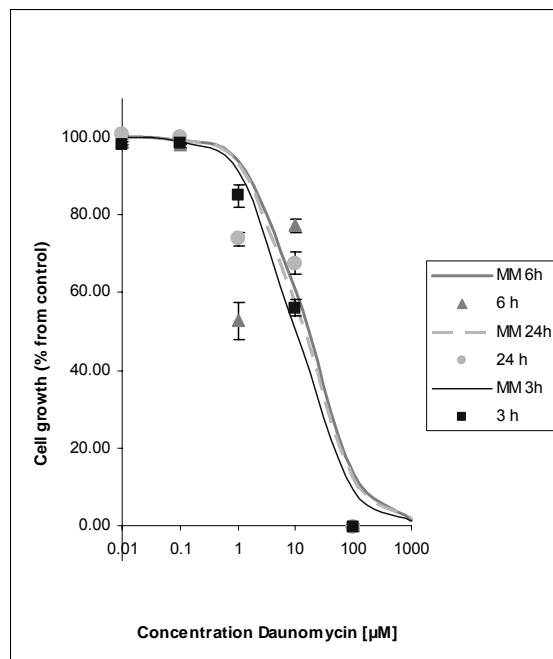
The next sets of experiments were based on something completely different. Drug delivery experiments using immunoliposomes were done with the aim to show a pharmacological *in vitro* effect. The cytotoxic substance daunomycin was therefore incorporated into OX26-immunoliposomes that were incubated with cells. The pharmacological action (i.e. cytotoxicity) and proliferation inhibition of daunomycin was determined in either a multidrug-resistant cell line and in a chemosensitive cell line using the sulforhodamine B cytotoxicity assay. Immortalized rat brain capillary endothelial cells (RBE4) overexpressing P-glycoprotein and the rat glioma RG2 cells were used for these experiments. LD<sub>50</sub> values of daunomycin cytotoxicity, determined for incubation periods of 3, 6 and 24 hours with increasing concentrations of the cytotoxic agent, are shown in Table 1 and Figure 24 (RBE4) and 25 (RG2). The sensitivity of the multi-drug resistant RBE4 cells (LD<sub>50</sub> after 3 hours 10.3 µM) towards daunomycin was significantly lower than the chemosensitivity of the RG2 cells, which showed a LD<sub>50</sub> of 0.5 µM under the same assay conditions (Figures 24 and 25). LD<sub>50</sub> values were not dependent on the duration of the daunomycin incubation: An increase of the daunomycin incubation period from 3 to 6 h and 24 h led to similar LD<sub>50</sub> values of 15.5 µM and 13.4 µM for RBE4 cells and 0.2 µM and 0.3 µM for RG2 cells, respectively.

Table 1: LD<sub>50</sub> values in µM of RBE4 and RG2 cells. Values are means (n = 3) for exposure times of 3 h, 6 h and 24 h.

Cell line	RBE4	RG2
LD <sub>50</sub> 3h	10.3	0.5
LD <sub>50</sub> 6h	15.5	0.2
LD <sub>50</sub> 24h	13.4	0.3



**Figure 24:** Dose-dependent cytotoxicity of daunomycin in rat brain endothelial RBE4 cells: influence of increasing concentrations of daunomycin on proliferation of RBE4 cells after 3 h (◆), 6 h (■) or 24 h (▲) of daunomycin exposure time. Values are means ± SEM, n = 6. Solid lines: Regression curves calculated by Michaelis Menten's equation.



**Figure 25:** Dose-dependent cytotoxicity of daunomycin in rat glioma RG2 cells: influence of increasing concentrations of daunomycin on proliferation of RG2 cells after 3 h (◆), 6 h (■) or 24 h (▲) of daunomycin exposure time. Values are means ± SEM, n = 6. Solid lines: Regression curves calculated by Michaelis Menten's equation.



These results indicate that daunomycin effectively inhibits growth in glioma RG2 cells and in endothelial RBE4 cells. As shown in Table 1, mean LD<sub>50</sub> values for three different incubation times were 44 times lower for chemosensitive RG2 cells (0.3 µM) than for P-glycoprotein expressing RBE4 cells (13.1 µM). As a consequence of P-glycoprotein drug efflux pump, RBE4 cells are expected to respond more sensitive to liposomal formulations than to free daunomycin. By-passing of P-glycoprotein using immunoliposomes can enhance the toxicity of a drug in a cell line that overexpresses this efflux pump, such as RBE4 cells. All further cytotoxicology experiments were therefore performed with chemoresistant REB4 cells.

#### 4.2.9 Cellular uptake of liposomal [<sup>3</sup>H]daunomycin

Cellular uptake of radiolabeled daunomycin by chemoresistant RBE4 cells did increase significantly if the drug was incorporated within biotinylated OX26-immunoliposomes (Figure 26). There was a more than 2-fold increase in cellular uptake of daunomycin during a 1 h incubation. After an incubation of three hours, the uptake was 12.7 % for liposomal and 5.2 % for free daunomycin respectively. The observed effect was time-dependent as longer incubation-times of liposomal daunomycin did result in a further and statistically significant increase in cellular accumulation of daunomycin (Figure 26). Preliminary incubation of the cells with free OX26 didn't change the uptake of liposomal daunomycin significantly.

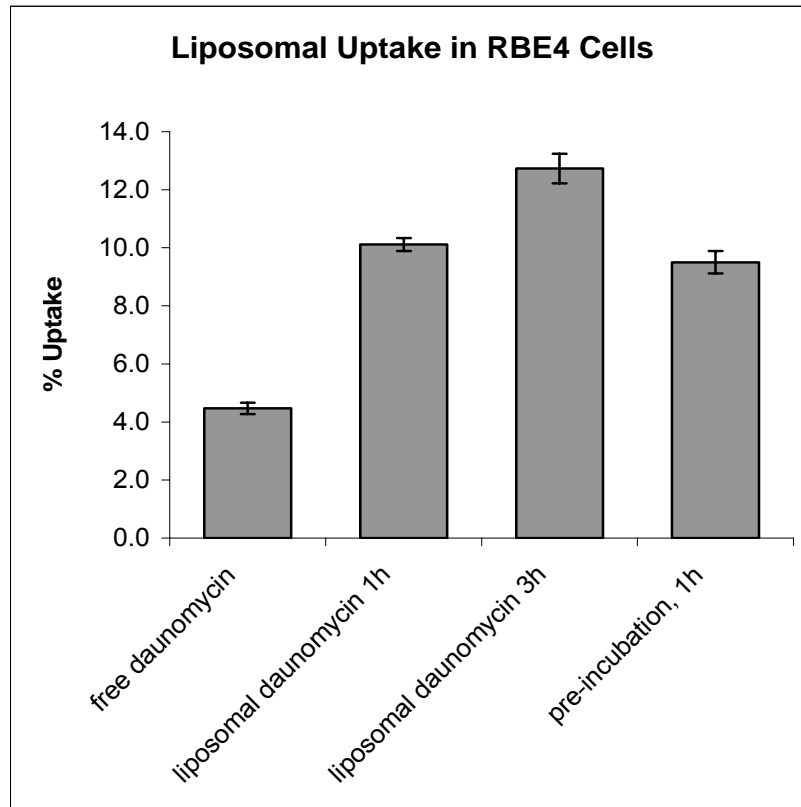


**Figure 26:** Cellular uptake of either free [ $^3\text{H}$ ]daunomycin or [ $^3\text{H}$ ]daunomycin incorporated in OX26-immunoliposomes after pre-incubation where indicated, by RBE4 brain endothelial cells. Values are means  $\pm$  SEM,  $n = 5$ . \*:  $P < 0.005$  by Student's t-test as compared to the indicated group.

#### 4.2.10 Pharmacological effects of daunomycin loaded immunoliposomes on RBE4 cells

Cellular uptake of liposomal daunomycin was associated with cytotoxic effects of daunomycin. Toxicity experiments were performed using the immortalised rat brain capillary endothelial cell line (RBE4) and are shown in Figures 27, 28, 29 and 30. Cell growth of RBE4 cells was inhibited by liposomal daunomycin.

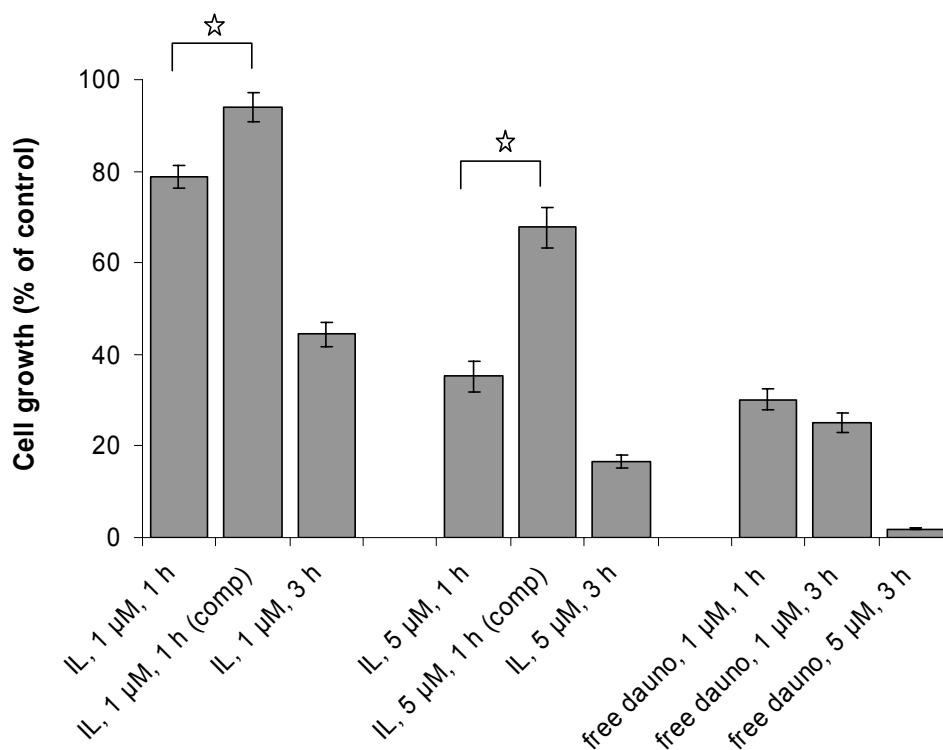


**Figure 27:** Cytotoxicity of different formulations of daunomycin in RBE4 brain endothelial cells: time-dependent inhibition of cell growth after exposure to different concentrations of daunomycin either incorporated in OX26-immunoliposomes (IL) or applied as free drug (free dauno). Control: 45 min pre-incubation of RBE4 cells with 1 mg/ml of free OX26 mAb (comp). Values are means  $\pm$  SEM,  $n = 8$ .  $P < 0.005$  (\*) by Student's t-test as compared to the indicated group.

Cellular toxicity did increase with increasing incubation times (i.e. 1 h versus 3 h). Cell growth after 1 h incubation with 1  $\mu$ M liposomal daunomycin was  $78.8 \pm 2.5$  % of the untreated control; prolongation of exposure time to 3 h entailed a reduction of cell growth to  $44.4 \pm 2.5$  % of untreated control cells. The observed pharmacological effects were dose-dependent (i.e. 1  $\mu$ M versus 5  $\mu$ M of daunomycin). Incubation with 5  $\mu$ M provoked even more important reductions in growth ( $35.2 \pm 3.2$  % of untreated control cells after 1 h and  $16.8 \pm 1.4$  % after 3 h, respectively). Effects were mediated by the OX26 monoclonal antibody since competitive inhibition of cellular uptake of liposomal

daunomycin by co-incubation with 100 µg/ml of free OX26 decreased cellular toxicity of the drug significantly (cell growth  $94.2 \pm 3.2$  % of untreated control for 1 µM daunomycin and  $67.7 \pm 4.3$  % for 5 µM, respectively).

The same experiments were performed on confluent cells (results not shown). Effects were notably more obvious on the sub-confluent cell layer. Results were statistically significant in both, sub-confluent and confluent cells.

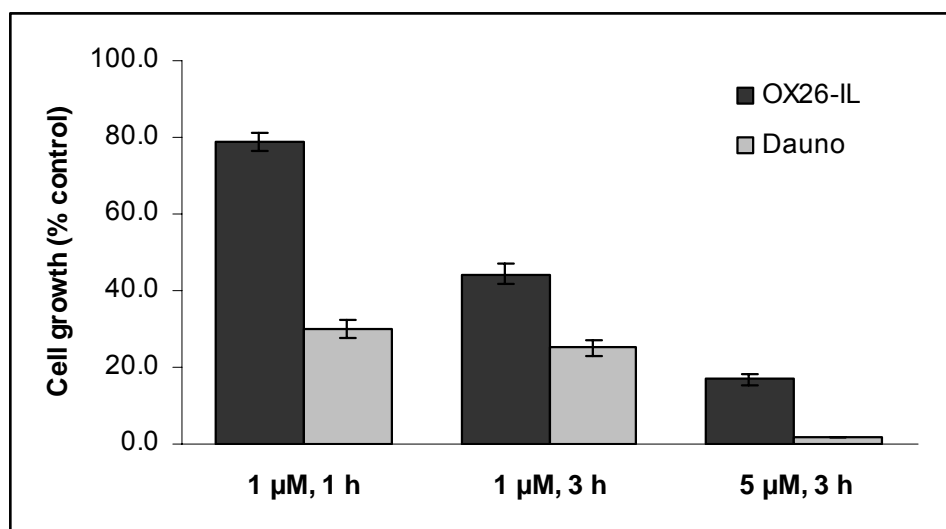


**Figure 28:** Daunomycin response of RBE4 brain endothelial cells: inhibition of cell growth after exposure to free or in OX26-immunoliposomes incorporated daunomycin for indicated times and concentrations. Values are means  $\pm$  SEM,  $n = 8$ .  $P < 0.005$  (\*).

Figure 28 presents same experiments in comparison with a formulation of free daunomycin. In these experiments, free daunomycin had a surprisingly strong cytotoxic effect which was significantly higher than the effect of liposomal daunomycin (Figure 28). Viability in RBE4 cells was lower throughout all experiments, when incubated with free daunomycin. This despite the fact that cellular uptake (and thus intracellular concentrations) of daunomycin were lower after incubations with free drug as opposed to incubations with liposomal drug (Figure 26). After one-hour incubation at 1 µM

daunomycin, cell growth was  $78.8 \pm 2.5$  from untreated control for liposomal daunomycin and  $30.1 \pm 2.3$  % for free daunomycin. After 3 h, values were  $44.4 \pm 2.5$  % for liposomal and  $25 \pm 2.1$  % for free daunomycin. Maximal toxicity was observed at the high concentration ( $5 \mu\text{M}$ ) after 3 hours incubation with free daunomycin. Viability was  $1.9 \pm 0.1$  % ( $16.8 \pm 1.4$  % for liposomal daunomycin).

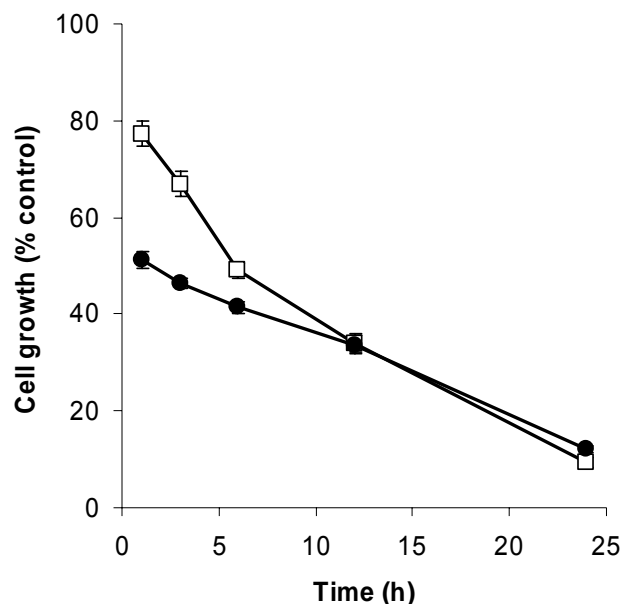


**Figure 29:** Time-dependent cytotoxicity of different formulations of daunomycin: RBE4 cells were incubated with either  $15 \mu\text{M}$  daunomycin incorporated in OX26-immunoliposomes ( $\square$ ) or  $15 \mu\text{M}$  free drug ( $\bullet$ ) for the indicated period of time. At 24 h, cytotoxicity of daunomycin was determined. Values are means  $\pm$  SEM,  $n = 6$ .

Figure 29 displays the time-response curves for  $15 \mu\text{M}$  daunomycin that was free or incorporated into OX26-immunoliposomes, for exposure times of 1, 3, 6, 12 and 24 h. Again, cells response of free daunomycin was more sensitive than of the OX26 coupled liposomal formulation. Differences were more obvious at the earlier time-points and approximated over experimentation course. Cell growth after 1 hour incubation was  $77.3 \pm 2.6$  % of controls for liposomal (OX26 controlled) daunomycin and  $51.2 \pm 1.8$  %

for free daunomycin. The importantly higher toxicity of free daunomycin, however, was present only in incubations which had a duration of less than 12 hours (Figure 29) as prolonged incubations with liposomal daunomycin led to a strong increase in cellular toxicity of the immunoliposomes. Values converged after 12 hours of incubation and curves even crossed after 24 hours of incubation.

Inhibition of cell growth in a dose-dependent way is illustrated in Figure 30. Both, liposomal (OX26 controlled) and free daunomycin caused a significant reduction of protein content measured by the SRB toxicity assay at higher doses for different exposure times (which is 3 hours in Figure 30). Again, free daunomycin causes significantly more cell growth inhibition than liposomal daunomycin formulations. However, values converge at higher concentrations; cell growth after 3 hours exposure to 15  $\mu\text{M}$  daunomycin was  $66.9 \pm 2.7$  % of controls for liposomal daunomycin and  $46.4 \pm 1.0$  % for free daunomycin, whereas at 1.5  $\mu\text{M}$ , values divergence more ( $100 \pm 2.7$  % and  $64.2 \pm 2.7$  % respectively). Daunomycin effect was tested up to 24 hours exposure with 15  $\mu\text{M}$  formulations. Under these conditions saturation occurred with both, liposomal and free daunomycin, generating very low cell growth values.

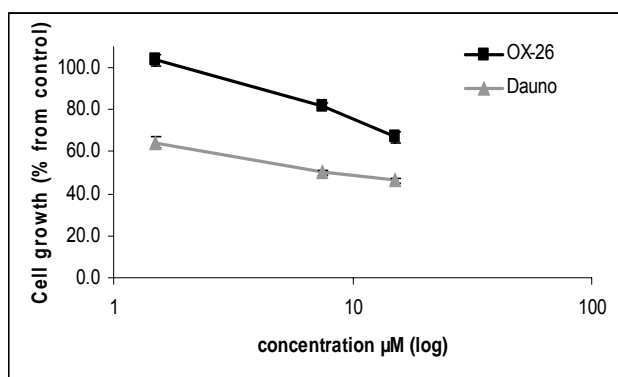


**Figure 30:** Daunomycin response of RBE4 brain endothelial cells: Concentration dependence of inhibition of cell growth after 3 hours exposure to free or OX26-immunoliposomes incorporated daunomycin for indicated concentrations. Values are means  $\pm$  SEM,  $n = 6$ .

Experiments were conducted several times and same trends persisted continuously. However, there was a substantial variability between individual values of different sets of experiments or cell batches. Broad relations between free and liposomal daunomycin were assessed by implementing average values of performed experiments. The response of RBE4 brain endothelial cells to daunomycin was compared for 15  $\mu\text{M}$  of free and liposomal daunomycin after a 1 hour incubation time throughout 3 independent sets of experiments. Toxicity of liposomal (OX26) daunomycin was  $50.9 \pm 29.4 \%$  (mean of  $n = 3$ ) of toxicity caused by free daunomycin.

In addition, total percent reversal caused by pre-incubation was analyzed statistically throughout all experiments. The reversal by pre-incubation with OX26 (means of  $n = 4$ ) was  $20.6 \pm 38.2 \%$ . These experiments were carried out at different daunomycin concentrations and OX26 competition concentrations.

### **4.3 IN VIVO ASSAYS AND RESULTS**

#### *4.3.1 Plasma concentrations of free and liposomal daunomycin in rat*

In order to explore the *in vivo* properties of biotinylated OX26-immunoliposomes, series of pharmacokinetic and tissue distribution studies were performed in the rat. Different formulations of liposomal radiolabeled daunomycin (equal doses of 20  $\mu\text{Ci}/\text{kg}$  equivalent to 0.6  $\mu\text{g}/\text{kg}$ ) were applied by jugular vein injection (including free drug). Five different types of liposomes were prepared and loaded with radiolabeled daunomycin using the pH gradient method. Daunomycin loading was achieved with a high reproducible yield ( $> 95 \%$  entrapment in most cases) (Huwyler et al., 1996). Fabricated types of liposomes were (1.) conventional, sterically stabilized (by incorporation of lipid-conjugated PEG) liposomes and (2.) additionally biotinylated (by incorporation of

DSPE-PEG-biotin phospholipids) liposomes that were either (3.) used directly or (4. and 5.) linked to a streptavidin coupled antibody by means of a biotin-streptavidin bond. In doing so, two antibodies were used: the monoclonal mAb OX26 against transferrin receptor in order to show a specific targeting, and the IgG<sub>2a</sub> isotope as an unspecific control antibody. Previous studies have shown that uptake of unchanged mouse IgG<sub>2a</sub> solely by rat tissue is minimal and behaves similar to a blood volume marker after i.v. injection (Pardridge et al., 1991). Pharmacokinetic parameters (Table 2) were calculated by non-compartmental data analysis of the plasma-concentration versus time profiles shown in Figure 31.

**Table 2:** Pharmacokinetics in the rat of different formulations of [<sup>3</sup>H]daunomycin: Area under the plasma concentration curve for the initial 60 min after intravenous bolus injection (AUC<sub>0-t</sub>), steady state volume of distribution (V<sub>D</sub>) and plasma clearance (Cl) of free drug (daunomycin) or drug incorporated within biotinylated PEG-liposomes, unspecific IgG<sub>2a</sub>-immunoliposomes and biotinylated OX26-immunoliposomes. Data are means ± SEM, n = 3.

Daunomycin Vehicle	Vehicle			AUC <sub>(0-1h)</sub>	T <sub>1/2</sub>	V <sub>D(SS)</sub>	Cl
	PEG	biotin	IgG	%ID*min/ml	min	l/kg	ml/min/kg
Free drug	-	-	-	3.69 ± 0.4	49.4 ± 7.6	3.85 ± 0.3	55.6 ± 6.4
PEG-liposomes	+	-	-	299.78 ± 13.0	38.0 ± 1.8	0.05 ± 0.0	0.9 ± 0.0
Bio-liposomes	+	+	-	210.38 ± 11.0	28.8 ± 1.6	0.05 ± 0.0	1.3 ± 0.0
OX26	+	+	+	30.17 ± 2.3	25.7 ± 1.8	0.35 ± 0.0	9.3 ± 0.5
IgG <sub>2a</sub>	+	+	+	47.67 ± 3.4	15.9 ± 1.8	0.15 ± 0.0	6.8 ± 0.7



Free daunomycin is rapidly removed from the circulation. The steady state volume of distribution ( $V_D = 3.9$  l/kg) and the systemic plasma clearance ( $CL = 56$  ml/min/kg) are very high. This is in contrast to the corresponding values for biotinylated PEG-liposomes (PEG-liposomes;  $V_D = 0.05$  l/kg and  $CL = 1.3$  ml/min/kg, Table 2). Biotinylation of conventional PEG-liposomes has a negligible impact on their plasma concentrations, volume of distribution or plasma clearance: Control experiments using non-biotinylated PEG-liposomes revealed a volume of distribution of 0.05 l/kg and a plasma clearance of 0.9 ml/min/kg. In view of these minimal differences, we assumed that it doesn't make a substantial difference whether biotinylated or non-biotinylated PEG-liposomes were used as a plasma volume marker ( $V_0$ ) for the calculation of organ PS products. We therefore decided to focus in our discussion solely on biotinylated PEG-liposomes and to use them as  $V_0$  for the calculation of PS products (Huwylar et al., 1996).

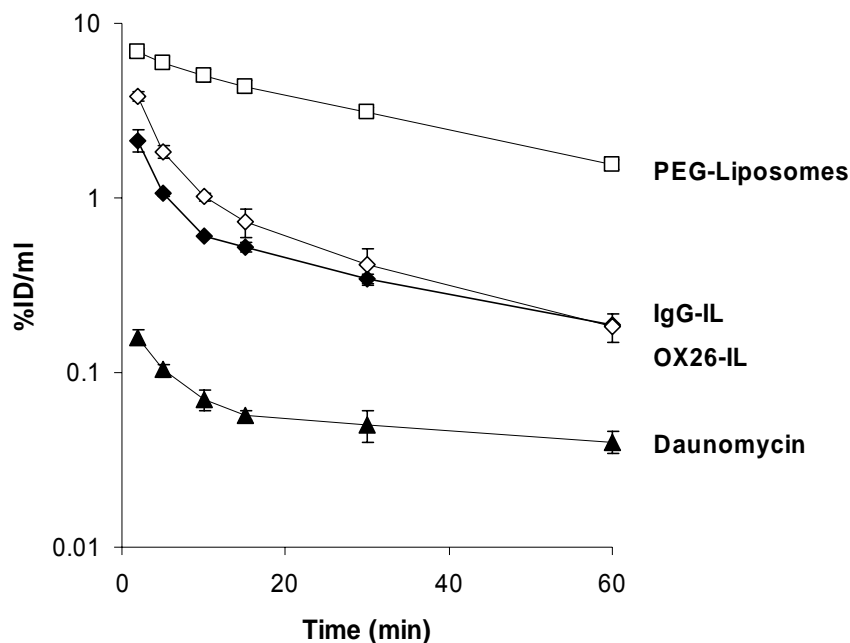


**Figure 31:** Plasma-concentration versus time profiles in the rat of different formulations of [ $^3\text{H}$ ]daunomycin: Intravenous bolus administration of daunomycin or daunomycin incorporated within biotinylated PEG-liposomes (PEG-liposomes), unspecific IgG<sub>2a</sub>-immunoliposomes (IgG-IL) and biotinylated OX26-immunoliposomes (OX26-IL). Plasma concentrations (%ID/ml) of [ $^3\text{H}$ ]daunomycin are plotted versus times. Data are means  $\pm$  SEM,  $n = 3$ .

The plasma clearance of radiolabeled drug was reduced 62-fold by incorporation into liposomes and solely PEG conjugation. An additional biotinylation resulted in a less pronounced 43-fold reduction of plasma clearance. These reductions are indicative of a long retention of the drug within sterically stabilized liposomes and the plasma compartment. The stability of PEG-liposomes in the circulation was investigated in previous studies where the presence of intact liposomes in the circulation for at least 6 hours after injection was evidenced (Huwyler et al., 1997). Conjugation of antibodies to pegylated liposomes reversed partially the effect of pegylation and led to an increase of the plasma clearance as well as the volume of distribution of these immunoliposomes. The plasma clearance of immunoliposomes was 9.3 ml/min/kg (OX26 coupled) and 6.8 ml/min/kg (IgG<sub>2a</sub> coupled). The effect of pegylation on the area under the plasma concentration curve after one hour (AUC<sub>0-t</sub>) was most conspicuous. Steric stabilized liposomes increased the daunomycin AUC<sub>0-t</sub> by a factor of 81 when compared to the free drug and additional biotinylation by a factor of 57 (Table 2).

#### 4.3.2 *Tissue distribution of free daunomycin and daunomycin loaded liposomes or immunoliposomes*

Several tissues (brain, liver, heart, kidney, lung, spleen, testes and muscle tissue) were analyzed for tissue clearance (PS product) and tissue uptake (%ID/g tissue) of different daunomycin formulations (Figure 32 and Table 3). Analysis revealed a very low volume of distribution of sterically stabilized and biotinylated liposomes which were used as a plasma volume marker (V<sub>0</sub>), leading per definition to a PS of zero (since V<sub>D</sub> – V<sub>0</sub> is zero) for this formulation ('BIO' in Figure 32). In sharp contrast to brain, no superiority of OX26-immunoliposomes could be shown with respect to %ID/g tissue for spleen, liver, heart, muscle or kidney. Spleen and liver are the two organs where substantially higher amounts of immunoliposomes accumulate as compared to free daunomycin (Figure 32

A and B). The high tissue clearance (PS product) of immunoliposomes is indicative of an active and unspecific sequestration of these particulate drug carriers by spleen and liver. In contrast, immunoliposomes are poorly retained by muscle tissue or the kidney. In these organs, free daunomycin had a 20- to 30-fold higher tissue clearance (Figure 32 F). The highest PS product was reached for free daunomycin in the kidney with a value for 120  $\mu\text{l}/\text{min}/\text{g}$  tissue (Figure 32 H).

**Table 3:** Tissue distribution in the rat after intravenous injection of different formulations of [ $^3\text{H}$ ]daunomycin: Tissue clearance (PS) and tissue uptake (%ID/g tissue) were determined 60 min after intravenous bolus administration of [ $^3\text{H}$ ]daunomycin or [ $^3\text{H}$ ]daunomycin incorporated within immunoliposomes (conjugated to the OX26 mAb or an unspecific IgG<sub>2a</sub> control). Biotinylated PEG-liposomes are used as plasma volume marker and have both a PS product and %ID/g value of zero. Data are means  $\pm$  SEM, n = 3.

Tissue	Formulation	PS ( $\mu\text{l}/\text{min}/\text{g}$ tissue)	%ID/g tissue
<b>Spleen</b>	free daunomycin	39.5 $\pm$ 6.5	0.15 $\pm$ 0.04
	OX26-liposomes	171.1 $\pm$ 42.3	5.21 $\pm$ 1.46
	IgG-liposomes	228.0 $\pm$ 47.3	10.10 $\pm$ 1.45
<b>Liver</b>	free daunomycin	54.3 $\pm$ 7.2	0.19 $\pm$ 0.01
	OX26-liposomes	47.3 $\pm$ 6.9	1.42 $\pm$ 0.22
	IgG-liposomes	49.9 $\pm$ 8.9	2.22 $\pm$ 0.24
<b>Heart</b>	free daunomycin	48.2 $\pm$ 1.1	0.177 $\pm$ 0.017
	OX26-liposomes	2.66 $\pm$ 0.19	0.079 $\pm$ 0.001
	IgG-liposomes	4.19 $\pm$ 0.67	0.188 $\pm$ 0.021
<b>Muscle</b>	free daunomycin	15.7 $\pm$ 1.3	0.058 $\pm$ 0.010
	OX26-liposomes	0.55 $\pm$ 0.14	0.016 $\pm$ 0.004
	IgG-liposomes	0.52 $\pm$ 0.05	0.023 $\pm$ 0.002
<b>Kidney</b>	free daunomycin	120.3 $\pm$ 5.0	0.444 $\pm$ 0.054
	OX26-liposomes	4.41 $\pm$ 1.40	0.139 $\pm$ 0.053
	IgG-liposomes	5.00 $\pm$ 0.62	0.227 $\pm$ 0.024

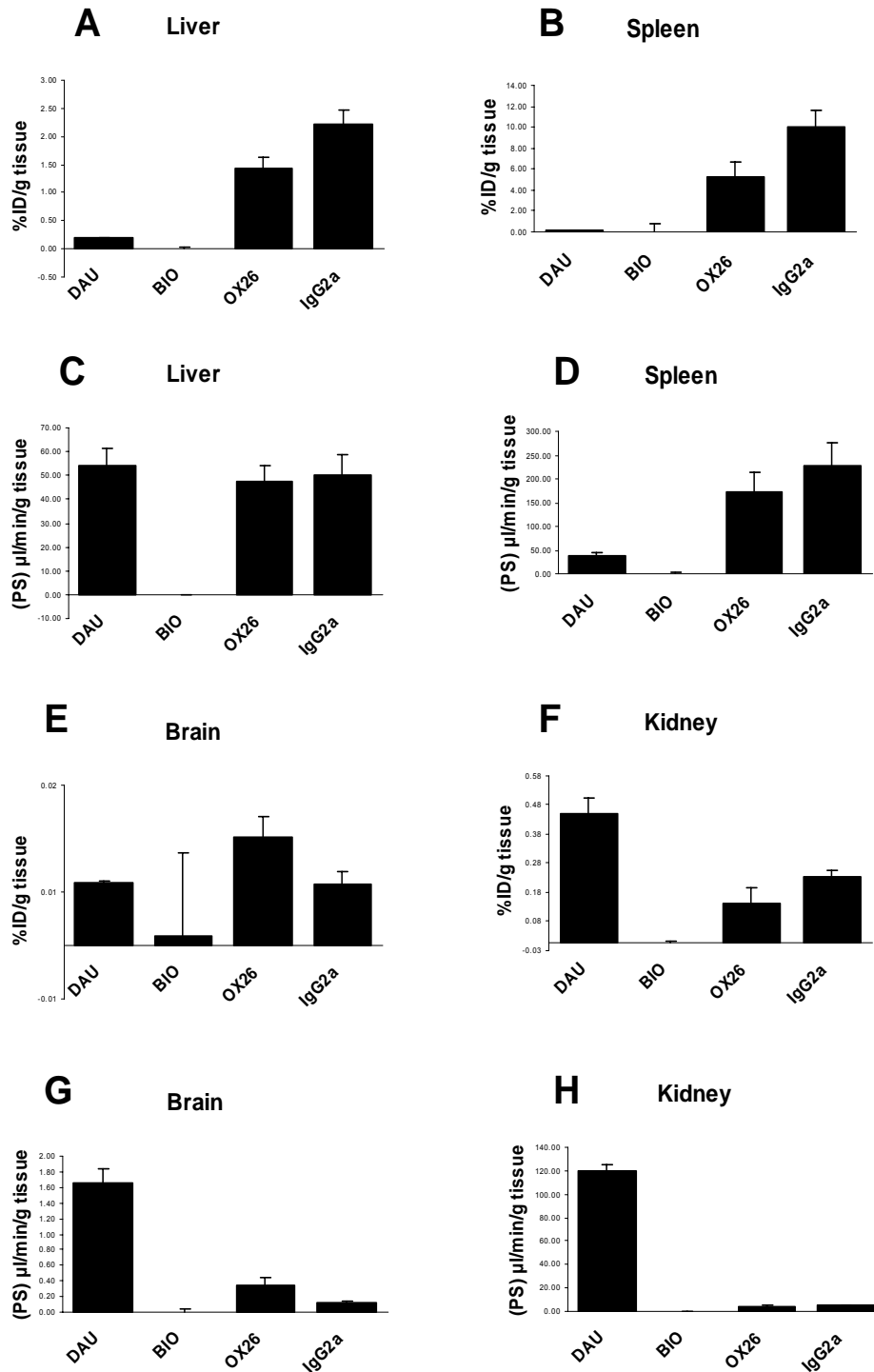


**Figure 32:** Tissue distribution in the rat after intravenous injection of different formulations of  $[^3\text{H}]$ daunomycin: free daunomycin (DAU), biotinylated PEG-liposomes (BIO), OX26-immunoliposomes (OX26) and IgG<sub>2a</sub>-immunoliposomes (IgG<sub>2a</sub>). Tissue clearance (PS) and uptake (%ID/g tissue) were determined 60 min after intravenous bolus administration of the relative  $[^3\text{H}]$ daunomycin formulation. Data are means  $\pm$  SEM, n = 3.

Interestingly, only in brain, PS product of OX26-immunoliposomes was higher than of IgG<sub>2a</sub>-immunoliposomes (Figure 32 G and Figure 33). All other organs showed a resembling pattern for PS products: free daunomycin >> IgG<sub>2a</sub>-immunoliposomes ≥ OX26-immunoliposomes > biotinylated PEG-liposomes (> PEG-liposomes) (Figure 32, C, D and H). Analysis of brain tissue at 60 min after intravenous administration of these different formulations of daunomycin revealed a permeability surface area (PS) product of free daunomycin of 1.7 μl/min/g brain. This in contrast to daunomycin incorporated within OX26-immunoliposomes which had a tissue clearance (i.e. PS product) of 0.4 μl/min/g brain. However, the area under the plasma concentration curve of daunomycin is very low (Table 2) resulting in a brain accumulation (%ID/g brain = 0.006) which is only half of the one of OX26-immunoliposomes (%ID/g brain = 0.01). The PS product of unspecific control IgG<sub>2a</sub>-immunoliposomes is 0.1 μl/min/g brain leading to a %ID/g brain value of 0.006. The difference between brain accumulation of OX26-immunoliposomes and IgG<sub>2a</sub>-immunoliposomes represents thereby the effect mediated specifically by the OX26 monoclonal antibody. It is important to note that the use of pegylated liposomes reduced the PS product to zero. As a consequence, no brain uptake of such PEG-liposomes was observed despite the high plasma AUC for this liposomal formulation.

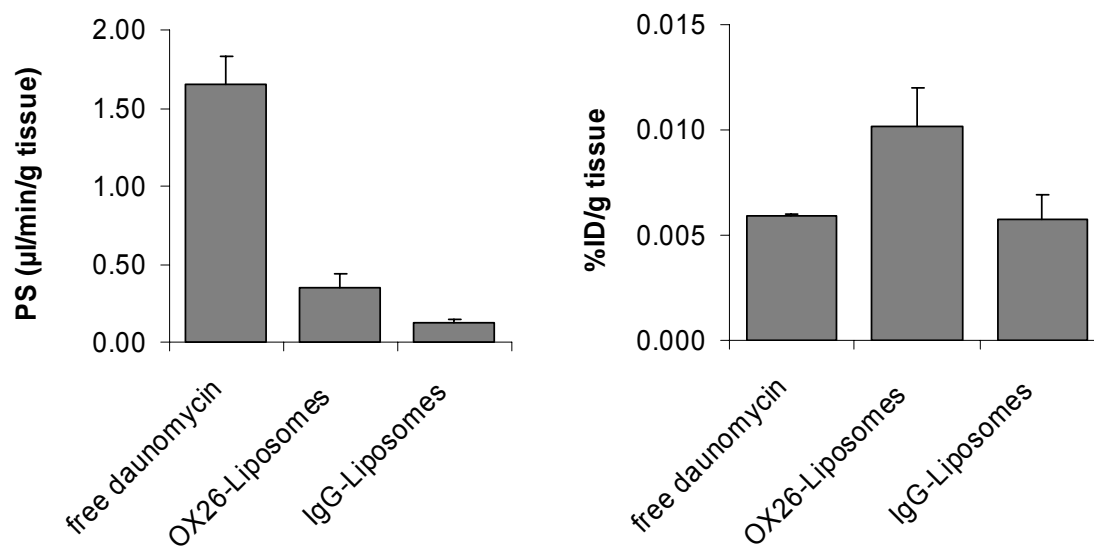


**Figure 33:** Brain delivery of [ $^3\text{H}$ ]daunomycin or [ $^3\text{H}$ ]daunomycin incorporated within OX26-immunoliposomes or control IgG<sub>2a</sub>-immunoliposomes: Brain tissue clearance (PS product, left panel) and brain uptake (%ID/g brain tissue, right panel) were determined 60 min after intravenous bolus administration in the rat. Data are means  $\pm$  SEM, n = 3.

## 5 DISCUSSION AND FUTURE PERSPECTIVES

### 5.1 CHARACTERIZATION AND OPTIMIZATION OF A NOVEL LIPOSOMAL CARRIER SYSTEM

Sterically stabilized liposomes have some significant advantages over conventional liposomes, including decreased uptake by macrophages of the reticuloendothelial system, increased blood residence times, increased stability to contents leakage, increased flexibility in lipid composition and dose-independent pharmacokinetics. Ganglioside GM1 appears to be unique among the glycolipids in conveying these properties to liposomes, and polyethylene glycolipid derivatives appear, so far at least, to be superior to other polymers in this regard (Allen, 1994b). The distinctive properties of stabilized liposomes or PEG-liposomes, makes them excellent candidates for many therapeutic applications including drug targeting (Maruyama et al., 1990b; Schnyder et al., 2004; Torchilin et al., 1992) as well as its use as a slow release formulation (Allen et al., 1992; Mayhew et al., 1992; Papahadjopoulos et al., 1991).

In the present thesis, a novel design of biotinylated PEG-immunoliposomes is presented, where a streptavidin-conjugated targeting vector (i.e. the OX26 mAb raised against the rat transferrin receptor) is attached to the surface of the liposome using a PEG spacer (Figure 5). Biotin was thereby coupled to the tip of the pegylated phospholipid PEG-DSPE, and subsequently incorporated into sterically stabilized liposomes (PEG-liposomes). A biotinylated PEG-liposome carries approximately 5500 strands of 2000 Da PEG and 30 strands of the linker lipid biotin-PEG-DSPE, and has a measured particulate size of 150 nm. The use of PEG as a flexible tether allows the biotin, and thereby the attached OX26 mAb, to extend away from the liposome surface,

which minimizes steric hindrance by unconjugated PEG moieties. Previous studies (Laverman et al., 2000) have indeed demonstrated that biotinylation of PEG-liposomes does not affect their *in vivo* pharmacokinetics in control rats, but promotes their accumulation in subcutaneous *Staphylococcus aureus* abscesses in the rabbit. Furthermore, direct measurement of the ligand-receptor interaction potential using biotinylated PEG-liposomes and streptavidin on a supported lipid bilayer indicated a markedly extended range of the interaction (Wong et al., 1997).

Biotinylated PEG-liposomes can be used for the non-covalent conjugation of any avidin- or streptavidin-conjugated ligand. Such ligands could include genetically engineered single chain antibody-streptavidin fusion proteins, such as the OX26 single chain Fv antibody-streptavidin fusion protein (Li et al., 1999), which can be produced on large scale in procaryotic or eucaryotic expression systems (Morrison and Shin, 1995). In the present work, streptavidin was chemically linked to the hybridoma-generated OX26 mAb. MBS was used as a hetero-bifunctional cross-linker reactive for primary amines in streptavidin and a single thiol group introduced into the OX26 mAb by thiolation with Traut's reagent (2-iminothiolane). This procedure has been shown previously to retain both, the antigen affinity of the OX26 mAb (Huwylar et al., 1996) and the biotin binding site of streptavidin (Zhang et al., 2002a). The OX26-streptavidin conjugate was purified and analyzed by gel-filtration chromatography (Figure 9). The conjugate was identified by a shift in molecular mass as compared with unconjugated OX26 mAb, and its ability to bind the fluorescent label biotin-fluorescein (Figure 9 A). A separation was achieved between cross-linked precipitates OX26-streptavidin (Figure 9 B, peak I) and unbound OX26 mAb (Figure 9 B, peak II), and this was confirmed by Tris-Glycine gel electrophoresis (Figure 10). Fractions containing the reaction product OX26 mAb conjugated to streptavidin were identified comparing electrophoresis pattern with the



molecular weight marker SeeBlue® Plus2 (Invitrogen) and bands of OX26 mAb (lane IV). The characteristic pattern of two light chain bands and one heavy chain band (Yoshikawa and Pardridge, 1992) have been confirmed. Except from lane II (peak II), samples analysed under non-reducing conditions (lanes I-III) show accumulation of signals above 250 kDa. Lane II exhibits the most intensive band at about 150 kDa, indicating free OX26 mAb (molecular weight of 150 kDa). Lane I (not reduced peak I) shows a band in the region of 200 kDa what corresponds to OX26-streptavidin by adding together molecular weights (molecular weight of streptavidin is 60 kDa). This peak is also present in the reaction mix before SEC purification (lane III). In addition, the band at approximately 150 kDa corresponds to the band (free OX26) in lane II. Cross-linking of OX26-streptavidin is supposed, considering the blurred signal above 250 kDa. Possible molecular weight of cross-linked conjugates are  $n * 150 \text{ kDa} + n * 60 \text{ kDa}$ , i.e. 270 kDa (1 OX26 linked to 2 streptavidin molecules), 360 kDa (2 OX26, 1 streptavidin), 420 kDa (2 and 2) and so on. Lower weights can be assumed but later on end in a inseparable blur of bands. Under reducing conditions, the interchain disulfide bonds of the antibody are cleaved, resulting in separation in heavy and light chains of the antibody. Conjugated streptavidin is not cleaved from the antibody, since it is connected by a stable thioether binding. Again, there are multiple weights possible, as a consequence of cross-linking with multiple streptavidin molecules bound per antibody. Starting with total molecular weights of 25, 50, 85 (light chain and streptavidin), 110 (heavy chain and streptavidin), 145 (two streptavidin molecules), continuation results in a blurred band likewise as it is possible to have inter-cross-linkages of two chains per streptavidin. These assumptions are confirmed in Figure 10, by the indefinite signals up from approximately 150 kDa in lane I (peak I) and III (reaction mix before purification) and it's absence in lane II (peak II). These findings confirm the presence of OX26-

streptavidin, cross-linked to a certain extent in pooled peak I and the occurrence of unconjugated OX26 in peak II.

The approximate yield of streptavidin-conjugated OX26 recovered after purification was 40 %. The binding capacity of the OX26-streptavidin conjugate for [<sup>3</sup>H]biotin was determined by an ultrafiltration method (Figure 11). There are normally four biotin-binding sites on the tetrameric streptavidin (Hermanson, 1996). Analysis of the biotin binding curve indicates that biotin binding is only partially impaired as a consequence of the coupling of streptavidin with the OX26 mAb. Owing to the extremely high affinity of biotin binding to streptavidin, with a  $K_D$  approximating  $10^{-15}$  M (Hermanson, 1996), the affinity constant of the OX26-streptavidin conjugate in itself cannot be determined. However, using 32 nM of OX26-streptavidin conjugate, saturation of biotin binding is observed between 64 and 100 nM biotin, indicating the presence of two to three biotin-binding sites on each OX26-streptavidin conjugate. The presence of multiple biotin-binding sites on each OX26-streptavidin conjugate may potentially lead to cross-linking of biotinylated liposomes, and thus to the formation of liposomal aggregates. To minimize this risk and to block excess biotin-binding sites, free biotin was added to OX26-streptavidin in a molar ratio of 1:1 prior to coupling of the OX26-streptavidin conjugate to biotinylated liposomes.

A vast number of different methods to synthesize liposomes are described. Phospholipids form spontaneously vesicles when transferred to water. The challenge is to produce liposomes which have the right size and structure and to entrap materials with high efficiency and in such a way that they do not leak out (New, 1990). The main difference between the various methods of production is in the way in which the membrane components are dispersed in aqueous media, before being allowed to coalesce in the form of bilayer sheets. In the present work, liposomes were

prepared after the simple physical dispersion method by drying down lipids and disperse them by addition of an aqueous medium, followed by shaking (New, 1990). Other methods, such as two-phase dispersion or detergent solubilization, are more complex or require more sophisticated equipment and components. The applied dispersion method is easy and fast, necessary facilities are a rotary evaporator apparatus for removing organic solvents (Figure 34) and an extruder to bring the liposomes to a defined size.

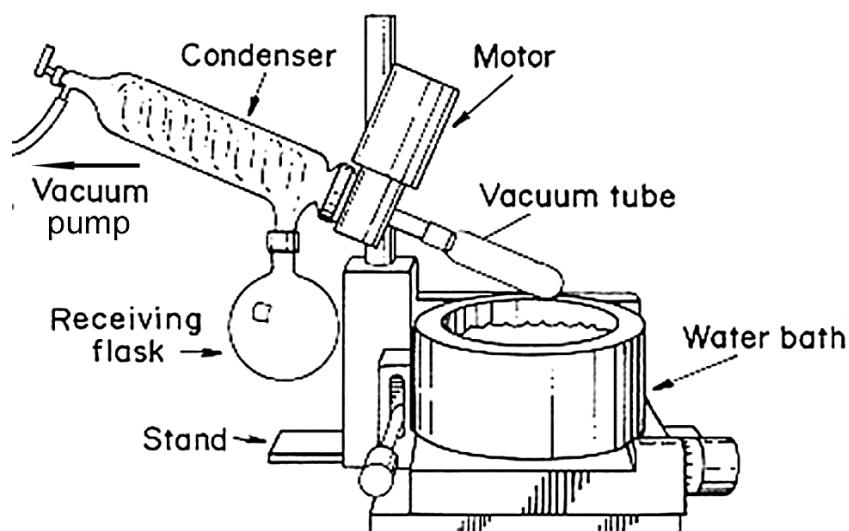


**Figure 34:** Rotary evaporator apparatus for evaporating off organic solvents. The evaporator consists of a heating bath with a rotating flask, in which the liquid is distributed as a thin film over the hot wall surfaces and can evaporate easily. The evaporation rate is regulated by the heating bath temperature, the size of flask, the pressure of distillation and the speed of rotation. (New, R. (1990) in *The practical approach series* (Rickwood, D. and Hames, B.D., eds.), pp. 301, Oxford University Press, Oxford)(New, 1990).



**Figure 35:** Hand-driven extrusion apparatus with a capacity of 1 ml (LiposoFast-Basic, Avestin, Ottawa, Canada). A 50 - 400 nm pore-size polycarbonate membrane is placed in the filter holder (middle). Back-and-forth passages of the sample between the two syringes result in a defined size of extruded liposomes.

We used for our studies a hand-driven extrusion apparatus with a capacity of 1 ml (LiposoFast-Basic, Avestin, Ottawa, Canada), which is easily made at low cost and meets the needs for our experiments (Figure 35). Alternatively, we had the possibility to use a Lipex™ high-pressure extruder (Northern lipids inc., Vancouver, Canada). However, the disadvantage of this device was a frequent congestion of the filter pores in consequence of the high pressure on the system.

The main difficulty is to develop liposomal systems that feature certain flexibility in composition, no drug leakage and long circulation half-lives. Therefore, efficient loading of material into the liposome and prevention of leakage presents a fundamental issue. Most of the water-soluble materials, such as carboxyfluorescein and propidium iodide, will be entrapped into liposomes by introducing aqueous solutions of these materials before or at some stage during the manufacture of the liposomes. However, this method is highly inefficient due to the fact that concentration is equal inside and outside the liposomes. As shown theoretical in Figure 6, the captured volume of liposomes is related to the liposome diameter, the surface area of the vesicles (which is proportional to the square of the radius), lipid weight and number of vesicles. It represents a small

percentage of the whole suspension only, explaining the inefficiency of passive entrapment. Some materials can not be incorporated by another, more efficient (active) loading method. Oligonucleotides and plasmids, for example, require a gentle working method at physiologic pH and temperatures. For inexpensive and simply available substances, though, losses can be accepted and it is not necessary to develop a specific drug incorporation procedure.

Certain types of compounds with ionizable groups and those that display both, lipid and water solubility, can also be introduced into liposomes after formation of the intact membranes (New, 1990). A substantial challenge with such substances is to retain them inside the liposomes and to circumvent leakage. Achieving equilibration between the liposome interior and exterior is a driving force in every system. If a lipophilic substance can pass the membrane and get inside the liposome, it is not hampered to go the same way back out again. However, there are substances that precipitate in a special form upon loading and pH change, respectively. Such compounds are the anticancer drugs daunomycin and doxorubicin that precipitate in the liposome interior in a form of gel with low solubility product. They practically do not leak out in the scale of days (Lasic et al., 1995). This is confirmed by the high loading efficiencies achieved in experiments with daunomycin in the present work. Furthermore, leakage was not excessive in the length of time, even after four days of storage at 4°C.

On the other hand, a too high stability of liposomes is rather disadvantageous than desired. Remaining inside of stable liposomes, entrapped materials are not delivered to the target tissue, organs or cells. The objective is, to find the right balance between stability in the circulation and rapid endosomal release when vesicles are taken up by the target cells. An approach to resolve this problem is the development of (sterically stabilized) pH-sensitive liposomes (Simoes et al., 2004). Such liposomes are stable at physiological pH 7.4 but undergo destabilization and acquire fusogenic properties under

acidic conditions, thus leading to the release of their aqueous contents. Liposomes encounter such changes in pH during the process of receptor mediated endocytosis as the pH in the endosomal compartment is characterized to be around 5.5 (Tycko et al., 1983). Destabilization of the liposomal membrane can also be induced by bound amphiphilic peptides that adopt an  $\alpha$ -helical conformation in an acidic environment (Vogel et al., 1996) or the use of mixtures of cationic and ionizable anionic lipids (Duezguenes and Nir, 1999). Such pH-sensitive liposomes are typically prepared from mixtures of dioleoylphosphatidylethanolamine (DOPE), which adopts a non-bilayer inverted hexagonal ( $H_{II}$ ) phase in isolation, and an ionizable anionic lipid such as cholesterolhemisuccinate (CHEMS). In its negatively charged form at elevated pH values, CHEMS stabilizes DOPE in its bilayer organization. Protonation of CHEMS at pH values below its pK abolishes its stabilizing effect, leading to membrane inversion, membrane fusion and the release of entrapped substances into the liposome-surrounding compartment (Hafez et al., 2000). This technology can be applied both to conventional liposomes as well as long-circulating, sterically stabilized liposomes (Slepshkin et al., 1997). Such pH-sensitive liposomes consisting of DOPE and CHEMS were produced and filled with propidium iodide in order to enhance endosomal drug release in the present work. It has been shown on Figure 18 that cells showed fluorescent signal one hour after incubation with pH-sensitive liposomes. However, despite this advantage of fast drug release, such liposomes were not sufficiently stable and incorporated substances leaked out when stored longer than 24 hours.

## 5.2 IN VITRO ASSAYS

Antibody conjugated liposomes can be used for targeting of organs and tissues *in vivo*. In order to study cellular uptake of OX26-immunoliposomes, rat glioma RG2 cells, which acquire transferrin by receptor mediated endocytosis, were used. This cell line was previously shown to take up OX26 mAb connected covalently to liposomes (Huwyler et al., 1999; Huwyler et al., 1997). The question rises if the developed novel design of biotinylated immunoliposomes, linked via a non-covalent streptavidin-biotin binding to the OX26-streptavidin conjugate, is taken up the same way by this cell line. Immunostaining of RG2 cells with free OX26 mAb and visualization by a secondary antibody against mouse antibody, confirmed the presence of transferrin receptor. It was expressed on cellular surface, as well as in the intracellular compartment when fixed cells were permeabilized prior to immunostaining (Figure 15). Examination by confocal microscopy showed a fluorescent staining pattern of the cell plasma whereas incubation at 4°C inhibited cellular uptake. Under these conditions, fluorescence signal was restricted to the cellular surface, since receptor-mediated endocytosis is inhibited at low temperatures.

Incubation at 37°C of RG2 cells with fluorescent-labeled OX26-streptavidin (Figure 17 A) resulted in accumulation of fluorescence within the cell, similarly. Furthermore, rat glioma RG2 cells incubated with biotinylated OX26-streptavidin immunoliposomes, which were filled with carboxyfluorescein to represent the liposomal cargo, exhibited a similar staining pattern (Figure 17 B). Fluorescent OX26-immunoliposomes were taken up by RG2 cells and did accumulate in distinct intracellular compartments, probably endosomes or lysosomes. After one hour of incubation, the entire cytoplasm showed a well-defined, particulate staining pattern. Background fluorescence of cells examined in

control experiments was not or only weakly fluorescent. This confirms that the signal originates from fluorescent immunoliposomes. This was further shown by competition experiments with free OX26 mAb, with the aim of occupying OX26 mAb binding-sites on the transferrin receptor (Figure 17 C). Fluorescence intensity was considerably diminished by this competition. In the face of the fact that it is hardly possible to achieve complete inhibition by competition, there is always some residual fluorescence present. Additionally, transferrin receptor does not disappear after mediating cellular (iron) uptake. The receptor is recycled after endocytosis with bound iron and release of the latter into the cell. Reoccurring on the cellular surface, the receptor is ready for the next endocytosis cycle. All these observations suggest that OX26-streptavidin conjugated biotinylated immunoliposomes penetrate RG2 cells by means of endocytosis as it was shown for other OX26-immunoliposomes.

The question arises of whether targeting of skeletal muscle could be achieved using OX26-streptavidin as a vector directed against the transferrin receptor. The transferrin receptor is expressed by different organs, such as the liver, spleen, general vascular endothelium and the blood-brain barrier. In skeletal muscle, transferrin has been shown to have an important role in muscle growth, i.e. the process of myoblast and satellite cell proliferation, their fusion to myotubes and their further differentiation into muscle fibers (Ozawa, 1989). Studies with, for example, primary cultures of chick muscle cells (Sorokin et al., 1987) have clearly demonstrated high expression levels of functional transferrin receptors regardless of the state of growth or differentiation of these cells. We confirmed, by immunostaining experiments using the OX26 mAb, the presence of the transferrin receptor in rat skeletal muscle tissue (Figure 13). Tissue sections perpendicular to the muscle fibers show an intense immunostaining at the periphery of the myofibers (which have a diameter of 50 - 100  $\mu\text{m}$ ), as well as at the periphery of the



enclosed myofibrils. The staining of the myofiber surface can also be seen in longitudinal sections. These findings were yet endorsed by the little or no fluorescence in control experiments using secondary antibody only or an unspecific mouse IgG<sub>2a</sub> isotype control antibody. Incubation of L6 cells, a cell line derived from rat skeletal muscle, with OX26 mAb at 37°C followed by visualization of the OX26 mAb using a fluorescent secondary antibody (Figure 14) reveals a fluorescent signal on the cell surface as well as a particulate intracellular staining pattern. This observation suggests that the OX26 mAb is internalized by L6 cells under cell-culture conditions, and subsequently accumulates within the endosomal compartment of these cells. At 4°C, binding of OX26 mAb to the cell surface only was observed (Figure 14 C) because of inhibition of receptor-mediated endocytosis at low temperature. Our findings are in line with previous reports on expression levels of the transferrin receptor in L6 cells, which indicated a receptor density of approximately 200000 receptors per L6 myocyte (Fava et al., 1981). We conclude from these experiments that the L6 cell line can be considered to be a representative cell-culture model of skeletal muscle that may be used to study transferrin receptor-mediated transport processes *in vitro*.

Uptake experiments in L6 cells (Figure 16) and RG2 cells (Figure 17) demonstrated that the functionality of the OX26 mAb is retained after chemical modification and coupling to streptavidin. Incubation of OX26-streptavidin, which was fluorescence-labeled using biotin-fluorescein, resulted in a strong intracellular accumulation of fluorescence in L6 cells (Figure 16 A). Similar results were obtained using carboxyfluorescein loaded OX26-immunoliposomes (Figure 16 B). The observed effects were mediated specifically by the OX26 mAb, since competitive inhibition of cellular uptake was observed in presence of free OX26 mAb (Figure 16 C). The percentage of positive cells in these experiments was estimated to be over 90 %. We conclude that biotinylated OX26-immunoliposomes, despite their big particulate size of 150 nm, are transported

across the plasma membrane of L6 muscle cells by means of receptor-mediated endocytosis. Experiments with RG2 cells confirmed these results (Figure 17) in rat glioma cells.

Recapitulating, these experiments confirm that the developed innovative drug carrier system (OX26 conjugated via streptavidin-biotin bond to biotinylated immunoliposomes) is taken up by the two transferrin receptor expressing cell lines, glioma RG2 and muscle L6 cells, by means of endocytosis.

It was been shown in several studies that liposomal cargo is released in a time-dependent manner to the cytoplasm. The kinetics of endosomal release (Cerletti et al., 2000) are very similar to the one described for other liposomal delivery systems, i.e. folate-targeted liposomes (Vogel et al., 1996). Among other groups, Vogel et al. also demonstrated that the process of drug release can be accelerated by the use of pH-sensitive liposomes. By taking advantage of the decreased pH within the endosomal compartment, drug incorporation into pH-sensitive liposomes can facilitate its release after uptake by transferrin receptor expressing cells. Two different liposome formulations, a pH-sensitive and a conventional formulation, were synthesized and their release of incorporated drug in transferrin receptor expressing RG2 cells was compared (Figures 18 and 19). Findings corresponded broadly to published data. Major differences could be manifested only at early time points, with the most notable distinction after 3 hours (Figure 18 B and E). Interestingly, comparison after one hour could not point out an evident distinction between pH-sensitive and conventional immunoliposomes. Propidium fluorescence is detected in the cell only when liposomes have successfully released their contents into the cytoplasm. Upon binding to RNA or diffusion into the nucleus and association with DNA, a dramatic increase in fluorescence is observed,

that is distinguishable from unbound PI (Vogel et al., 1996). However, leakage of liposomes and absence of free PI was not controlled and may explain similar results for the two formulations after one hour, but a distinctive differentiation after only 3 hours. Figures 18 and 19 reveal an outstanding staining pattern with most of the fluorescence localized in the nucleoli and the cytoplasm. As nucleoli are the organelles in the nucleus where ribosomes are synthesized, they are particularly important and multiplied when protein expression is required, hence when cells are in division state. PI is used to visualize DNA and RNA. What may explain fluorescence of nucleoli. The peculiar nucleolus staining has been shown by Vogel et al. similarly. Fluorescence was less pronounced after 24 and 36 hours for both formulations what may be due to a dilution effect of dividing cells (liposomes were removed after 3 hours).

We can summarize our preliminary results as follows: OX26-immunoliposomes have been taken up by RG2 cells and released their cargo into the cells. Release was time-dependent and could be accelerated by incorporating the dye into pH-sensitive liposomes. Further experiments will be needed to get a quantitative assessment of the process of endosomal release.

A variety of gene delivery systems have been tested including viruses and liposomes. Because of the risk of infectivity and their possible immunogenic, cytopathic or recombinogenic effects, there are potential complications associated with viral vectors (Xu et al., 2002). Consequently, a significant amount of attention has been directed at nonviral vectors for the delivery of molecular therapeutics. The lack of immunogenicity may be the most important advantage of the liposome approach. Gene expression of “immunoliposomal” administered expression vectors *in vitro* was examined using two different, commercially available and highly sensitive plasmids: pGL3-Basic Luciferase

Vector (Promega) and  $\beta$ -galactosidase plasmid DNA (pcDNA<sup>TM</sup>3.1/myc-His/lacZ, Invitrogen, Carlsbad, CA). Luciferase expression vector incorporated into OX26-immunoliposomes and administered on RG2 and L6 cells, did lead to a marginal luciferase expression only (Figure 21). The presence of complete DNA within the liposomes was proofed by agarose electrophoresis (Figure 20) and corresponded to the indicated molecular weight of the commercial plasmids, controlled by a 1 kb DNA ladder. Furthermore, the control experiment of DNA transfection by using a well established transfection reagent (lipofectamine) that revealed very high luciferase expression on both examined cell lines, confirmed the function of the plasmid. The expression level of the positive control was 400 fold higher than the level of OX26-immunoliposomes. Since incubation time was 24 hours, incubation time was not a limiting factor in these experiments That should be largely sufficient for endosomal uptake (Note:  $T_{1/2}$  values for transferrin receptor endocytosis in erythroid cells were shown to be approximately 1.5 min (Ponka and Lok, 1999)) and gene expression, and does not explain the outstanding difference between lipofectamine transfection and gene delivery by using immunoliposomes. Gene expression experiments using a  $\beta$ -galactosidase expression vector (pcDNA<sup>TM</sup>3.1/myc-His/lacZ), with at least similar sensitivity, did not show better results for liposomal gene delivery. Cells transfected with lipofectamine likewise expressed  $\beta$ -galactosidase in a pronounced extend, clearly distinguishable from liposomal transfected cells that didn't exhibit the characteristic blue staining of X-gal, confirming  $\beta$ -galactosidase expression.

The results of these studies of gene expression via liposomal administration can be summarized with the conclusion that RG2 and L6 cells can be used both to study gene expression of luciferase and  $\beta$ -galactosidase expression vectors but that gene expression could not be achieved by administration plasmids incorporated into immunoliposomes.

In summary, marginal gene-transfer by immunoliposomes could be achieved only. The question arises if incomplete cellular uptake of DNA or intracellular enzymatic degradation of the transported DNA might be the reason for this low transfection efficiency. To clarify this point, additional DNA uptake experiments were performed.

To investigate endosomal release and location of liposome incorporated DNA, Cy3-labeled oligonucleotides were encapsulated into immunoliposomes and administered to RG2 cells. OX26-immunoliposomes were loaded by the gentle freeze-thaw method and as a control, unconjugated liposomes were examined in parallel. Figure 22 confirms the uptake of the oligonucleotides incorporated into OX26-immunoliposomes. Furthermore, fluorescence signal after 24 h incubation with unconjugated liposomes is apparently decreased, compared to immunoliposomes. That confirms a more rapid uptake of targeted OX26-immunoliposomes in a directly measurable form. Simultaneously, these observations also show an uptake, even if decreased, of “unspecific” liposomes without connected targeting vector. Additionally, after an incubation of 40 hours, no difference between antibody conjugated OX26-immunoliposomes and unspecific biotinylated PEG-liposomes could be recognized. In spite of the more rapid uptake by OX26-targeted immunoliposomes, signals could not be distinguished from those, obtained with bare liposomes after longer incubation times. This extensive unspecific uptake may result from interactions of biotin with cell surface structures, such as other receptors or uptake mediating proteins. Another possibility could be the fusion of liposomal bilayer with cell membranes or unspecific uptake mechanisms via other transporters. An explicit location of the fluorescence within the cells was difficult to determine. Figure 23 evidences a predominantly fluorescence signal in the cytoplasm, but not in the nucleus. Thus, neither oligonucleotides delivered by OX26-immunoliposomes, nor by bare liposomes reach nucleus within 40 hours and rather remain in the cytoplasm. DNA

plasmids containing a (therapeutic) gene need to enter the nuclear compartment for transcription and integration into the host cell genome for stable expression (Belting et al., 2005). Small inhibitory RNA (siRNA) on the contrary, are processed for specific targeting of complementary mRNA sequences in the cytosol and have to escape therefore through the liposomal and endosomal membrane into the cytosol. Thus, if immunoliposomes are filled with bioactive RNA structures, delivery to the nucleus has not to be achieved as protein synthesis takes place in the cytosol. For liposomal DNA plasmids, however, delivery to the nucleus is mandatory and may not be reached, relating to used immunoliposomes. Moreover, once inside the nucleus, plasmid mediated effects will not persist, unless extraneous DNA integration into the host cell chromatin structure is attained. Whereas retroviral vectors are capable of integrating into the host genome, non-viral delivery systems are restricted to extra chromosomal plasmid expression and may even exit the nucleus during cell division (Belting et al., 2005). Considering all this, a detailed understanding of how bioactive peptides and nucleic acids are processed and targeted in the intracellular compartment, is essential to develop an eligible gene delivery system.

Zhang et al. (Zhang et al., 2002b) used a liposomal drug delivery system to bring therapeutic genes to the nuclear compartment of implanted cancer cells by conjugating two different receptor-specific monoclonal antibodies to the surface of PEG-liposomes. Mice were implanted with intracranial human glial brain tumors. The mAb against mouse transferrin receptor enabled transport across the tumor vasculature, which is of mouse brain origin. The mAb against human insulin receptor, which was simultaneously connected to the liposomes, caused transport across the plasma membrane and the nuclear membrane of the human brain cancer cell. This study showed that such sophisticated liposomal gene delivery systems can produce significant therapeutic effects in an experimental brain cancer model. These findings suggest linkage of OX26-

immunoliposomes with a second antibody that controls transport within the cells. It was not examined in the present work and may be the objective of future projects.

We can summarize that liposomal contents passed the cellular plasma membrane and were delivered into the cytoplasm, where the exact localization could not be defined. Uptake of targeted OX26-immunoliposomes in RG2 cells occurred earlier than uptake of biotinylated liposomes; therefore cells should not be incubated longer than 24 hours in order to discern specific uptake from unspecific interactions. Overcoming this first barrier of the cellular membrane, delivery to the nucleus seemed to be incomplete. Solutions therefore may be coupling liposomes with multiple antibodies, responsible for mediating overcoming of the different barriers to optimize gene expression.

Targeting of small molecules to tumour cells using immunoliposomes may enhance considerably intracellular accumulation of the transported pharmaceuticals. This technique is of special interest when it comes to the treatment of drug-resistant tumours (Mamot et al., 2003). In these cells, overexpression of drug-efflux transporters, such as the ABC-transporter P-glycoprotein (Eytan and Kuchel, 1999; Roninson, 1992), prevents cellular uptake of free drug and thus confers the multidrug resistance phenotype to these cells. Previous studies (Goren et al., 2000; Huwyler et al., 2002; Suzuki et al., 1997) have indeed demonstrated that by-passing of plasma membrane-associated P-glycoprotein using liposomal carriers leads to an enhanced intracellular accumulation of the transported molecules. However, this did not necessarily translate to enhanced pharmacological effects (Goren et al., 2000). In a set of toxicity *in vitro* experiments, the immunoliposome-based drug delivery system was used as a more specific strategy in order to promote cellular uptake of liposomal cargo, tritium-labeled daunomycin ( $[^3\text{H}]$ daunomycin). Daunomycin was therefore incorporated within

biotinylated OX26-immunoliposomes to induce a cytotoxic effect in RBE4 cells. These cells express P-glycoprotein (Begley et al., 1996) and are therefore resistant to the anthracycline antibiotic: the LD<sub>50</sub> dose of 10 µM determined in the sulforhodamine B cytotoxicity was 20-fold higher as compared to the corresponding value in the chemosensitive RG2 rat glioma cell line (Figures 24 and 25). As observed earlier with non-biotinylated immunoliposomes (Huwylar et al., 2002), cellular uptake of daunomycin increased significantly (2- to 3-fold) if the drug was incorporated within biotinylated OX26-immunoliposomes (Figure 26). Growth inhibition of RBE4 cells was analyzed to show that intracellular accumulation of liposomal daunomycin was associated with a pharmacological effect, which was both, time- and dose-dependent (Figure 27). Since competitive inhibition of cellular uptake with free OX26 mAb led to a statistically significant reduction of cytotoxicity, we can assume that the observed effects were mediated by the OX26 mAb. Surprisingly, however, the pharmacological effect of liposomal daunomycin was lower than the one of the free drug (Figure 28). An explanation for this finding could be the observation, that endosomal release of drugs incorporated within OX26-immunoliposomes is a rather slow process. Quantitative determination of intracellular unloading of liposomal propidium iodide (Cerletti et al., 2000) indicated that this fluorescent dye was released from the endosomal compartment to the cytoplasm with an initial rate of 4 % of total intracellular dose per hour only. Data from Figure 29 support this view in that an increase of the incubation time has a considerably higher impact on cytotoxicity of liposomal daunomycin as compared to the free drug. As opposed to the situation after 1 or 3 hours (Figures 27, 28 and 29), after incubations longer than 12 hours, both formulations of daunomycin showed equivalent pharmacological effects. It is tempting to speculate that modifications of the phospholipid composition of the liposomes could be used to adjust the rate of intracellular release and thus the kinetics of pharmacological effects. Such a



strategy could be based on the principle of pH-sensitive liposomes: The endosomal compartment is characterized by a low pH value of 5.0 to 5.5 (Tycko et al., 1983). Incorporation of pH-sensitive peptides (which adopt an amphiphilic  $\alpha$ -helical conformation on a mildly acidic environment) were shown to promote endosomal release of a liposomal cargo (Parente et al., 1988; Vogel et al., 1996). pH-sensitive liposomes that transform into an inverted hexagonal phase and release the liposomal content within shorter times have been mentioned before and will be described subsequently in more details (5.5. Future perspectives).

### **5.3 IN VIVO ASSAYS**

Antibody conjugated liposomes can be used for targeting of organs and tissues *in vivo*. Previous studies have demonstrated that brain drug delivery of small molecules can be achieved *in vivo* using immunoliposomes conjugated to the OX26 mAb to the rat transferrin receptor (Huwyler et al., 1996; Huwyler et al., 1997). In previous experiments, free OX26 mAb has been shown to permeate across the blood-brain barrier (Bickel et al., 1994). Labeled OX26 mAb were detected after internal carotid artery infusion at the luminal plasma membrane of brain capillary endothelia, within endocytotic vesicles of 50 - 100 nm and beyond the abluminal plasma membrane. Studies demonstrated that immunoliposomes with a similar composition to the liposomes used in present work had favorable *in vivo* pharmacokinetic properties, e.g. minimal unspecific tissue binding (Huwyler et al., 1996; Huwyler et al., 1997). Tissue distribution of the immunoliposomes was mediated by the OX26 mAb with selective accumulation in brain tissue.

The pharmacokinetics and tissue distribution of free daunomycin and different liposomal formulations of daunomycin were determined in the rat after intravenous injection

(Figure 31). Free daunomycin is rapidly removed from the circulation. The apparent volume of distribution ( $V_D$ ) as well as the systemic plasma clearance of the free drug is high. The clearance value of 56 ml/min/kg is close to liver blood flow in the awake rat (60 to 80 ml/min/kg (Davies and Morris, 1993; Kawasaki et al., 1990)). This is in sharp contrast to the situation where daunomycin is incorporated within biotinylated PEG-liposomes. As expected from literature data (Lasic and Papahadjopoulos, 1995), the plasma clearance is very low and reduced 43-fold as compared to free daunomycin. Such pegylated liposomes have a very low apparent volume of distribution of 0.05 l/kg, which is almost identical to the plasma volume (0.032 l/kg (Davies and Morris, 1993)). Biotinylated PEG-liposomes were therefore used as a plasma volume marker for the calculation of organ PS products. Both, unspecific control immunoliposomes as well as OX26-immunoliposomes, have a higher plasma clearance than PEG-liposomes since decoration of the liposome surface with antibodies reverses partially the protective effect of PEG. This effect has been described for other particulate targets as well (Frank, 1993). It is important to note, however, that liposomes conjugated to the specific OX26 mAb are characterized by a higher  $V_D$  and plasma clearance as compared to control IgG<sub>2a</sub>-immunoliposomes. Analysis of brain tissue at 1 hour after intravenous administration (Figure 32) revealed indeed a two-fold higher tissue accumulation (in terms of %ID/ g brain tissue) as well as brain permeability (PS product) of OX26-immunoliposomes as compared to IgG<sub>2a</sub>-immunoliposomes. OX26-immunoliposomes showed also a higher brain accumulation than free daunomycin, this despite the fact that the PS product of free daunomycin is very high. The brain delivery of a given drug (%ID/g) can be described as the product of its PS product and its plasma AUC at a given time after injection (Pardridge, 1995a). Thus, brain delivery of free daunomycin is poor due to its rapid clearance from the circulation resulting in a short and low exposure of brain tissue. Note that no brain uptake is observed for PEG-liposomes, which results

in PS and %ID/g values of zero for this plasma volume marker. Figure 33 shows the advantages of OX26-immunoliposomes. The only difference between this formulation and OX26-immunoliposomes is the antibody and it shows effects that are not due to the OX26 mAb. In summary, these *in vivo* results obtained with biotinylated OX26-immunoliposomes are similar to previous results from studies with OX26-immunoliposomes prepared by covalent chemical coupling (Huwylar et al., 1996) indicating a low impact of the used coupling procedure.

Receptor mapping studies in cynomolgous monkey using monoclonal antibodies against the human transferrin receptor showed that distribution of such antibodies was not confined to brain tissue but that a significant percentage of the injected dose did accumulate in other tissues expressing the transferrin receptor such as skeletal muscle (Friden et al., 1996). Interestingly, the over-all pattern of tissue distribution was quite different for the two monoclonal antibodies which were tested. This may be a consequence of binding of the antibodies to different structural motives on the transferrin receptor. These results together with our findings suggest that *in vivo* drug targeting to skeletal muscle may be achieved by targeting of the transferrin receptor; using the streptavidin-conjugated OX26 mAb directed against the rat transferrin receptor, targeting of immunoliposomes to L6 skeletal muscle cells *in vitro* followed by intracellular accumulation was achieved and published (Schnyder et al., 2004). Two important questions were therefore if OX26-immunoliposomes, which have a particulate size of 100 - 150 nm, could be used for drug targeting to the brain as well as to skeletal muscle *in vivo*.

Besides brain tissue, skeletal muscle as well as several other tissues such as spleen, liver, heart and kidney were therefore analyzed (Table 3). Neither in skeletal muscle nor in any other of these tissues (and in sharp contrast to the brain), a superior targeting of

OX26-immunoliposomes as compared to IgG<sub>2a</sub>-immunoliposomes was observed. In these tissues, unspecific tissue interactions with antibody-conjugated liposomes seemed to mask effects mediated by the OX26 mAb. This can be explained by the fact that the brain is the only examined tissue where the OX26 antibody has been shown to permeate across the endothelial cell barrier of the vasculature by an active transport process (i.e. receptor mediated transcytosis (Pardridge et al., 1991)). Spleen and liver were two tissues, where immunoliposomes accumulated to a higher degree than free daunomycin. This could be indicative for their clearance by macrophages of the reticuloendothelial system. The opposite effect was observed for the kidney: this organ showed very high tissue permeability (PS product) for free daunomycin. This is in line with the observation that renal excretion of parent drug (25 % of applied dose in man) is a major pathway for elimination (Dollery, 1999). However, in muscle tissue, OX26-immunoliposomes did not mediate specific tissue uptake of daunomycin. This observation is in agreement with previous studies in rhesus monkey (Zhang et al., 2003c), where gene delivery using immunoliposomes directed against the human insulin receptor did result in a pronounced expression of the reporter gene ( $\beta$ -galactosidase) in brain, liver and spleen, but not in heart or skeletal muscle. The latter organs are perfused by capillaries with continuous endothelium. The endothelial pore system of this vasculature is too small to allow for a passive passage of 100 nm liposomes. For targeting of muscle tissue, a second antibody would be needed to trigger transport across the muscle capillary endothelial wall prior to OX26-mediated endocytosis of the immunoliposomes by muscle cells (Schnyder et al., 2004). Such a concept of double antibody targeting was applied recently (Zhang et al., 2002b) to anti-sense mRNA targeting of tumour tissue: A mouse anti-transferrin receptor antibody was used for transport across the tumour vasculature whereas an anti-insulin receptor

antibody did mediate transport across the plasma- and nuclear-membranes of the target cell.

## **5.4 FUTURE PERSPECTIVES**

One of the most interesting and promising challenges in drug targeting by the use of targeted immunoliposomes is the combination with gene targeting. However, this potential technology is in the fledging stages and has to be elaborated and optimized onward until it can be administered in a large-scale way. As discussed earlier (1.6. gene targeting), several groups have shown very promising results of gene expression after incorporating expression vectors into immunoliposomes (Shi et al., 2001a; Zhang et al., 2002a). Further, it has been shown that targeting can be obtained on two different stages. First, by the use of a specific targeting vector coupled to the liposome, and second, by incorporation of a specific promoter controlling the incorporated DNA plasmid (Shi et al., 2001b). We integrated a human alpha-skeletal actin gene into the before described pGL3 expression vector, in order to direct the expression of luciferase protein in muscle cells. However, this approach of gene expression of a muscle specific promoter containing plasmid was of limited success. Skeletal muscle cells transfected by lipofectamine with the modified pGL3 plasmid did not express luciferase in a higher extend than glioma cells (results not shown) and no distinction between cells originating from muscle or from brain could be demonstrated. Nevertheless, this concept will be followed up sure enough, considering the growth of impact over the last few years of this subject and further, promising results.

A basic knowledge about the intracellular processing of any drug delivery system remains to be fundamental for the development of future applications. Characterization

of intracellular fate, i.e. of immunoliposomes, has to be elucidated therefore in order to understand uptake mechanism and liposomal release. In the present work, electron spin resonance (ESR) technique was applied to examine intracellular fate of immunoliposomes *in vitro*. We developed a method to monitor *in vitro* pH-changes of the environment of liposomes. Two spin labels were used to be incorporated into liposomes or liposomal bilayer (Figure 36).

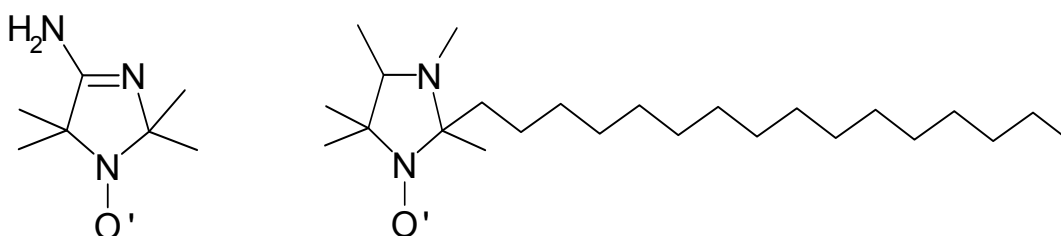


**Figure 36:** The chemical structure of spin labels. Left panel: 4-Amino-2,2,5,5-tetramethyl-3-imidazoline-1-yloxy, pK = 6.1 (hydrophil); Right panel: 2-Heptadecyl-2,3,4,5,5-pentamethylimidazolidine-1-yloxy, pK = 4.5 (lipophil). Both purchased from Magnettech GmbH (Berlin, FRG).

The lipophil spin label 2-Heptadecyl-2,3,4,5,5-pentamethylimidazolidine-1-yloxy (HP) (Magnettech GmbH, Berlin, FRG) possesses in addition to the spin trap (nitroxyl radical) a long, saturated hydrocarbon chain (heptadecyl) that can be incorporated within the liposomal bilayer. The other used spin label 4-Amino-2,2,5,5-tetramethyl-3-imidazoline-1-yloxy (AT) (Magnettech) is water soluble and was incorporated into liposomes by the freeze-thaw technique. The molecular structures of the spin probes are shown in Figure 36. Nitroxyl radicals are spin labels for electron spin resonance (ESR), an investigative tool for the study of radicals (spins) formed in solid and liquid materials. Due to charge-dipol interactions, one of the two isomeric forms of a nitroxyl

radical is favored in a polar environment and therefore depends also on pH (Bittner et al., 2001). Transitions can be induced between spin states by applying a magnetic field and then supplying electromagnetic energy.

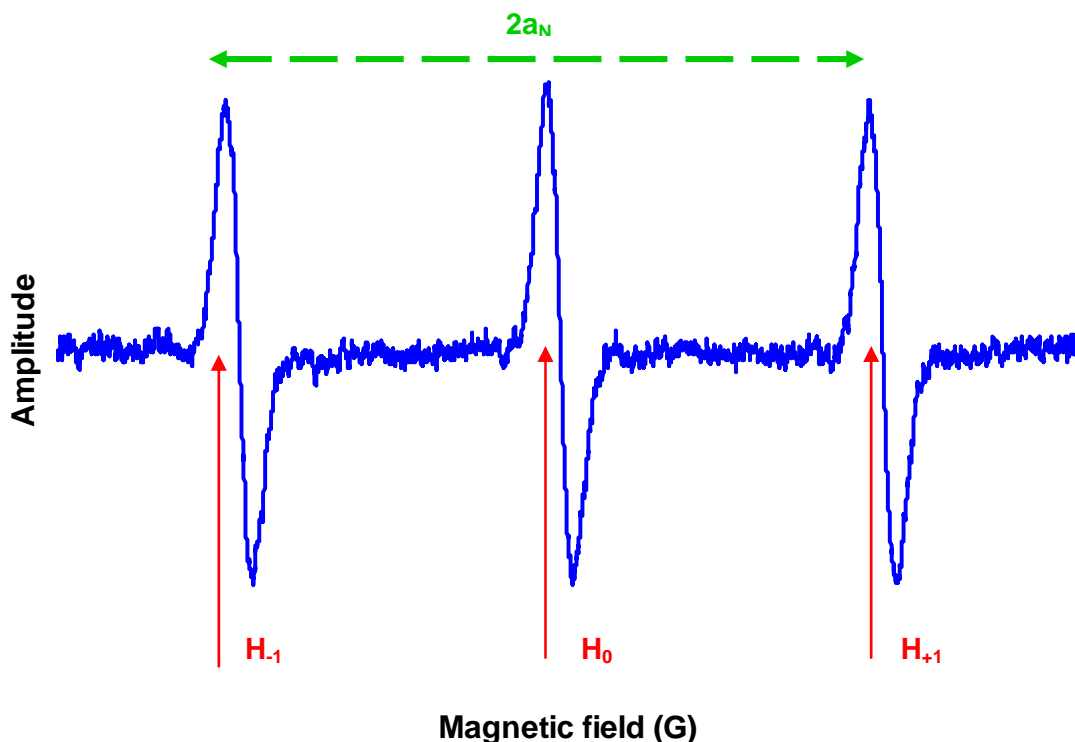


**Figure 37:** ESR spectra of a freely movable spin label.  $2a_N$  (distance between the first and the third peak) and H-Values (intersection with baseline) can be read off from the spectral shape.

The resulting absorption spectra are described as electron spin resonance (ESR) spectra (Figure 37). The distance between the first and the third peak in the ESR spectrum ( $2a_N$ ) is directly proportional to the spin density on the nitrogen atom of the nitroxyl moiety. Thus,  $2a_N$  is sensitive to the polarity of the environment of the spin probe and depends on pH. Moreover, the ratios between the signal amplitudes are indicative for the mobility of the spin probe. Spin labels in an environment where

mobility is high, result in an isotropic spectrum characterized by three absorption peaks with comparable signal amplitudes.

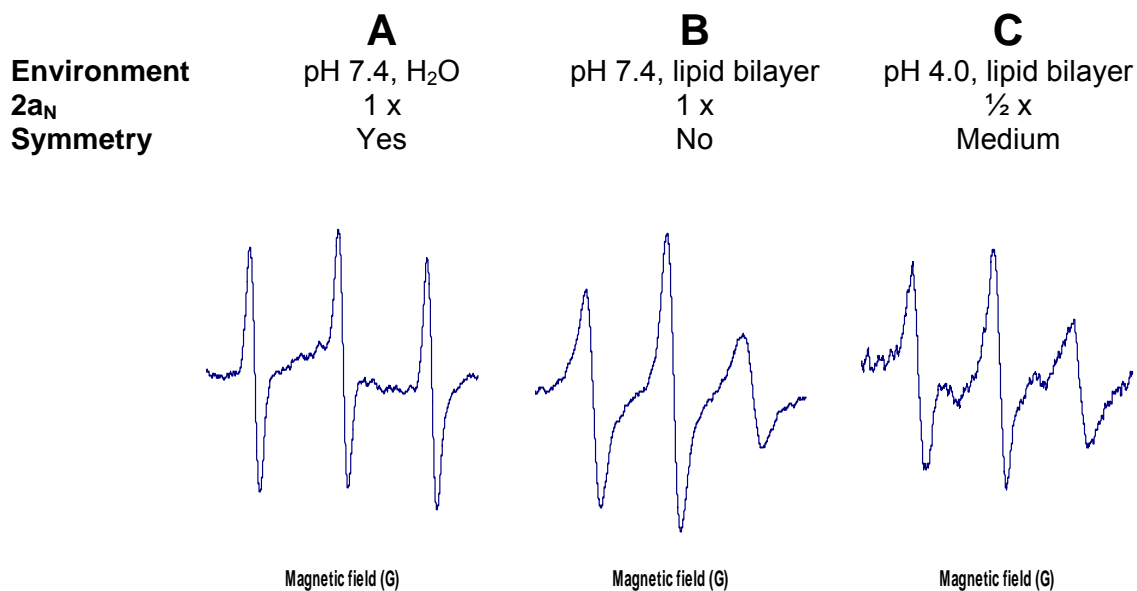


**Figure 38:** ESR spectra and trends of values of spin labels in different environments. **A:** hydrophil spin label (4-Amino-2,2,5,5,-tetramethyl-3-imidazoline-1-yloxy) dissolved in a buffer where it is freely movable; **B:** lipophil spin label (2-Heptadecyl-2,3,4,5,5,-pentamethylimidazolidine-1-yloxy ) incorporated in liposomal bilayer at pH 7.4; **C:** same as B at pH 5.0.

This is shown in Figure 38 A where the hydrophil spin label AT was dissolved in an aqueous buffer pH 7.4, where it is freely movable. Its spectrum presents three identical, even peaks. When the lipophil spinlabel HT was incorporated into the bilayer membrane of liposomes (by its hydrocarbon chain), its free movement is limited by other phospholipid-, cholesterol- and PEG molecules building up the membrane of the liposome. Spectra of such spin labels are not symmetric any longer as shown in Figure 38 B with pH-sensitive liposomes. These pH-sensitive liposomes were structured by DOPE, CHEMS and optionally PEG, as described before. Symmetry of the three peaks increased with lower pH, indicating more flexibility of the spin. This enhancement of freedom may be a consequence of formed H<sub>II</sub> phase (non-bilayer inverted hexagonal



phase), a liquid-crystalline phase allowing freer scope than the bilayer structure of intact liposomes at pH 7.4. This is illustrated only in a minor extent in Figure 38 C (primarily peak one and two), in the spectrum of the same spin label but at decreased pH of 5.0. As  $H_{II}$  phase seems to be a highly instable state and liposomes therefore decomposed at slightly lower pH, more crucial adjustments of symmetry could not be measured anymore. Decomposition of liposomes upon pH decrease was detected by a sudden disappearance of the characteristic opalescence of the dispersion and a formulation of a fine precipitate. As a consequence of leakage, these pH studies could not be carried out with the hydrophil spin label AT incorporated in pH-sensitive liposomes.

In order to examine behavior of spin labels in dependence of pH in a larger scale, the hydrophil spin label AT was titrated and analyzed at different pH. The spin probe was therefore dissolved in an appropriate aqueous buffer and ESR spectra were recorded at decreasing pH. The overall spectrum width  $2a_N$  (distance between first and third peak) from unprotonated AT (high pH) was greater than from protonated label (low pH).  $2a_N$  values and a simulation of a pH-titration-curve crossing the diagram points are shown in Figure 39.

These results suggest that *in vitro* characterization of intracellular fate of immunoliposomes can be done by ESR monitoring to some degree. Phase transition from liposomal bilayer to  $H_{II}$  phase was detected in liposomal suspension with a lipophil spin label. Further experiments with more stable (pH-sensitive) liposomes are required for same examinations with a hydrophil spin label that is incorporated into the liposomes. ESR is a convenient, rapid and simple method to monitor pH changes and drug release *in vitro* as well as *in vivo* and has been used by other groups (Bittner et al., 2001; Mäder et al., 1998). A study was made by Foster et al. (Foster et al., 2003) of the *in vivo* detectability of a pH-sensitive spin probe, and the efficacy of ESR-based techniques for pH measurement *in vitro* and *in vivo* in rats. Moreover, Mäder et al.

(Mäder et al., 1995) monitored *in vivo* drug release and polymer erosion from biodegradable polymers by ESR spectroscopy. A special implant composed of different layers was thereby manufactured and the mobility of introduced nitroxides was monitored by ESR spectroscopy. Evaluation of spectra gave information about motion of spin traps towards the border of the implant.

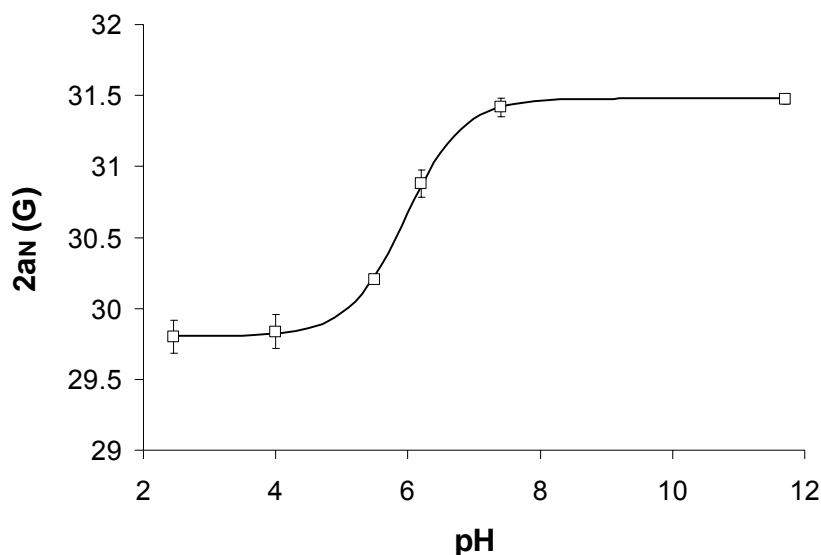


**Figure 39:** pH dependence of hydrophil spin label AT.  $2a_N$  values (distance between first and third peak in ESR spectra) of spin label dissolved in aqueous buffer. Spin probe was monitored at decreasing pH and a sigmoid pH-titration-curve simulation was fitted through the data points. **Data are means SEM (n = 3)**

We incubated cells with pH-sensitive immunoliposomes containing spin label in order to analyze cellular uptake. No ESR signals could be monitored in harvested cells, neither in supernatant medium. pH-sensitive immunoliposomes containing hydrophil spin probe AT could not be monitored because of leakage of this liposome formulation. Another reason responsible for this limited success is intracellular metabolism of the spin label radical by reduction and thus loss of the ESR signal, leading to sensitivity problems. Considering these difficulties, we decided not to go on with ESR projects and

focused on other methods to examine drug delivery and drug release that are described earlier in the other chapters.

The development of pH-sensitive liposomes is a possibility to enhance intracellular release of liposomal drug by the use of multifunctional liposomes. Such liposomal formulations release their contents spontaneously in an environment with a decreased pH. Liposomes encounter such changes in pH during the process of receptor mediated endocytosis as the pH in the endosomal compartment is characterized by a pH of ~5.5 (Tycko et al., 1983). Destabilization of the liposomal membrane can be induced by bound amphiphilic peptides which adopt an  $\alpha$ -helical conformation in an acidic environment (Vogel et al., 1996) or the use of mixtures of cationic and ionizable anionic lipids (Duezguenes and Nir, 1999). Such pH-sensitive liposomes are typically prepared from mixtures of dioleoylphosphatidylethanolamine (DOPE), which adopts a non-bilayer inverted hexagonal ( $H_{II}$ ) phase in isolation, and a ionizable anionic lipid such as cholesterolhemisuccinate (CHEMS). In its negatively charged form at elevated pH values, CHEMS stabilizes the DOPE in its bilayer organization. Protonation of the CHEMS at pH values below its pK abolishes its stabilizing effect leading to membrane inversion, membrane fusion and the release of entrapped substances into the liposome-surrounding compartment (Hafez et al., 2000). This technology can be applied both to conventional liposomes as well as long-circulating, sterically stabilized liposomes (Slepushkin et al., 1997).

There are other approaches to develop 'multifunctional' liposomes with the aim of optimizing liposomal design. Long circulating pegylated liposomes can be seen as a starting point for the design of multifunctional drug carrier systems. The properties of such targeted liposomes can be modulated and adopted to different needs by the combination of different types of vectors and enzymes bound to the liposome surface.

Previous reports describe the design of immuno-enzymosomes, i.e. immunoliposomes bearing enzymes on their surface that catalyze the conversion of prodrugs into active parent compounds (Vingerhoeds et al., 1993). Vingerhoeds et al. (Vingerhoeds et al., 1996) used a  $\beta$ -glucuronidase bearing enzymosome drug targeting system, directed against ovarian carcinoma cells by F(ab')<sub>2</sub> fragments of the mouse monoclonal 323/A3 antibody. This antibody recognizes a surface glycoprotein on a variety of carcinomas. After binding of immuno-enzymosomes to the target cells, the prodrug is administered and converted into the active drug in close proximity of the tumor cell. The density of the enzyme is thus increased substantially at the target cell surface using such a liposome-based targeting strategy. This is in particular valuable for tumors with little antigen expression.

In addition to these approaches, liposomes can be decorated with two or even more different peptidomimetic antibodies or targeting fragments to increase liposomal delivery of an incorporated drug or plasmid DNA to both extracellular epitopes as well as intracellular compartments. For example, one vector might be responsible for brain tissue targeting and another for inducing cellular uptake or intracellular transport, as already discussed. This strategy is based on the observation that some antigens may be attractive targets in terms of patterns of expression, yet, they are poor at delivering their cargo (i.e. DNA) to the appropriate cellular (i.e. nuclear) compartment (Tan et al., 2003).

In another set of experiments (Tan et al., 2003), liposomes were linked to a first antibody to the transferrin receptor and a second antibody specific for E-selectin. Targeting of the transferrin receptor offers a rapid internalization of the liposomal complex by receptor-mediated endocytosis. Tissue selectivity of the immunoliposomes is thereby enhanced by the antibody against E-Selectin, which exhibits a distinct and endothelial-selective pattern of expression.

Besides this promising construction of multifunctional liposomal carrier systems, another future perspective is the binding of liposomes to vectors that target structures in human, i.e. human insulin receptor. The use of such targeting antibodies and proteins is a further step towards development of liposomal delivery systems for clinical administration. With the coupling technology described in present study, where a streptavidin-biotin binding is used to link antibodies to biotinylated liposomes, such exchange of targeting vectors is easy and rapid. We used the mouse mAb OX26 against the rat transferrin receptor and showed the flexibility of this delivery system by the use of streptavidin-coupled IgG<sub>2a</sub> antibody as control. The basic tool for drug delivery to human cells is therefore represented, the only lacking component is an appropriate vector with a human target that merely has to be coupled with a streptavidin molecule.

The OX26 mAb targets the transferrin receptor and we consequently studied delivery to tissues and organs with above-average expression of transferrin receptor, such as the brain. Delivery systems to other organs and tissues have also been developed. Derycke et al. (Derycke et al., 2004) examined whether transferrin-mediated liposomal targeting of a photosensitizer is an effective strategy to attain tumor-selective accumulation of this compound when applied intravesically in rats. Bladder transitional-cell carcinoma cells overexpress the transferrin receptor on their surface. They could show a specific targeting into carcinoma cells of transferrin-conjugated liposomes, compared to unconjugated liposomes and they concluded that transferrin-mediated liposomal targeting of photosensitizing drugs is a promising potential tool for photodynamic therapy of superficial bladder tumors. Additionally, selective transferrin receptor mediated uptake by HeLa cells was shown by the same group (Gijssens et al., 2002).

A cooperating group in nephrology (Tuffin et al., Inselspital, Bern) used liposomes of the same composition as described in the present work, to target rat mesangial cells that

are characterized by expression of the Thy1.1 antigen. The OX7 monoclonal antibody directed against the Thy1.1 antigen was coupled to the liposomes by a covalent binding. Specific targeting of mesangial cells in kidney as well as specific pharmacologic effects were shown (publication in preparation).

Closing this chapter of future perspectives and to-be uses of liposomal delivery systems, it must be kept in mind that there are other fields where a drug targeting is desirable. In addition to therapeutic applications, a possible future use of immunoliposomes might include their use as diagnostic tools to localize, for example, tumor tissue (Mamot et al., 2004) or amyloid plaques in Alzheimer's disease (Kurihara and Pardridge, 2000; Lee et al., 2002), as described before.

## 6 CONCLUSIONS

In summary, this study demonstrates that biotinylated immunoliposomes can be used to target incorporated drugs to target cells *in vitro* or *in vivo*. The observed pharmacokinetics and tissue distribution in the rat confirmed findings from previous studies using an alternative design of covalently conjugated immunoliposomes. *in vitro*, cellular uptake of OX26-immunoliposomes by multidrug-resistant target cells expressing the transferrin receptor resulted in by-passing of P-glycoprotein and thus to an enhanced intracellular accumulation of the cytotoxic agent daunomycin. Intracellular accumulation of daunomycin was mediated by the OX26 mAb and associated with a pharmacological effect. While the presented data demonstrates the feasibility of targeting using biotinylated immunoliposomes, further experimentation will be needed to optimize the properties of the liposomal carrier. In particular, modifications of the phospholipid membrane composition may be needed to accelerate intracellular release of the transported cargo. The target specificity of biotinylated immunoliposomes may be tailored to specific needs by substitution of the OX26 mAb for an alternative, streptavidin-conjugated targeting vector. Such modifications can be realized with ease using the proposed immunoliposome design and may bring the described technology to its full potential.

## 7 REFERENCES

- Allen, T. M. (1994a). "Long-circulating (sterically stabilized) liposomes for targeted drug delivery." *Trends Pharmacol. Sci.*, 15, 215-220.
- Allen, T. M. (1994b). "The Use of Glycolipids and Hydrophilic Polymers in Avoiding Rapid Uptake of Liposomes by the Mononuclear Phagocyte System." *Advanced Drug Delivery Reviews*, 13(3), 285-309.
- Allen, T. M., Brandeis, E., Hansen, C. B., Kao, G. Y., and Zalipsky, S. (1995). "A new strategy for attachment of antibodies to sterically stabilized liposomes resulting in efficient targeting to cancer cells." *Biochim. Biophys. Acta*, 1237(2), 99-108.
- Allen, T. M., and Chonn, A. (1987). "Large unilamellar liposomes with low uptake into the reticuloendothelial system." *FEBS Lett*, 223(1), 42-6.
- Allen, T. M., Mehra, T., Hansen, C., and Chin, Y. C. (1992). "Stealth liposomes: an improved sustained release system for 1-beta-D-arabinofuranosylcytosine." *Cancer Res.*, 52(9), 2431-2439.
- Allen, T. M., Sapra, P., Moase, E., Moreira, J., and Iden, D. (2002). "Adventures in targeting." *J. Liposome Res.*, 12(1-2), 5-12.
- Arnold, D. L., and Matthews, P. M. (2002). "MRI in the diagnosis and management of multiple sclerosis." *Neurology*, 58(8 Suppl 4), S23-31.
- Basanez, G., Goni, F. M., and Alonso, A. (1997). "Poly(ethylene glycol)-lipid conjugates inhibit phospholipase C-induced lipid hydrolysis, liposome aggregation and fusion through independent mechanisms." *FEBS Lett*, 411(2-3), 281-6.
- Begley, D. J., Lechardeur, D., Chen, Z. D., Rollinson, C., Bardoul, M., Roux, F., Scherman, D., and Abbott, N. J. (1996). "Functional expression of P-glycoprotein in an immortalised cell line of rat brain endothelial cells, RBE4." *J. Neurochem.*, 67(3), 988-995.
- Belting, M., Sandgren, S., and Wittrup, A. (2005). "Nuclear delivery of macromolecules: barriers and carriers." *Adv Drug Deliv Rev*, 57(4), 505-27.
- Bendas, G., Krause, A., Bakowsky, U., Vogel, J., and Rothe, U. (1999). "Targetability of novel immunoliposomes prepared by a new antibody conjugation technique." *Int. J. Pharm.*, 181(1), 79-93.
- Bickel, U., Kang, Y. S., Yoshikawa, T., and Pardridge, W. M. (1994). "In vivo demonstration of subcellular localization of anti-transferrin receptor monoclonal antibody-colloidal gold conjugate in brain capillary endothelium." *J. Histochem. Cytochem.*, 42(11), 1493-1497.



- Bickel, U., Yoshikawa, T., and Pardridge, W. M. (1993). "Delivery of peptides and proteins through the blood-brain barrier." *Adv. Drug Deliv. Rev.*, 10, 205-245.
- Bittner, B., Gonzalez, R. C., Walter, I., Kapps, M., and Huwyler, J. (2003). "Impact of Solutol HS 15 on the pharmacokinetic behaviour of colchicine upon intravenous administration to male Wistar rats." *Biopharm Drug Dispos*, 24(4), 173-81.
- Bittner, B., Isle, H., and Mountfield, R. J. (2001). "The use of election paramagnetic resonance spectroscopy in early preformulation experiments: the impact of different experimental formulations on the release of a lipophilic spin probe into gastric juice." *Eur J Pharm Biopharm*, 51(2), 159-162.
- Bobo, R. H., Laske, D. W., Akbasak, A., Morrison, P. F., Dedrick, R. L., and Oldfield, E. H. (1994). "Convection-enhanced delivery of macromolecules in the brain." *Proc. Natl. Acad. Sci. U S A*, 91(6), 2076-2080.
- Bulte, J. W., Douglas, T., Mann, S., Frankel, R. B., Moskowitz, B. M., Brooks, R. A., Baumgarner, C. D., Vymazal, J., Strub, M. P., and Frank, J. A. (1994). "Magnetoferritin: characterization of a novel superparamagnetic MR contrast agent." *J. Magn. Reson. Imaging*, 4(3), 497-505.
- Carlsson, J., Kullberg, E. B., Capala, J., Sjoberg, S., Edwards, K., and Gedda, L. (2003). "Ligand liposomes and boron neutron capture therapy." *J. Neurooncol.*, 62(1-2), 47-59.
- Cerletti, A., Drewe, J., Fricker, G., Eberle, A. N., and Huwyler, J. (2000). "Endocytosis and transcytosis of an immunoliposome-based brain drug delivery system." *J. Drug Targeting*, 8(6), 435-447.
- Cullis, P. R., and de Kruijff, B. (1978). "The polymorphic phase behaviour of phosphatidylethanolamines of natural and synthetic origin. A <sup>31</sup>P NMR study." *Biochim Biophys Acta*, 513(1), 31-42.
- Davies, B., and Morris, T. (1993). "Physiological parameters in laboratory animals and humans." *Pharm Res*, 10(7), 1093-5.
- Derycke, A. S., Kamuhabwa, A., Gijssens, A., Roskams, T., De Vos, D., Kasran, A., Huwyler, J., Missiaen, L., and de Witte, P. A. (2004). "Transferrin-conjugated liposome targeting of photosensitizer AIPcS4 to rat bladder carcinoma cells." *J Natl Cancer Inst*, 96(21), 1620-30.
- Dollery, C. (1999). "Daunorubicin (hydrochloride)." In Dollery, C. (ed). *Therapeutic drugs* (London: Churchill Livingstone), pp. D18-D23.
- Duezguenes, N., and Nir, S. (1999). "Mechanisms and kinetics of liposome-cell interactions." *Adv. Drug Deliv. Rev.*, 40(1-2), 3-18.
- Dufresne, I., Desormeaux, A., Bestman-Smith, J., Gourde, P., Tremblay, M. J., and Bergeron, M. G. (1999). "Targeting lymph nodes with liposomes bearing anti-HLA-DR Fab' fragments." *Biochim Biophys Acta*, 1421(2), 284-94.

- Dunnick, J. K., McDougall, I. R., Aragon, S., Goris, M. L., and Kriss, J. P. (1975). "Vesicle interactions with polyamino acids and antibody: in vitro and in vivo studies." *J Nucl Med*, 16(6), 483-7.
- Emanuel, N., Kedar, E., Bolotin, E. M., Smorodinsky, N. I., and Barenholz, Y. (1996). "Targeted delivery of doxorubicin via sterically stabilized immunoliposomes: pharmacokinetics and biodistribution in tumor-bearing mice." *Pharm. Res.*, 13(6), 861-868.
- Eytan, G. D., and Kuchel, P. W. (1999). "Mechanism of action of P-glycoprotein in relation to passive membrane permeation." *Int. Rev. Cytol.*, 190, 175-250.
- Fava, R. A., Comeau, R. D., and Woodworth, R. C. (1981). "Specific membrane receptors for diferric-transferrin in cultured rat skeletal myocytes and chick-embryo cardiac myocytes." *Biosci. Rep.*, 1(5), 377-385.
- Foster, M. A., Grigor'ev, I. A., Lurie, D. J., Khramtsov, V. V., McCallum, S., Panagiotelis, I., Hutchison, J. M., Koptioug, A., and Nicholson, I. (2003). "In vivo detection of a pH-sensitive nitroxide in the rat stomach by low-field ESR-based techniques." *Magn Reson Med*, 49(3), 558-67.
- Frank, M. M. (1993). "The reticuloendothelial system and bloodstream clearance." *J. Lab. Clin. Med.*, 122, 487-488.
- Friden, P. M., Olson, T. S., Obar, R., Walus, L. R., and Putney, S. D. (1996). "Characterization, receptor mapping and blood-brain barrier transcytosis of antibodies to the human transferrin receptor." *J. Pharmacol. Exp. Ther.*, 278(3), 1491-1498.
- Gabizon, A., Catane, R., Uziely, B., Kaufman, B., Safra, T., Cohen, R., Martin, F., Huang, A., and Barenholz, Y. (1994). "Prolonged circulation time and enhanced accumulation in malignant exudates of doxorubicin encapsulated in polyethylene-glycol coated liposomes." *Cancer Res*, 54(4), 987-92.
- Gabizon, A., and Papahadjopoulos, D. (1988). "Liposome formulations with prolonged circulation time in blood and enhanced uptake by tumors." *Proc. Natl. Acad. Sci. U S A*, 85(18), 6949-6953.
- Gabizon, A., Shmeeda, H., and Barenholz, Y. (2003). "Pharmacokinetics of pegylated liposomal Doxorubicin: review of animal and human studies." *Clin. Pharmacokinet.*, 42(5), 419-436.
- Gabizon, A. A. (2001). "Pegylated liposomal doxorubicin: metamorphosis of an old drug into a new form of chemotherapy." *Cancer Invest.*, 19(4), 424-436.
- Gagne, J. F., Desormeaux, A., Perron, S., Tremblay, M. J., and Bergeron, M. G. (2002). "Targeted delivery of indinavir to HIV-1 primary reservoirs with immunoliposomes." *Biochim. Biophys. Acta.*, 1558(2), 198-210.

- Gijssens, A., Derycke, A., Missiaen, L., De Vos, D., Huwyler, J., Eberle, A., and de Witte, P. (2002). "Targeting of the photocytotoxic compound AIPcS4 to HeLa cells by transferrin conjugated PEG-liposomes." *Int J Cancer*, 101(1), 78-85.
- Goren, D., Horowitz, A. T., Tzemach, D., Tarshish, M., Zalipsky, S., and Gabizon, A. (2000). "Nuclear delivery of doxorubicin via folate-targeted liposomes with bypass of multidrug-resistance efflux pump." *Clin. Cancer Res.*, 6(5), 1949-1957.
- Gulati, M., Bajad, S., Singh, S., Ferdous, A. J., and Singh, M. (1998). "Development of liposomal amphotericin B formulation." *J. Microencapsul.*, 15(2), 137-151.
- Hafez, I. M., Ansell, S., and Cullis, P. R. (2000). "Tunable pH-sensitive liposomes composed of mixtures of cationic and anionic lipids." *Biophys. J.*, 79(3), 1438-1446.
- Hafez, I. M., and Cullis, P. R. (2000). "Cholesteryl hemisuccinate exhibits pH sensitive polymorphic phase behavior." *Biochim Biophys Acta*, 1463(1), 107-14.
- Hansen, C. B., Kao, G. Y., Moase, E. H., Zalipsky, S., and Allen, T. M. (1995). "Attachment of antibodies to sterically stabilized liposomes: evaluation, comparison and optimization of coupling procedures." *Biochim Biophys Acta*, 1239(2), 133-44.
- Heath, T. D., Fraley, R. T., and Papahadjopoulos, D. (1980). "Antibody targeting of liposomes: cell specificity obtained by conjugation of F(ab')<sub>2</sub> to vesicle surface." *Science*, 210, 539-541.
- Heath, T. D., Montgomery, J. A., Piper, J. R., and Papahadjopoulos, D. (1983). "Antibody-targeted liposomes: increase in specific toxicity of methotrexate-gamma-aspartate." *Proc Natl Acad Sci U S A*, 80(5), 1377-81.
- Hermanson, G. T. (1996). *Bioconjugate techniques*, Academic Press, San Diego.
- Herrlinger, U., Kramm, C. M., Aboody-Guterman, K. S., Silver, J. S., Ikeda, K., Johnston, K. M., Pechan, P. A., Barth, R. F., Finkelstein, D., Chiocca, E. A., Louis, D. N., and Breakefield, X. O. (1998). "Pre-existing herpes simplex virus 1 (HSV-1) immunity decreases, but does not abolish, gene transfer to experimental brain tumors by a HSV-1 vector." *Gene Ther.*, 5(6), 809-819.
- Hosokawa, S., Tagawa, T., Niki, H., Hirakawa, Y., Nohga, K., and Nagaike, K. (2003). "Efficacy of immunoliposomes on cancer models in a cell-surface-antigen-density-dependent manner." *Br. J. Cancer*, 89(8), 1545-51.
- Huwyler, J., Cerletti, A., Fricker, G., Eberle, A. N., and Drewe, J. (2002). "By-passing of P-glycoprotein using immunoliposomes." *J. Drug Targeting*, 10(1), 73-79.
- Huwyler, J., Froidevaux, S., Roux, F., and Eberle, A. N. (1999). "Characterization of transferrin receptor in an immortalized cell line of rat brain endothelial cells, RBE4." *J. Recept. Signal Transduct. Res.*, 19, 729-739.

- Huwylar, J., Wu, D., and Pardridge, W. M. (1996). "Brain drug delivery of small molecules using immunoliposomes." *Proc Natl Acad Sci U S A*, 93(24), 14164-9.
- Huwylar, J., Yang, J., and Pardridge, W. M. (1997). "Receptor mediated delivery of daunomycin using immunoliposomes: pharmacokinetics and tissue distribution in the rat." *J. Pharmacol. Exp. Ther.*, 282(3), 1541-1546.
- Hwang, S. H., Maitani, Y., Qi, X. R., Takayama, K., and Nagai, T. (1999). "Remote loading of diclofenac, insulin and fluorescein isothiocyanate labeled insulin into liposomes by pH and acetate gradient methods." *Int J Pharm*, 179(1), 85-95.
- Hyde, R., Peyrollier, K., and Hundal, H. S. (2002). "Insulin promotes the cell surface recruitment of the SAT2/ATA2 system A amino acid transporter from an endosomal compartment in skeletal muscle cells." *J Biol Chem*, 277(16), 13628-34.
- Iden, D. L., and Allen, T. M. (2001). "In vitro and in vivo comparison of immunoliposomes made by conventional coupling techniques with those made by a new post-insertion approach." *Biochim Biophys Acta*, 1513(2), 207-16.
- Jefferies, W. A., Brandon, M. R., Williams, A. F., and Hunt, S. V. (1985). "Analysis of lymphopoietic stem cells with a monoclonal antibody to the rat transferrin receptor." *Immunology*, 54(2), 333-341.
- Kaasgaard, T., Mouritsen, O. G., and Jorgensen, K. (2001). "Screening effect of PEG on avidin binding to liposome surface receptors." *Int. J. Pharm.*, 214(1-2), 63-65.
- Kajiwara, K., Byrnes, A. P., Ohmoto, Y., Charlton, H. M., Wood, M. J., and Wood, K. J. (2000). "Humoral immune responses to adenovirus vectors in the brain." *J. Neuroimmunol.*, 103(1), 8-15.
- Kang, Y. S., and Pardridge, W. M. (1994). "Use of neutral avidin improves pharmacokinetics and brain delivery of biotin bound to an avidin-monoclonal antibody conjugate." *J. Pharmacol. Exp. Ther.*, 269(1), 344-350.
- Kawasaki, T., Carmichael, F. J., Saldivia, V., Roldan, L., and Orrego, H. (1990). "Relationship between portal venous and hepatic arterial blood flows: spectrum of response." *Am J Physiol*, 259(6 Pt 1), G1010-8.
- Kirpotin, D., Hong, K., Mullah, N., Papahadjopoulos, D., and Zalipsky, S. (1996). "Liposomes with detachable polymer coating: destabilization and fusion of dioleoylphosphatidylethanolamine vesicles triggered by cleavage of surface-grafted poly(ethylene glycol)." *FEBS Lett*, 388(2-3), 115-8.
- Kirpotin, D., Park, J. W., Hong, K., Zalipsky, S., Li, W. L., Carter, P., Benz, C. C., and Papahadjopoulos, D. (1997). "Sterically stabilized anti-HER2 immunoliposomes: design and targeting to human breast cancer cells in vitro." *Biochemistry*, 36(1), 66-75.
- Klibanov, A. L., Maruyama, K., Beckerleg, A. M., Torchilin, V. P., and Huang, L. (1991). "Activity of amphipathic poly(ethylene glycol) 5000 to prolong the circulation time

- of liposomes depends on the liposome size and is unfavorable for immunoliposome binding to target." *Biochim. Biophys. Acta*, 1062(2), 142-148.
- Kung, V. T., Vollmer, Y. P., and Martin, F. J. (1986). "Large liposome agglutination technique for the serological detection of syphilis." *J Immunol Methods*, 90(2), 189-96.
- Kurihara, A., and Pardridge, W. M. (2000). "Abeta(1-40) peptide radiopharmaceuticals for brain amyloid imaging: (111)In chelation, conjugation to poly(ethylene glycol)-biotin linkers, and autoradiography with Alzheimer's disease brain sections." *Bioconjug Chem*, 11(3), 380-6.
- Laemmli, U. K. (1970). "Cleavage of structural proteins during the assembly of the head of bacteriophage T4." *Nature*, 227(5259), 680-5.
- Lai, M. Z., Vail, W. J., and Szoka, F. C. (1985). "Acid- and calcium-induced structural changes in phosphatidylethanolamine membranes stabilized by cholesteryl hemisuccinate." *Biochemistry*, 24(7), 1654-61.
- Lasic, D. D. (1996). "Doxorubicin in sterically stabilized liposomes." *Nature*, 380, 561-562.
- Lasic, D. D., Ceh, B., Stuart, M. C. A., Guo, L., Frederik, P. M., and Barenholz, Y. (1995). "Transmembrane gradient driven phase transitions within vesicles: lessons for drug delivery." *Biochimica et Biophysica Acta*, 1239, 145-156.
- Lasic, D. D., and Papahadjopoulos, D. (1995). "Liposomes revisited." *Science*, 267(5202), 1275-1276.
- Laverman, P., Zalipsky, S., Oyen, W. J., Dams, E. T., Storm, G., Mullah, N., Corstens, F. H., and Boerman, O. C. (2000). "Improved imaging of infections by avidin-induced clearance of 99mTc- biotin-PEG liposomes." *J. Nucl. Med.*, 41(5), 912-918.
- Lee, H. J., Zhang, Y., Zhu, C., Duff, K., and Pardridge, W. M. (2002). "Imaging brain amyloid of Alzheimer disease in vivo in transgenic mice with an Abeta peptide radiopharmaceutical." *J Cereb Blood Flow Metab*, 22(2), 223-31.
- Lee, R. J., and Low, P. S. (1994). "Delivery of liposomes into cultured KB cells via folate receptor-mediated endocytosis." *J. Biol. Chem.*, 269, 3198-3204.
- Leserman, L. D., Machy, P., and Barbet, J. (1981). "Cell-specific drug transfer from liposomes bearing monoclonal antibodies." *Nature*, 293(5829), 226-8.
- Li, J. Y., Sugimura, K., Boado, R. J., Lee, H. J., Zhang, C., Duebel, S., and Pardridge, W. M. (1999). "Genetically engineered brain drug delivery vectors: cloning, expression and in vivo application of an anti-transferrin receptor single chain antibody-streptavidin fusion gene and protein." *Protein Eng.*, 12(9), 787-796.

- Liu, Y., Mounkes, L. C., Liggitt, H. D., Brown, C. S., Solodin, I., Heath, T. D., and Debs, R. J. (1997). "Factors influencing the efficiency of cationic liposome-mediated intravenous gene delivery." *Nat. Biotechnol.*, 15(2), 167-173.
- Mäder, K., Bacic, G., Domb, A., Elmalak, O., Langer, R., and Swartz, H. M. (1995). "Noninvasive in vivo monitoring of drug release and polymer erosion from biodegradable polymers by EPR spectroscopy and NMR imaging." *J Pharm Sci*, 86(1), 126-134.
- Mäder, K., Bittner, B., Li, Y., Wohlauf, W., and Kissel, T. (1998). "Monitoring microviscosity and microacidity of the albumin microenvironment inside degrading microparticles from poly(lactide-co-glycolide) (PLG) or ABA-triblock polymers containing hydrophobic poly(lactide-co-glycolide) A blocks and hydrophilic poly(ethyleneoxide) B blocks." *Pharm Res*, 15(5), 787-793.
- Mamot, C., Drummond, D. C., Hong, K., Kirpotin, D. B., and Park, J. W. (2003). "Liposome-based approaches to overcome anticancer drug resistance." *Drug Resist Updat*, 6(5), 271-9.
- Mamot, C., Nguyen, J. B., Pourdehnad, M., Hadaczek, P., Saito, R., Bringas, J. R., Drummond, D. C., Hong, K., Kirpotin, D. B., McKnight, T., Berger, M. S., Park, J. W., and Bankiewicz, K. S. (2004). "Extensive distribution of liposomes in rodent brains and brain tumors following convection-enhanced delivery." *J Neurooncol.*, 68(1), 1-9.
- Mandel, J. L., and Pearson, M. L. (1974). "Insulin stimulates myogenesis in a rat myoblast line." *Nature*, 251(5476), 618-620.
- Martin, F. J., and Papahadjopoulos, D. (1982). "Irreversible coupling of immunoglobulin fragments to preformed vesicles. An improved method for liposome targeting." *J Biol. Chem.*, 257(1), 286-288.
- Maruyama, K., Holmberg, E., Kennel, S. J., Klibanov, A., Torchilin, V. P., and Huang, L. (1990a). "Characterization of in vivo immunoliposome targeting to pulmonary endothelium." *J Pharm Sci*, 79(11), 978-84.
- Maruyama, K., Kennel, S. J., and Huang, L. (1990b). "Lipid composition is important for highly efficient target binding and retention of immunoliposomes." *Proc Natl Acad Sci U S A*, 87(15), 5744-8.
- Maruyama, K., Takizawa, T., Yuda, T., Kennel, S. J., Huang, L., and Iwatsuru, M. (1995). "Targetability of novel immunoliposomes modified with amphipathic poly(ethylene glycol)s conjugated at their distal terminals to monoclonal antibodies." *Biochim. Biophys. Acta*, 1234(1), 74-80.
- Matsumura, Y., Gotoh, M., Muro, K., Yamada, Y., Shirao, K., Shimada, Y., Okuwa, M., Matsumoto, S., Miyata, Y., Ohkura, H., Chin, K., Baba, S., Yamao, T., Kannami, A., Takamatsu, Y., Ito, K., and Takahashi, K. (2004). "Phase I and pharmacokinetic study of MCC-465, a doxorubicin (DXR) encapsulated in PEG immunoliposome, in patients with metastatic stomach cancer." *Ann Oncol*, 15(3), 517-25.

- Mayer, L. D., Bally, M. B., and Cullis, P. R. (1986). "Uptake of adriamycin into large unilamellar vesicles in response to a pH gradient." *Biochim Biophys Acta*, 857(1), 123-6.
- Mayhew, E. G., Lasic, D., Babbar, S., and Martin, F. J. (1992). "Pharmacokinetics and antitumor activity of epirubicin encapsulated in long-circulating liposomes incorporating a polyethylene glycol-derivatized phospholipid." *Int. J. Cancer*, 51(2), 302-309.
- Moghimi, S. M., and Patel, H. M. (1992). "Opsonophagocytosis of liposomes by peritoneal macrophages and bone marrow reticuloendothelial cells." *Biochim. Biophys. Acta*, 1135(3), 269-274.
- Moradpour, D., Compagnon, B., Wilson, B. E., Nicolau, C., and Wands, J. R. (1995). "Specific targeting of human hepatocellular carcinoma cells by immunoliposomes in vitro." *Hepatology*, 22(5), 1527-1537.
- Mori, A., Klibanov, A. L., Torchilin, V. P., and Huang, L. (1991). "Influence of the steric barrier activity of amphipathic poly(ethyleneglycol) and ganglioside GM1 on the circulation time of liposomes and on the target binding of immunoliposomes in vivo." *Febs Lett*, 284(2), 263-6.
- Morrison, S. L., and Shin, S. U. (1995). "Genetically engineered antibodies and their application to brain delivery." *Adv. Drug Delivery Rev.*, 15(1-3), 147-175.
- Nakano, S., Matsukado, K., and Black, K. L. (1996). "Increased brain tumor microvessel permeability after intracarotid bradykinin infusion is mediated by nitric oxide." *Cancer Res.*, 56, 4027-4031.
- Nassander, U. K., Steerenberg, P. A., Poppe, H., Storm, G., Poels, L. G., De, J. W., and Crommelin, D. J. (1992). "In vivo targeting of OV-TL 3 immunoliposomes to ascitic ovarian carcinoma cells (OVCAR-3) in athymic nude mice." *Cancer Res.*, 52(3), 646-653.
- New, R. (1990). "Preparation of liposomes in Liposomes: A Practical Approach." The practical approach series, D. Rickwood and B. D. Hames, eds., Oxford University Press, Oxford, 301.
- O'Connell, J. P., Campbell, R. L., Fleming, B. M., Mercolino, T. J., Johnson, M. D., and McLaurin, D. A. (1985). "A highly sensitive immunoassay system involving antibody-coated tubes and liposome-entrapped dye." *Clin Chem*, 31(9), 1424-6.
- Osaka, G., Carey, K., Cuthbertson, A., Godowski, P., Patapoff, T., Ryan, A., Gadek, T., and Mordenti, J. (1996). "Pharmacokinetics, tissue distribution, and expression efficiency of plasmid [33P]DNA following intravenous administration of DNA/cationic lipid complexes in mice: use of a novel radionuclide approach." *J. Pharm. Sci.*, 85(6), 612-618.
- Ozawa, E. (1989). "Transferrin as a muscle trophic factor." *Rev. Physiol. Biochem. Pharmacol.*, 113, 89-141.

- Papahadjopoulos, D., Allen, T. M., Gabizon, A., Mayhew, E., Matthay, K., Huang, S. K., Lee, K. D., Woodle, M. C., Lasic, D. D., Redemann, C., and Martin, F. J. (1991). "Sterically stabilized liposomes: improvements in pharmacokinetics and antitumor therapeutic efficacy." *Proc. Natl. Acad. Sci. USA*, 88(24), 11460-11464.
- Pardridge, W. M. (1993). "Brain drug delivery and blood-brain barrier transport." *Drug Delivery*, 1, 83-101.
- Pardridge, W. M. (1995a). "Transport of small molecules through the blood-brain barrier: biology and methodology." *Adv. Drug Delivery Rev.*, 15, 5-36.
- Pardridge, W. M. (1995b). "Vector-mediated peptide drug delivery to the brain." *Adv. Drug Delivery Rev.*, 15, 109-146.
- Pardridge, W. M., Buciak, J. L., and Friden, P. M. (1991). "Selective transport of an anti-transferrin receptor antibody through the blood-brain barrier." *J. Pharmacol. Exp. Ther.*, 259, 66-70.
- Pardridge, W. M., Eisenberg, J., and Yang, J. (1987). "Human blood-brain barrier transferrin receptor." *Metabolism*, 36, 892-895.
- Parente, R. A., Nir, S., and Szoka, F. C., Jr. (1988). "pH-dependent fusion of phosphatidylcholine small vesicles. Induction by a synthetic amphipathic peptide." *J Biol Chem*, 263(10), 4724-30.
- Ponka, P., and Lok, C. N. (1999). "The transferrin receptor: role in health and disease." *Int. J. Biochem. Cell Biol.*, 31(10), 1111-1137.
- Radler, J. O., Koltover, I., Salditt, T., and Safinya, C. R. (1997). "Structure of DNA-cationic liposome complexes: DNA intercalation in multilamellar membranes in distinct interhelical packing regimes." *Science*, 275(5301), 810-814.
- Richardson, D. R., and Ponka, P. (1997). "The molecular mechanisms of the metabolism and transport of iron in normal and neoplastic cells." *Biochim Biophys Acta*, 1331(1), 1-40.
- Roninson, I. B. (1992). "The role of the MDR1 (P-glycoprotein) gene in multidrug resistance in vitro and in vivo." *Biochem. Pharmacol.*, 43(1), 95-102.
- Saito, R., Bringas, J. R., McKnight, T. R., Wendland, M. F., Mamot, C., Drummond, D. C., Kirpotin, D. B., Park, J. W., Berger, M. S., and Bankiewicz, K. S. (2004). "Distribution of liposomes into brain and rat brain tumor models by convection-enhanced delivery monitored with magnetic resonance imaging." *Cancer Res.*, 64(7), 2572-2579.
- Schnyder, A., Krahenbuhl, S., Torok, M., Drewe, J., and Huwyler, J. (2004). "Targeting of skeletal muscle in vitro using biotinylated immunoliposomes." *Biochem J*, 377(Pt 1), 61-7.



- Shahinian, S., and Silviu, J. R. (1995). "A novel strategy affords high-yield coupling of antibody Fab' fragments to liposomes." *Biochim. Biophys. Acta*, 1239(2), 157-167.
- Shek, P. N., and Heath, T. D. (1983). "Immune response mediated by liposome-associated protein antigens. III. Immunogenicity of bovine serum albumin covalently coupled to vesicle surface." *Immunology*, 50(1), 101-6.
- Shi, N., Boado, R. J., and Pardridge, W. M. (2001a). "Receptor-mediated gene targeting to tissues in vivo following intravenous administration of pegylated immunoliposomes." *Pharm Res*, 18(8), 1091-5.
- Shi, N., and Pardridge, W. M. (2000). "Noninvasive gene targeting to the brain." *Proc Natl Acad Sci U S A*, 97(13), 7567-7572.
- Shi, N., Zhang, Y., Zhu, C., Boado, R. J., and Pardridge, W. M. (2001b). "Brain-specific expression of an exogenous gene after i.v. administration." *Proc Natl Acad Sci U S A*, 98(22), 12754-9.
- Simoes, S., Moreira, J. N., Fonseca, C., Duzgunes, N., and de Lima, M. C. (2004). "On the formulation of pH-sensitive liposomes with long circulation times." *Adv Drug Deliv Rev*, 56(7), 947-65.
- Skehan, P., Storeng, R., Scudiero, D., Monks, A., McMahon, J., Vistica, D., Warren, J. T., Bokesch, H., Kenney, S., and Boyd, M. R. (1990). "New colorimetric cytotoxicity assay for anticancer-drug screening." *J Natl Cancer Inst*, 82(13), 1107-12.
- Slepushkin, V. A., Simoes, S., Dazin, P., Newman, M. S., Guo, L. S., Pedroso, d. L. M., and Duzgunes, N. (1997). "Sterically stabilized pH-sensitive liposomes. Intracellular delivery of aqueous contents and prolonged circulation in vivo." *J. Biol. Chem.*, 272(4), 2382-2388.
- Sorokin, L. M., Morgan, E. H., and Yeoh, G. C. (1987). "Transferrin receptor numbers and transferrin and iron uptake in cultured chick muscle cells at different stages of development." *J. Cell Physiol.*, 131(3), 342-353.
- Stevens, P. J., and Lee, R. J. (2003). "Formulation kit for liposomal doxorubicin composed of lyophilized liposomes." *Anticancer Res*, 23(1A), 439-42.
- Storm, G., and Crommelin, D. J. A. (1998). "Liposomes: quo vadis?" *Pharmaceutical Science & Technology Today*, 1, 19-31.
- Suzuki, S., Inoue, K., Hongoh, A., Hashimoto, Y., and Yamazoe, Y. (1997). "Modulation of doxorubicin resistance in a doxorubicin-resistant human leukaemia cell by an immunoliposome targeting transferrin receptor." *Br. J. Cancer*, 76(1), 83-89.
- Suzuki, S., Uno, S., Fukuda, Y., Aoki, Y., Masuko, T., and Hashimoto, Y. (1995a). "Cytotoxicity of anti-c-erbB-2 immunoliposomes containing doxorubicin on human cancer cells." *Br. J. Cancer*, 72(3), 663-668.

- Suzuki, S., Watanabe, S., Masuko, T., and Hashimoto, Y. (1995b). "Preparation of long-circulating immunoliposomes containing adriamycin by a novel method to coat immunoliposomes with poly(ethylene glycol)." *Biochim. Biophys. Acta*, 1245(1), 9-16.
- Tan, P. H., Manunta, M., Ardjomand, N., Xue, S. A., Larkin, D. F., Haskard, D. O., Taylor, K. M., and George, A. J. (2003). "Antibody targeted gene transfer to endothelium." *J Gene Med*, 5(4), 311-23.
- Torchilin, V. P., Goldmacher, V. S., and Smirnov, V. N. (1978). "Comparative studies on covalent and noncovalent immobilization of protein molecules on the surface of liposomes." *Biochem Biophys Res Commun*, 85(3), 983-90.
- Torchilin, V. P., Klibanov, A. L., Huang, L., O'Donnell, S., Nossiff, N. D., and Khaw, B. A. (1992). "Targeted accumulation of polyethylene glycol-coated immunoliposomes in infarcted rabbit myocardium." *Faseb J*, 6(9), 2716-9.
- Torchilin, V. P., and Weissig, V. (2003). *Liposomes*, Oxford University Press, New York.
- Triguero, D., Buciak, J., and Pardridge, W. M. (1990). "Capillary depletion method for quantification of blood-brain barrier transport of circulating peptides and plasma proteins." *J. Neurochem.*, 54(6), 1882-1888.
- Tycko, B., DiPaola, M., Yamashiro, D. J., Fluss, S., and Maxfield, F. R. (1983). "Acidification of endocytic vesicles and the intracellular pathways of ligands and receptors." *Ann. N Y Acad. Sci.*, 421, 424-433.
- Uster, P. S., Allen, T. M., Daniel, B. E., Mendez, C. J., Newman, M. S., and Zhu, G. Z. (1996). "Insertion of poly(ethylene glycol) derivatized phospholipid into preformed liposomes results in prolonged in vivo circulation time." *FEBS Lett*, 386(2-3), 243-6.
- Vingerhoeds, M. H., Haisma, H. J., Belliot, S. O., Smit, R., Crommelin, D., and Storm, G. (1996). "Immunoliposomes as enzyme-carriers (immuno-enzymosomes) for antibody-directed enzyme prodrug therapy (adept) - optimization of prodrug activating capacity." *Pharm. Res.*, 13(4), 604-610.
- Vingerhoeds, M. H., Haisma, H. J., van, M. M., van, de, Rijt, Rb, Crommelin, D. J., and Storm, G. (1993). "A new application for liposomes in cancer therapy. Immunoliposomes bearing enzymes (immuno-enzymosomes) for site-specific activation of prodrugs." *FEBS Letters*, 336(3), 485-490.
- Vogel, K., Wang, S., Lee, R. J., Chmielewski, J., and Low, P. S. (1996). "Peptide-mediated release of folate-targeted liposome contents from endosomal compartments." *J. Am. Chem. Soc.*, 118, 1581-1586.
- Wang, S., and Low, P. S. (1998). "Folate-mediated targeting of antineoplastic drugs, imaging agents, and nucleic acids to cancer cells." *J. Control. Release*, 53(1-3), 39-48.

- Wong, J. Y., Kuhl, T. L., Israelachvili, J. N., Mullah, N., and Zalipsky, S. (1997). "Direct measurement of a tethered ligand-receptor interaction potential." *Science*, 275(5301), 820-822.
- Woodle, M. C., Matthay, K. K., Newman, M. S., Hidayat, J. E., Collins, L. R., Redemann, C., Martin, F. J., and Papahadjopoulos, D. (1992). "Versatility in lipid compositions showing prolonged circulation with sterically stabilized liposomes." *Biochim. Biophys. Acta*, 1105, 193-200.
- Wu, D., Yang, J., and Pardridge, W. M. (1997). "Drug targeting of a peptide radiopharmaceutical through the primate blood-brain barrier in vivo with a monoclonal antibody to the human insulin receptor." *J Clin Invest*, 100(7), 1804-12.
- Xu, L., Huang, C. C., Huang, W., Tang, W. H., Rait, A., Yin, Y. Z., Cruz, I., Xiang, L. M., Pirollo, K. F., and Chang, E. H. (2002). "Systemic tumor-targeted gene delivery by anti-transferrin receptor scFv-immunoliposomes." *Mol Cancer Ther*, 1(5), 337-46.
- Yoshikawa, T., and Pardridge, W. M. (1992). "Biotin delivery to brain with a covalent conjugate of avidin and a monoclonal antibody to the transferrin receptor." *J. Pharmacol. Exp. Ther.*, 263(2), 897-903.
- Zelphati, O., Zon, G., and Leserman, L. (1993). "Inhibition of HIV-1 replication in cultured cells with antisense oligonucleotides encapsulated in immunoliposomes." *Antisense Res Dev*, 3(4), 323-38.
- Zhang, Y., Calon, F., Zhu, C., Boado, R. J., and Pardridge, W. M. (2003a). "Intravenous nonviral gene therapy causes normalization of striatal tyrosine hydroxylase and reversal of motor impairment in experimental parkinsonism." *Hum. Gene Ther.*, 14(1), 1-12.
- Zhang, Y., Jeong Lee, H., Boado, R. J., and Pardridge, W. M. (2002a). "Receptor-mediated delivery of an antisense gene to human brain cancer cells." *J Gene Med*, 4(2), 183-94.
- Zhang, Y., Schlachetzki, F., and Pardridge, W. M. (2003b). "Global non-viral gene transfer to the primate brain following intravenous administration." *Mol. Ther.*, 7(1), 11-18.
- Zhang, Y., Schlachetzki, F., and Pardridge, W. M. (2003c). "Global non-viral gene transfer to the primate brain following intravenous administration." *Mol Ther*, 7(1), 11-8.
- Zhang, Y., Zhang, Y. F., Bryant, J., Charles, A., Boado, R. J., and Pardridge, W. M. (2004). "Intravenous RNA interference gene therapy targeting the human epidermal growth factor receptor prolongs survival in intracranial brain cancer." *Clin. Cancer Res.*, 10(11), 3667-3677.
- Zhang, Y., Zhu, C., and Pardridge, W. M. (2002b). "Antisense gene therapy of brain cancer with an artificial virus gene delivery system." *Mol. Ther.*, 6(1), 67-72.

## 8 CURRICULUM VITAE

### PERSONAL DATA

Name: Anita Schnyder  
Date and place of birth: Solothurn, 25.4.1976  
Nationality: Swiss  
Marital status: Single  
Present address: Nidwaldnerstrasse 47  
CH-4055 Basel

### EDUCATION

10/1996-11/2001 University of Basel, Basel, CH  
Master degree in Pharmacy and approbation as Eidg.  
Dipl. Apothekerin  
08/1991-01/1996 Grammar school at Kantonsschule Solothurn,  
examination certificate type C

### PROFESSIONAL TRAINING AND EXPERIENCE

01/2002-present F. Hoffmann–La Roche Basel, Pharma Research, in  
collaboration with University of Basel, Division of clinical  
pharmacology and toxicology, Basel, CH PhD Student in  
clinical pharmacology under the supervision of Prof. Dr.  
Stephan Krähenbühl, Prof. Dr. Jürgen Drewe and PD Dr.  
Jörg Huwyler

- 02/2001-07/2001 University of Basel, Departement Forschung,  
Kantonsspital of Basel, CH  
Diploma thesis: "Synchronisation des Zellzyklus von  
Mammakarzinomzellkulturen"  
Mentor: PD Dr. Heinz Müller
- 10/1998-10/1999 University of Lausanne and Pharmacie de Chailly,  
Lausanne, CH  
One-year internship to fulfill diploma requirements,  
included three-month-trainee at Hôpital de Samaritain in  
Vevey, CH
- 10/1999-present Regular substitutions in different pharmacies in Solothurn,  
Nidau, La Chaux-de-Fonds, Ebnet-Kappel

### **SCIENTIFIC PUBLICATIONS, PATENT AND AWARD**

- 03/2005 Review Article:  
Schnyder, A. and Huwyler, J. (2005): Targeting of  
daunomycin using biotinylated immunoliposomes:  
Pharmacokinetics, tissue distribution and in vitro  
pharmacological effects. (submitted)
- 01/2005 Review Article:  
Schnyder, A. and Huwyler, J. (2005): Drug Transport to  
Brain with Targeted Liposomes. *NeuroRx* 2, 99-107
- 01/2004 Paper:  
Schnyder, A., Krähenbühl, S., Török, M., Drewe, J. and  
Huwyler, J. (2004): Targeting of skeletal muscle in vitro

- using biotinylated immunoliposomes. *Biochem. J.* 377, 61-67
- 01/2004 Amedis Award 2003 received for the publication in *Biochemical Journal* (2004, 377: 61-67)
- 11/2003 US-Patent:  
A non-covalent coupling method for the preparation of pegylated immunoliposomes. Huwyler J. and Schnyder A.  
Patent pending (case No. S-22306)

### **ATTENDED CONGRESSES / SYMPOSIA**

- BBB 2003 5. Blut-Hirn Schranke Expertentreffen Bad Herrenalb, Germany, 26. – 28.  
May 2003
- BBB 2004 6. Blut-Hirn Schranke Expertentreffen Bad Herrenalb, Germany, 17. – 19.  
May 2003
- Pharma-Day 2004, Center of Pharmaceutical Sciences Basel – Zürich, Switzerland, 5.  
February 2004 (with presentation: Amedis lecture: Drug targeting using immunoliposomes)
- Certificate “Key Issues in Drug Discovery and Development”, 7-Day-Graduate-Course,  
Center of Pharmaceutical Sciences Basel-Zürich, CH, November 2004

### **LANGUAGE SKILLS**

- |         |   |
|---------|---|
| German  | native speaker                          |
| French  | fluently spoken and written             |
| English | fluently spoken and written             |
| Spanish | basic skills (Spanish language courses) |